MICROSTRUCTURAL DESIGN OF FOOD GELS TO CONTROL MATERIAL PROPERTIES AND RELEASE OF NUTRIENTS

By

KELSEY MICHELE KANYUCK

A thesis submitted to the

University of Birmingham

for the degree of

DOCTOR OF PHILOSOPHY

School of Chemical Engineering

College of Engineering and Physical Sciences

University of Birmingham

March 2021

Abstract

Hydrocolloid systems can be used to tailor sugar release to match the needs of specific populations such as diabetics and athletes. A chewable gel with controllable release of sugars is of interest to food manufacturers, but first a fundamental understanding of the impacts of hydrocolloid structure on texture and release must be developed. Literature has shown a strong relationship between the structure and function of hydrocolloids and demonstrated the ability to optimise properties through control of the microstructure. The structure and gelation of maltodextrin (MD) and high acyl (HA) gellan gum have been established in previous research and were built upon to understand this more complex system.

The microstructure of MD gels and mixed gels with HA gellan gum were examined using techniques such as differential scanning calorimetry, large deformation gel fracture, Young's Modulus, and microscopy. Lower holding temperatures (5 °C compare to 45 °C and 60 °C) increased the enthalpy of MD gels which resulted in a more brittle gel with a higher modulus. The microstructure of these gels was more heterogeneous with larger pockets of water and smaller but an increased number of crystallites. The work suggested that concentration and temperature effected the helix-coil transition of maltodextrin and the subsequent formation of the aggregate network. An interpenetrating network (IPN) was observed between mixed gels MD and HA gellan which ranged in texture from hard and brittle to easily deformable based on the relative amounts of each polymer and the subsequent changes in microstructure. Aggregation of MD occurred within the pores of the HA gellan gum network which added brittleness and an increased modulus to the composite

gel. Determining the type of network allowed prediction of the behaviour using characteristics of the existing model.

Compared to smaller molecular weight carbohydrates (such as glucose and maltose), MD was slower to be released from the gel and required the digestive enzyme amylase for breakdown into smaller units. In comparison with other hydrocolloid gels, an IPN with MD resulted in lower release than phase separated gels, and both types of mixed gels were lower than maltodextrin alone. Swelling of HA gellan gum also reduced the release of carbohydrates and the swelling was found to be driven by an osmotic imbalance. This work provides a fundamental understanding of MD and HA gellan gum gels and the ways the microstructure can be developed to select for specific textures and release profiles. Examination of the underlying principles of gelation and the methods to create specific microstructures allowed this understanding.

Acknowledgements

I would first like to thank my supervisors Prof. Ian Norton, Dr. Tom Mills, and Dr. Abigail Norton-Welch for their guidance and support throughout my time as a student.

I would also like to thank all of the members of the microstructure group for sharing their knowledge and their friendships that have made my time so enjoyable. Additional thanks goes to SIS and the School of Chemical Engineering for the funding.

I am also forever thankful to my family for their continued support and encouragement.

Table of contents

List of figures..... x

List of tables..... xvi

List of abbreviations xviii

List of symbols xix

Chapter 1. Introduction 1

1.1. Project context.....1

1.2. Aims 2

1.3. Thesis structure 4

1.4. Publications and presentations 6

Chapter 2. Literature review 8

2.1. Introduction 8

2.2. Gelation of hydrocolloids 8

2.2.1. Single hydrocolloid systems.....8

2.2.2. Methods of analysis 11

2.2.2.1. Texture Analysis 11

2.2.2.2. Nuclear magnetic resonance (NMR) 12

2.2.2.3. Differential scanning calorimetry (DSC).....13

2.2.3. Mixed hydrocolloids systems.....13

2.3. Functionality of hydrocolloid gels 16

2.3.1. Carbohydrate release from gels 16

2.3.1.1. Diffusional release 17

2.3.1.2. Enzyme triggered release 17

2.3.1.3. Testing methodology 19

2.3.2. Swelling of gels 20

2.4. Maltodextrin 23

2.4.1 Maltodextrin structure 23

2.4.2 Maltodextrin gelation 25

2.4.2.1. Influences of dissolution process 28

2.4.2.2. Influences of gel setting method 29

2.5. Gellan gum 32

2.5.1. Gellan gum structure 32

2.5.2. High acyl gellan gelation 33

2.5.3. Low acyl gellan gelation 35

2.5.4. Functionality of gellan gum 36

Chapter 3. Temperature influences on network formation of low DE maltodextrin gels ... 39

Abstract 40

3.1. Introduction 41

3.2. Materials and methods 43

3.2.1. Materials 43

3.2.2. Preparation of gels 44

3.2.3. Large deformation properties 44

3.2.4. Differential scanning calorimetry 45

3.2.5. NMR analysis 45

3.2.6. Transmission electron microscopy 46

3.2.7. Statistical analysis 47

3.3. Results and discussion 47

3.3.1. Concentration of maltodextrin 47

3.3.2. Temperature influence on gelation 50

3.3.2.1 Temperature influence on fracture and bulk properties 51

3.3.2.2 Temperature influence on water distribution within network 53

3.3.2.3 Temperature influence on aggregation enthalpy, entropy, and free energy 56

3.3.2.4 Temperature influence on aggregate structure 62

3.3.3. Thermal hysteresis of gel network 63

3.4. Conclusion 68

Chapter 4. Structural characterization of interpenetrating network of high acyl gellan and maltodextrin mixed gels 70

Abstract 71

4.1. Introduction 73

4.2. Materials and methods....76
4.2.1. Materials and gel preparation....76
4.2.2. Compression and fracture of gels....77
4.2.3. Differential scanning calorimetry....78
4.2.4. Modelling by polymer blending laws....78
4.2.5 Scanning electron microscopy (SEM)....80
4.2.6 Statistical analysis....80
4.3. Results and discussion....81
4.3.1 Network characterization....81
4.3.1.1 Material properties....81
4.3.1.2. Microstructure analysis....85
4.3.2. Polymer contributions....94
4.3.3. Gelation mechanism....98
4.4. Conclusion....100
Chapter 5. Release of glucose and maltodextrin DE 2 from gellan gum gels and the impacts of gel structure....101
Abstract....102
5.1. Introduction....103
5.2. Materials and Methods....106
5.2.1 Materials....106

5.2.2. Sample preparation 106

5.2.3. Release measurements 108

5.2.4. Modelling of glucose release 110

5.2.5. Swelling 112

5.2.6. DSC 113

5.2.7. Statistical Analysis 113

5.3. Results and discussion 113

5.3.1. Diffusion based release of small MW carbohydrates 116

5.3.2. Impacts of gel stimuli-driven structural changes on release 122

5.3.3. Amylase-triggered release of MD 124

5.3.3.1. MD aggregation 125

5.3.3.2. Gelling agents 127

5.4. Conclusion 133

Chapter 6. Swelling of high acyl gellan gum hydrogel: characterization of network strengthening and slower release 134

Abstract 135

6.1. Introduction 136

6.2. Materials and methods 140

6.2.1. Materials 140

6.2.2. Sample preparation 141

6.2.3. Swelling measurement 141

6.2.4. Gel compression and fracture 142

6.2.5. Differential scanning calorimetry (DSC) 143

6.2.6. Rheology 143

6.3. Results and discussion 145

6.3.1. Swelling of gellan gum gels 145

6.3.2. Ionic influence on HA gellan gum swelling 147

6.3.2.1. Mechanical properties 149

6.3.3. Characterization of gel network changes 152

6.3.3.1. DSC 153

6.3.3.2. Temperature dependence of modulus 156

6.3.3.3. Mixed solution swelling 158

6.4. Conclusion 164

Chapter 7. Conclusions and Future Work 165

7.1. Conclusions 165

7.2. Future Work 167

Chapter 8. References 170

Appendix 185

List of figures

Figure 2.1. Schematic of the coil-to-helix transition (a) of polymer chains followed by an aggregation of helices (b) that led to a sol-gel transition 10

Figure 2.2. Illustrations of each type of network arrangement for maltodextrin (aggregates) and HA gellan gum (fibrous network). 16

Figure 2.3. Visual representation of maltodextrin gelation through double helix association, aggregation of double helix into crystalline regions, and connection of crystalline regions by long chains 27

Figure 2.4. Molecular structure of (A) HA and (B) LA gellan gum 33

Figure 2.5. Schematic models of gelation for (a) HA gellan, (b) LA gellan with monovalent cations, and (c) LA gellan with divalent cations 35

Figure 3.1. Comparison of the impact of concentration on force to fracture a gel [N] (■) and relaxation rate [s-1] (●) of maltodextrin gels 49

Figure 3.2. Influence of gelling time and temperature on strength of a 40% maltodextrin gel, after holding at the specified temperature 51

Figure 3.3. Influence of gelation temperature on gel strength 53

Figure 3.4. Melting DSC endotherm of 40% maltodextrin gels set for four days at the indicated temperature. 58

Figure 3.5. Holding temperature influence on Free Energy (Δ G) calculated from DSC thermograms. 61

Figure 3.6. TEM images of maltodextrin networks (at 40%) held for four days at (A) 10 ^{o}C, (B) 22 ^{o}C and (C) 60 ^{o}C. 62

Figure 3.7. Reversibility of gel structure for a 40% maltodextrin, after holding at the initial temperature for 4 days.....64
Figure 3.8. Melting DSC endotherm of 40% maltodextrin gels set for four days first temperature, and another 6 days at the second temperature. 67
Figure 4.1. Compression curves for 30% MD and 1% HA gellan (HAG) (- - - -) with comparison to 30% MD (—), 1% HA gellan (—), 20% MD and 1 % HA gellan (HAG) (— —) using calculated true stress and true strain values. Arrows show the points of fracture for each gel. 82
Figure 4.2. Comparison of the strain at failure for increasing levels of MD with HA gellan concentrations of 0 % (☐), 0.25% (▲), 0.5% (■), 0.75% (■), 1% (●), 1.5% (▲), and 2% (◆). Images show the appearance of 1% HA gellan with maltodextrin after compression. 84
Figure 4.3. Small deformation mechanics before failure as indicated by the Young's Modulus for HA gellan concentrations from 0 % (☐), 0.25% (▲), 0.5% (■), 0.75% (■), 1% (●), 1.5% (▲), and 2% (◆) at increasing levels of MD. 85
Figure 4.4. Comparison of measured network modulus of (A) 0.5% HA gellan, (B) 1% HA gellan and (C) 1.5% HA gellan with added MD (●) to calculated moduli from the isostrain (☐) and isostress (■) phase separation models and (D) 0.5% HA gellan, (E) 1% HA gellan and (F) 1.5% HA gellan for models utilizing one phase concentrations. 87
Figure 4.5. DSC heating (A) and cooling (B) curves for gels of 1% HA gellan (—), 20% MD (–), and 1% HA gellan with 20% MD (- - -) after four days of gelation. After baseline subtraction, the error bars represent a standard deviation of triplicate samples. 91
Figure 4.6. DSC curves comparing melting temperature of 1% HA gellan gum with and without 20% MD to 1.25% HA gellan gum. 92
Figure 4.7. SEM images of 30% MD (A and C) and 1% HA gellan with 25% MD (B and D). 94

Figure 4.8. Contribution of MD aggregation to the composite Young's Modulus at 0 % (◇), 10% (●), 15% (X), 20% (■), 25% (▲), and of 30 % (●) to a 1% HA Gellan network and 30% MD without HA gellan (☐) from 24 hours to 14 days. 97

Figure 4.9. Contribution of MD aggregation to the true strain at fracture for mixed gels with 30% MD and 1% (●), 0.75% (■), 0.5% (▲), and 0% (☐) HA gellan from 24 hours to 14 days. 97

Figure 4.10. Proposed schematic for HA gellan network alone (A) and contributing to an interpenetrating network with MD (aggregates) below (B) and above (C) the critical gelation concentrations of MD. 99

Figure 5.1. Diagram of release experimental setup showing the gels within dialysis tubing and inside of a larger bulk phase (150 mL) which was shaken at 200 rpm at 37 °C 110

Figure 5.2. Release of carbohydrates from 1% HA gellan (A) and 2% LA gellan (C) gels formulated with 30% glucose (▲), maltose (◊), and with MD DE 2 (●) and DE 10 (■) with amylase (black) and without (white). Total release from the gels at 48 hours shown for 1% HA gellan (B) and 2% LA gellan (D). 115

Figure 5.3. Concentration dependence of release profiles from LA gellan (squares) and HA gellan (circles) formulated with 30% glucose. 117

Figure 5.4. Modelling glucose release for 2% HA gellan gum (A) and LA gellan gum (B) comparing the Peppas-Sahlin Model (solid black line), single exponential (dashed grey line), and COMSOL mass transfer model (grey line). Equations are shown in Table 5.2. 119

Figure 5.5. Proportional contributions of Fickian diffusion (·····) and case II transport (– · – · –) mass transfer based on the Peppas-Sahlin Model for 2% HA gellan gum (A) and 2% LA gellan gum (B).....120

Figure 5.6. Release of glucose from 2% HA gellan gum (●), LA gellan gum (■), alginate (◆), kappa-carrageenan (◆), and gelatin (△) at 37 °C. 121
Figure 5.7. Release of glucose from gelling agents at 25 °C to compare the non-melting 2% gelatin (△) to 2% LA gellan (■) and HA gellan (●) gum. 123
Figure 5.8. Swelling of 1% HA gellan during the timeframe of release experiments (X) compared to formulations with 30% glucose (▲), maltose (◊), and with MD DE 2 (●) and DE 10 (■). Part B displays the swelling after 48 hours. 124
Figure 5.9. Carbohydrate release by amylase hydrolysis compared by gelling temperature for DE 2 MD at 30% (●), 40% (■), and 30% with 1% HA gellan gum (▲). Percentage released at 90 minutes shown by open symbols and final release shown by filled symbols. Samples were held at the indicated gelling temperature for 4 days prior to measurements and release experiments were all conducted at the same temperature (37 °C). 127
Figure 5.10. Release profiles (A) of 30% DE 2 MD without any gelling agent (X), HA gellan gum at 0.25% (○), 0.5% (●), 1% (●), and 2% (●), and with LA gellan gum at 0.25% (□), 0.5% (■), 1% (■), and 2% (■). Part B displays the total release after 48 hours for only MD (X) and each concentration of HA gellan (●) and LA gellan (■). 128
Figure 5.11. Release profiles at 37 131
Figure 5.12. Maltodextrin release from gelatin (△) at non-melting conditions (25 °C) compared to no gelling agent (X), another phase separated network 1% agarose (♦), and IPN 1% HA gellan (●). Total release (B) and for IPN (black), phase separated (grey), and no gelling agent (white) where lettering indicates significantly different values. 132
Figure 5.13. DSC heating curves for 30% MD, 2% gelatin, and 30% MD with 2% gelatin after four days of gelling at room temperature. 132

Figure 6.1. Changes in swelling ratio of 2% HA gellan (●) and LA gellan (■) during submersion in deionized water (filled symbol) and in 50 mM KCl (unfilled symbol ○ and □) for up to 7 days at room temperature. 146

Figure 6.2. Influence of salt concentrations on swelling of 2% HA gellan gels after soaking in 150mL of the indicated solution of KCl (■), NaCl (●), and $CaCl_2$ (Δ) for 48 hours and images show the change in appearance for gellan soaked in KCl solutions. Maximum swelling occurred in zone 1 and the equivalence salt concentration was estimated between 10 and 50 mM salt in zone 2. 148

Figure 6.3. Influence of ionic effect on the Young's Modulus of 2% HA gellan gels after soaking in 150mL solutions of KCl (■), NaCl (●), and $CaCl_2$ (Δ) compared to a fresh sample (dotted line) for 48 hours. Maximum swelling occurred in zone 1 and the equivalence salt concentration was estimated between 10 and 50 mM salt in zone 2. 151

Figure 6.4. Changes in gel fracture of 2% HA gellan after soaking in 150mL of of KCl (■), NaCl (●), and $CaCl_2$ (Δ) compared to a fresh sample (dotted line). Maximum swelling occurred in zone 1 and the equivalence salt concentration was estimated between 10 and 50 mM salt in zone 2. Image shows the appearance of HA gellan gum gels at the indicated concentration (A) before treatment and (B) fractured gels after soaking in DI water. 152

Figure 6.5. DSC heating thermograms for 2% HA gellan gum fresh (without any treatment) and after soaking in deionized (DI) water or 50 mM KCl for 48 hours. 155

Figure 6.6. Temperature dependence of storage modulus for 2% HA gellan (black) and after soaking in deionized water (blue) and 50mM KCl (dashed orange) utilizing small deformation rheology with controlled heating. 157

Figure 6.7. Solvent effects on swelling ratio (A), Young's Modulus (B), and strain at fracture (C) of 2% HA gellan gels after soaking in 150mL of water mixed with the indicated percentage of glucose (♦), glucose plus 100mM KCl (●), and ethanol (▲) for 48 hours and compared to a fresh gel (dotted line).....160

Figure 6.8. Release of glucose from gels prepared with 30% glucose and 2% HA gellan (●) and 2% LA gellan (■) into a bulk phase of deionized water (filled symbols) and 50mM KCl (unfilled symbols ○ and □ respectively). 163

Appendix A. NMR relaxation rates ($1/T_2$) used to estimate phase separation volumes for MD (☐), MD with 1% HA gellan (●). A Bruker mq20 minispec benchtop NMR was used for the measurement with a CPMG pulse sequence and tau of 0.25 ms. 185

List of tables

Table 2.1. Parameters of critical gelling factors for maltodextrins reported in the literature28

Table 2.2. Summary of reported network type using a low DE maltodextrin at or greater than a 10% w/w concentration and above the critical gelation point of the 2nd polymer. 31

Table 2.3. Summary of swelling behaviour for HA gellan gum gels. Reported values were either normalized to the freeze dried weight (Q) or the gel weight (q). 38

Table 3.1. Measured relaxation rates at 25 °C for 30 %, 40%, and 50% maltodextrin gels, after holding at the indicated temperature for 4 days. 56

Table 3.2. Calculated melting temperatures, enthalpy, and entropy values from DSC heating endotherms of maltodextrin gels set for four days at the indicated temperature 61

Table 3.3. Water relaxation rates, measured at 25 °C, for 40% maltodextrin gels, after holding at the initial temperature for 4 days and the secondary temperature for 6 days. 65

Table 3.4. Calculated melting onset temperatures, enthalpy of melting values, and entropy from DSC curves after holding at the initial temperature for 4 days and the secondary temperature for 6 days.....68

Table 4.1. Comparison of material properties of 1% HA gellan gels with 30% carbohydrate additives. Time dependence refers to a significant change ($p < 0.05$) in Young's Modulus or true strain at fracture over the period of 1 and 14 days.....89

Table 4.2. Calculated enthalpy values (J/g) from DSC heating and cooling cycles based on grams of total sample. Values are reported as the average with one standard deviation for three replicates. Different letters indicate significantly different sample means. 92

Table 5.1. A summary of the hydrocolloids used in formulation of the carbohydrate gels. 107

Table 5.2. Equations modelled to the release of glucose shown in Figure 5.4. 119

Table 5.3. Peak melting temperatures and enthalpy from DSC heating thermograms for MD and gelatin independently and the mixed gel of both hydrocolloids. 133
Table 6.1. Swelling ratio of HA gellan and LA gellan gum gels after submersion in 150mL of solution the indicated solution. Averages are reported with ± the standard deviation.....146
Table 6.2. Enthalpy of melting (J/g of polymer) and peak melting temperature (°C) for 2% HA gellan gum from Figure 6.5 and calculated entropy and Gibbs free energy (ΔG). Values were normalized to the grams of gellan gum in each sample and are reported as the average with one standard deviation. Means were compared for each column and different lettering is indicative of a significant difference between sample means. 156

List of abbreviations

Da	Daltons
DE	Dextrose equivalent
DI	Deionized [water]
DSC	Differential scanning calorimetry
GI	Gastrointestinal
HA	High acyl [gellan gum]
IPN	Interpenetrating network
LA	Low acyl [gellan gum]
MD	Maltodextrin
MW	Molecular weight
NMR	Nuclear magnetic resonance
PBS	Phosphate buffered saline
q	Swelling ratio
Q	Swelling degree
RI	Refractive index
U	Enzyme activity

List of symbols

E	Young's Modulus (Pa)
G	Gibbs Free Energy (J/g)
G_c	Predicted modulus of composite gel (Pa)
H	Enthalpy (J/g)
k	Rate constant of release (s^{-1})
ℓ	Distance of compression (mm)
ℓ_0	Initial height of gel (mm)
M	Mass of the gel (g)
M_0	Initial gel mass (g)
M_∞	Maximum concentration of sugar (g/mL)
M_t	Concentration of sugar (g/mL)
R^2	Correlation coefficient
S	Entropy (J/g·K)
t	Time (s)
Δ	Change
ε	Strain
ε_T	True strain
ξ	pore size (nm)
Π	Osmotic pressure (Pa)
σ	Stress (Pa)
σ_T	True stress (Pa)
ϕ_{HAG}	Phase volume of HA gellan
ϕ_{MD}	Phase volume of MD

Chapter 1. Introduction

1.1. Project context

Adequate consumption of water and food is necessary for the body to function properly. Specific populations, such as athletes and diabetics, require specific nutritional profiles to maintain appropriate blood glucose levels (Gidley, 2013; Norton et al., 2014b). Controlling carbohydrate release profiles to be able to maintain digestion over a specific period of time could improve the nutrition of these groups (Norton et al., 2014b).

During sustained exercise, the body requires refuelling to maintain optimal functioning (Maughan, 1991; Brouns and Kovacs, 1997; Jeukendrup and Jentjens, 2000). Consumption of carbohydrates during endurance-based exercise improves athlete performance (Jeukendrup and Jentjens, 2000). However, carbohydrates consumed at high levels can cause gastric distress and slower digestion rates (Maughan, 1991). A sustained level of carbohydrate intake is necessary to limit stress on the digestive system (Shi and Passe, 2010). A range of 1 – 1.1 g/min has been suggested as the maximum an athlete should consume (Jeukendrup and Jentjens, 2000). Consumption of traditional sugar-based (glucose) beverages have a high osmolality and cause slower emptying rates and GI distress (Hofman et al., 2016). Controlling the release by controlling structure of maltodextrin or mass transfer of sugars could improve athletic performance (Norton et al., 2014b).

Within the sports nutrition field, quick energy products which do not upset the stomach and control sugar release are of particular interest. Towards this need, beverages and fluid gels have been developed with balanced formulas, but there is consumer desire for a chewable energy gel. As an alternative to sugar, maltodextrin (a short and branched glucose polymer)

has been proposed as a better energy source. Maltodextrin still has quick digestion, but without the GI stress associated with high osmolality of sugar solutions.

A solution to reducing gastrointestinal stress is to create structures that slow the release of carbohydrates. This will be investigated by looking at maltodextrin as a carbohydrate source and how self-aggregation and hydrocolloid gels can be used to modify release profiles. Maltodextrin has been used for its functional properties in mixed gels, but there is a lack of knowledge on the digestibility of MD aggregates and how that structure formation may impact the caloric availability. Factors such as temperature, concentration, and gelation time have been suggested to effect the structure formation of maltodextrin by altering the stability associated with helix-coil transitions (Chronakis, 1998). A detailed understanding of the behaviour and structure formation of maltodextrin was necessary to facilitate the use of self-structuring to modify the speed of release. For development of a range of chewable textures, the influence of a secondary gelling agent within the mixed-gel systems is of interest. Literature has suggested the inclusion of a hydrocolloid decreases the availability of starch for carbohydrate digestion (Koh et al., 2009). It was therefore important to measure the effects of HA gellan gum on maltodextrin availability in the mixed gel and to compare the release to other carbohydrate. Development and optimization of the microstructure for both of these systems, with consideration to release and texture, will aim to develop a technology for commercial product application.

1.2. Aims

The goal of this PhD project was to develop the optimal microstructure of an energy gel using maltodextrin as the carbohydrate source. Determination of the physical properties

was key for developing a desirable texture of the gel, and analysis of the microstructure was used to predict the effects of structuring on release and digestion. To achieve this goal, the following three objectives were pursued:

1) Evaluate the gelation of maltodextrin (MD) and the ability to control structure formation using concentration, temperature, and gelation time;

2) Evaluate the inclusion of a secondary hydrocolloid high acyl (HA) gellan gum to create a less brittle gel than with maltodextrin alone. Examine the impacts of this second gelling agent on MD aggregation and gelation;

3) Investigate structural influences of MD gelation and mixed gel structure on the release of sugars and MD to predict stomach digestion behaviour;

Analysis of these objectives will build an understanding of each component's contribution to the texture and microstructure and allow for recommendations in developing a commercial energy gel product.

Structure-function relationships of MD were explored through analysis of the physical properties of gels formed under different conditions. Gelling temperature was shown to modify the gelation mechanism of MD by shifting the balance of enthalpy and entropy and could be used to selectively modify the microstructure. Characterization of mixed gels used composite properties and polymer theories to examine changes in gel network formation. Both small and large deformation behaviours were essential for determining the structure formation of the MD and HA gellan gum gels. This work will show how the microstructure determines the physical properties (texture) and the functional properties (release behaviour) of gels and how they can be selectively controlled.

1.3. Thesis structure

There is a need to understand carbohydrate structure and the influence of gelling agents to create a specific textures and release behaviour in functional products. This thesis provides a detailed characterization of maltodextrin and gellan gum structures and utilizes this structural information to explain the texture and release behaviour of the composite gels.

Chapter 2 is a literature review that provides an overview of hydrocolloid gelation followed by a critical review of maltodextrin and gellan gum. Additionally, a summary of work to date on swelling of gels and release from gels will be presented and applied in Chapters 5 and 6.

Chapter 3 investigates the gelation behaviour of maltodextrin and examines how temperature can be used to create different structures.

Chapter 4 examines the gel structure of maltodextrin with inclusion of a second hydrocolloid (HA gellan gum). The texture of MD alone was not appropriate for a commercial food gel and thus an additional hydrocolloid was needed. A series of experiments, including a utilization of the temperature dependence observed in the previous chapter, was used to characterize the mixed gel of the two polymers.

Chapter 5 measures the release of carbohydrates from the gel structures that were characterized in Chapters 3 and 4. The importance of carbohydrate size was analysed and a comparison to other gelling agents provided context for the behaviour of gellan and maltodextrin.

Chapter 6 examines an interesting behaviour that was observed with the HA gellan gum during release – a high degree of swelling. The swelling is characterized by examining the

influence of ionic environments of the swelling ratio, material properties, and network. The impacts of swelling on the release of glucose were measured.

Overall conclusion are provided in Chapter 7 and a suggestion of future work.

1.4. Publications and presentations

Publications:

Kanyuck, K. M., Mills, T. B., Norton, I. T., & Norton-Welch, A. B. (2019). Temperature influences on network formation of low DE maltodextrin gels. Carbohydrate Polymers, (218), 170-178.

Kanyuck, K. M., Norton-Welch, A. B., Mills, T. B., & Norton, I. T. (2021). Structural characterization of interpenetrating network of high acyl gellan and maltodextrin mixed gels. Food Hydrocolloids, (112), 106295.

Kanyuck, K. M., Mills, T. B., Norton, I. T., & Norton-Welch, A. B. (2021). Swelling of high acyl gellan gum hydrogel: Characterization of network strengthening and slower release. Carbohydrate Polymers, (259), 117758.

Kanyuck, K. M., Mills, T. B., Norton, I. T., & Norton-Welch, A. B. (2022). Release of glucose and maltodextrin DE 2 from gellan gum gels and the impacts of gel structure. *Food Hydrocolloids*, (122), 107090.

Oral presentations: (speaker underlined)

Kanyuck, K. M., Norton-Welch, A. B., Mills, T. B., & Norton, I. T. Temperature influences on network formation of low DE maltodextrin gels. *20th Gums and Stabilisers for the Food Industry*, San Sebastian, Spain, June 2019.

Kanyuck, K. M., Norton-Welch, A. B., Mills, T. B., & Norton, I. T. Microstructure influence on rheology of high acyl gellan and maltodextrin mixed gels. *8th International Symposium on Food Rheology and Structure*, Zurich, Switzerland, June 2019.

Kanyuck, K. M., Norton-Welch, A. B., Mills, T. B., & Norton, I. T. Structural characterization of interpenetrating network of high acyl gellan and maltodextrin mixed gels. *15th International Hydrocolloids Conference*, Melbourne, Australia, March 2020.

Kanyuck, K. M., Norton-Welch, A. B., Mills, T. B., & Norton, I. T. Release of carbohydrates from high acyl gellan gum gels and the impacts of swelling. *International Conference on Formulations in Food and Healthcare*, Virtual, March 2021.

Chapter 2. Literature review

2.1. Introduction

Designing food gels for delivery of carbohydrates requires an understanding of the structure and function of the hydrocolloids used to create them. Characterization of these materials and their impacts on release was the focus of this thesis. The proceeding literature review will give an overview of the theory of hydrocolloid structure-function relationships. Functionality of hydrocolloids gels will be reviewed with an overview of swelling and release from hydrocolloid gels to describe the current approaches used to describe and model these behaviours. Then a detailed summary specific to maltodextrin and HA gellan gum will be presented to identify gaps in the literature.

2.2. Gelation of hydrocolloids

2.2.1. Single hydrocolloid systems

Hydrocolloids are widely used in the food industry for thickening, stabilization, texture modification, and film formation (Nishinari et al., 2000; Williams and Phillips, 2009). They are also widely used in pharmaceutical and personal care industries for the same functionalities (Nishinari et al., 2000). Many of these polymers are large carbohydrate-based molecules such as carrageenan, alginate, and gellan. Gelatin, another common hydrocolloid, is a protein. Sources of the most common food hydrocolloids are plants, algae, microbes, and animals (Williams and Phillips, 2009).

Formulations typically contain only 0.1-2% by mass of these ingredients, but their interactions with water cause functional changes at even low concentrations. The large

molecular weight (MW) and aggregation ability of these molecules allow this unique functionality. Behaviour of each hydrocolloid is dictated by the concentration of polymer in solution. Below a critical concentration (C*) the polymer chains are in a dilute region such that molecules do no overlap and solutions are generally of low viscosity (Williams and Phillips, 2009). Above the C*, is the semi-dilute region in which polymer chains interact through topological entanglement and a shear thinning behaviour is observed (Williams and Phillips, 2009). The exact concentration for each polymer depends on the size and chemistry of the molecule. Some hydrocolloids are able to form physical interactions between molecules via ionic bridges, hydrophobic interactions, or hydrogen bonds (Williams and Phillips, 2009). At low concentrations these associations form aggregates, and above a critical gelling concentration (C_0) a continuous network of polymer spans the solution (Clark, 1991). Addition of salts or changes in temperature or pH are usually needed to trigger the gelation of hydrocolloids (Clark, 1991; Williams and Phillips, 2009).

The point a hydrocolloid solution becomes a gel is known as the sol-gel transition (Nishinari et al., 2000) (Figure 2.1). By definition a gel is a solid; although many are soft solids and easily deformable, a network must span the entire sample to provide the elastic behaviour (Clark, 1991). Changes in temperature, such as lowering below ~35 °C to set gellan gels or increasing temperature to denature proteins, can induce the aggregation and gelation of polymers (Clark, 1991). Other mechanisms of gelation, such as pH changes or addition of salt, either cause a conformation change or participate in the aggregation itself (Clark, 1991). Cold-set gelation from conformation changes occurs for many carbohydrate hydrocolloids e.g. gellan, carrageenan, and maltodextrin. At a certain temperature (often influenced by the amount of salt), the chains convert from random coils to an ordered

double helix conformation (Clark, 1991). Coil-helix transition represents the point the enthalpy of association becomes larger than the entropy associated with remaining in solution and the random coils form ordered helical structures. Double or triple helices are formed most often although sometimes a single helix. The presence of sufficient helices to form a continuous network becomes the point of gelation (Tanaka, 2003) (Figure 2.1). The balance between solution and gelation (sol-gel) is often discussed as a more general balance of solubility and aggregation (Djabourov et al., 2013). Factors such as the ionic properties and temperature effect this balance. Frequently used techniques to study these mechanism are differential scanning calorimetry (DSC) and rheology, both of which take advantage of the thermal dependency of the gelation (Clark, 1991; Nishinari et al., 2000).

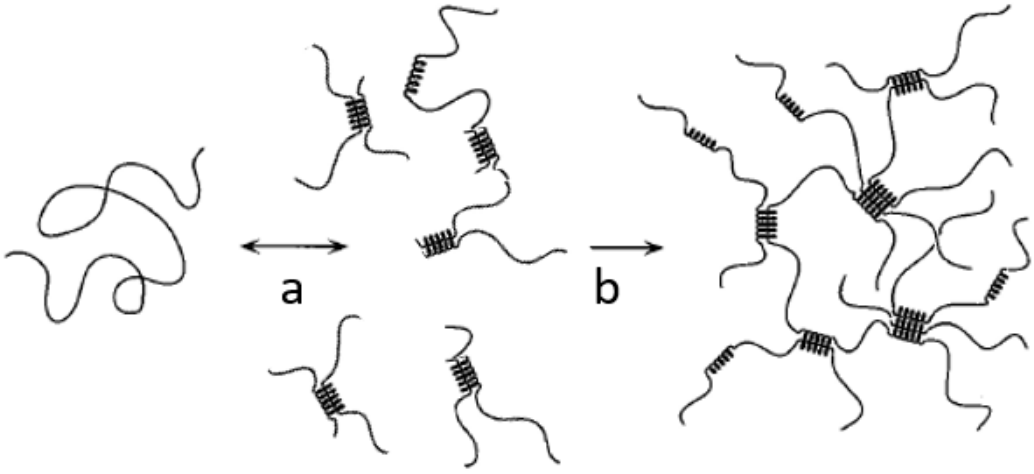

Figure 2.1. Schematic of the coil-to-helix transition (a) of polymer chains followed by an aggregation of helices (b) that led to a sol-gel transition (adapted from Tanaka, 2003)

2.2.2. Methods of analysis

2.2.2.1. Texture Analysis

Physical properties of gels are often characterized by applying stresses or strains and measuring the deformation. A test called squeeze-flow, in which a cylindrical sample is compressed between two parallel plates, is commonly used for food gels (Engmann et al. 2005). During compression, the upper plate moves at a set speed and measures the force required to achieve the set deformation. From the instrumental measurement of force (F) and distance (ℓ), and the sample properties initial contact area (A_0) and initial height (ℓ_0) the stress (σ) and strain (ε) can be calculated:

$$\sigma = F/A_0 \qquad \text{(Eq. 2.1)}$$

$$\varepsilon = (\ell - \ell_0)/ \ell_0 \qquad \text{(Eq. 2.2)}$$

Curves of the stress vs. strain are plotted to show the deformation behaviour. The stress at fracture gives an indication of the gel strength, and the strain at fracture is a measure of the gel's deformability. A small strain at fracture is indicative of a brittle gel, while a large strain to fracture corresponds to a deformable gel. To measure the elastic response, the Young's Modulus (E) is calculated from the ratio of stress to strain by the equation:

$$E = \sigma/\varepsilon \text{ from } \varepsilon = 0 \text{ to } \varepsilon = 0.05 \qquad \text{(Eq. 2.3)}$$

Young's Modulus of a material is calculated at the initial linear portion of the stress strain curve (approximately $\varepsilon = 0$ to $\varepsilon = 0.05$). This ratio is a very commonly used material property to engineers and material scientists for a wide variety of material from metals to hydrogels.

For deformable gels, a true strain (ε_T), and true stress (σ_T) are often calculated which take into consideration the change in shape during compression:

$$\varepsilon_T = \ln((\ell_0 + (\ell_0 - \ell) / \ell_0) \quad \text{(Eq. 2.4)}$$

$$\sigma_T = (F/A_0) (1 + \varepsilon) \quad \text{(Eq. 2.5)}$$

These parameters are used to describe the material properties of gels and are indicative of the underlying network structures of the gels. The Young's Modulus relates to the spacing of junction zones and the strain to fracture is a measure of the ability to structurally rearrange (Djabourov et al., 2013).

2.2.2.2. Nuclear magnetic resonance (NMR)

Nuclear magnetic resonance (NMR) is a widely used technique with many different applications based on instrument capabilities. For hydrogels, the use of T_2 relaxation (spin-spin relaxation) is of particular use to study the water mobility inside of gels (Lillford et al., 1980). The measurement begins by applying a magnetic pulse through the sample to align the spins. As the spin alignment decays, the kinetics of the process are measured by the instrument. Pulse sequences, such as the Carr-Purcell-Meiboom-Gill (CPMG), are used to lengthen the relaxation time for easier detection. The decay curves are fit to a mono or bi-exponential decay function and the exponent taken as the relaxation time.

Changes in arrangement of gel networks can be monitored with this technique. The relaxation time is an averaged measure of the relative distance between water protons and a solid surface, and in total reflects the distribution of water. Larger relaxation times indicate more mobile protons and are suggestive of larger water droplets and a less solid

sample (Lillford et al., 1980). Processes such as freeze-thaw separation of gels and cooked meats, which create a heterogeneous water distribution, have been demonstrated with this method (Lillford et al., 1980).

2.2.2.3. Differential scanning calorimetry (DSC)

Differential scanning calorimetry (DSC) is a technique that measures the thermal dependence of a sample during heating or cooling in reference to a standard material. Phase changes, such as melting or crystalizing, are classic examples of a thermal events that can be measured. The heat given off or absorbed during any phase change or other thermal event are measured by the instrument as a change in heat flow. By graphing heat flow over time, the temperature at which the event occurred and the total energy can be calculated.

In the study of hydrocolloids, DSC is widely used to determine the melting and gelling temperature. By integration of the heat flow curve, the enthalpy of these transitions can be calculated. In combination these parameters give important information about the conformational changes of a hydrocolloid (Djabourov et al., 2013). For example, the helix-coil transition of gellan is exothermic and the heat the conformation change gives off is detected. Using DSC, among other techniques, the effects of salt and pH on the coil-helix transition temperature can be quantified.

2.2.3. Mixed hydrocolloids systems

Mixtures of two or more hydrocolloids are commonly used to create ideal properties such as texture, breakdown, and functionality (Norton and Frith, 2001). Arrangements of these mixtures can be categorized into three types of gel networks: phase separated,

interpenetrating network (IPN), and coupled (Morris, 1986; Kasapis, 1995; Norton et al., 2014a). Illustrations of the three network types hypothesized for MD and HA gellan are shown in Figure 2.2.

A phase separated network is a water-in-water dispersion in which one polymer forms droplets within a continuous network of the second polymer (Morris, 2009; Norton et al., 2014a). This leads to an increased effective concentration of each polymer in the respective phase (Djabourov et al., 2013). Concentration of each polymer and the ionic environment effect the equilibrium. At dilute concentrations of both polymers, phase mixing is typically observed. Only at sufficiently high concentrations (approximately 4% total mass) is phase separation generally observed. Classic examples of phase separated networks are gelatin and maltodextrin (Kasapis et al., 1993a) and agarose and maltodextrin (Loret et al., 2005).

An IPN network is formed by both polymers spanning the gel without separation into different phases (Kasapis, 1995; Norton et al., 2014a). A polymer mixture known to form an IPN is gellan and agarose (Amici et al., 2000a).

A coupled network remains a single phase and additionally involves an ionic or electrostatic associated between the polymer chains, and this type is the least common (Morris, 1995; Kasapis, 1995; Morris, 2009). Some examples include konjac glucomannan with xanthan and locust bean gum and xanthan (Morris 2009).

The phase behaviour is controlled by the entropic and enthalpic favourability of mixing and alike polymer interactions respectively (Norton and Frith, 2001). Phase separation is common among mixtures, especially at higher concentrations and lower temperatures, due

to the enthalpy associated with chemically similar molecules (Kasapis et al., 1993a; Clark, 1996; Norton and Frith, 2001; Morris, 2009). Interpenetrating networks are more common for polymers with a charge due to the unfavorablity to aggregate like-charged chains (Norton and Frith, 2001). Changes in environment, such as salt and temperature can shift the balance and allow for a selected behaviour (Morris, 2009).

Examination of mixed hydrocolloids typically begins with a characterization of the type of network structure using several different methods. Polymer blending laws can be used to estimate the composite modulus of a phase separated system using the phase volumes and individual hydrocolloid modulus at the estimated concentration (Morris, 2009; Djabourov et al., 2013). Isostress and isostrain models are calculated which gives an estimate for the upper and lower bounds for the composite, and the true composite modulus is compared to evaluate consistency with phase separation (Morris, 2009; Djabourov et al., 2013). Differential scanning calorimetry (DSC) is used to compare gelation of each individual polymer to that of the composite gel. Changes in enthalpy (size of the melting peak) or melting temperature can indicate binding between polymers characteristic of a coupled network (Nishinari et al., 1996b; Djabourov et al., 2013). Microscopy is another commonly used technique when staining of one phase is possible, and therefore it is most commonly used for protein – polysaccharide mixtures (Lorén et al., 1999; Djabourov et al., 2013). Each method has limitations and thus in practice a combination of methods are used together to predict the network type.

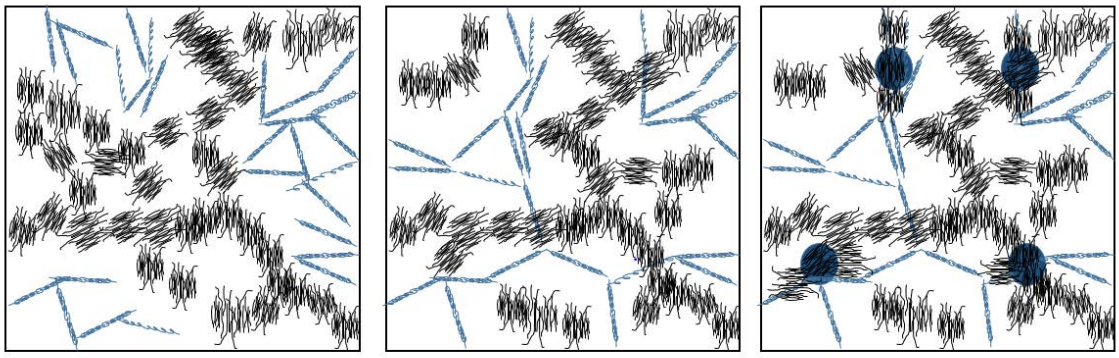

Figure 2.2. Illustrations of each type of network arrangement for maltodextrin (aggregates) and HA gellan gum (fibrous network).

2.3. Functionality of hydrocolloid gels

2.3.1. Carbohydrate release from gels

Food technologies which are able to control carbohydrate digestion are important for groups such as athletes and diabetes which have tailored needs (Norton et al., 2014b). When used strategically, formulation with gelling hydrocolloids can prolong digestion and have the possibility to enhance satiety or modify glycaemic levels (Jenkins et al., 1977; Gidley, 2013). Generally, higher concentrations of polymer decrease the speed of release of an entrapped small MW active (McClements and Xiao, 2014).

A gel network predominately acts as a barrier to movement unless an interaction occurs between the hydrocolloid and the analyte (McClements, 2017; Wee and Henry, 2020). Size of the analyte relative to the gel pores (Andersson et al., 1997) and the presence of covalent or ionic bonds between the analyte and the gel pores (McClements, 2017) both can have large impacts. Structural effects of a gel network depend on the size of the carbohydrate

and the path for release. Small MW carbohydrates (such as glucose and maltose) do not form aggregates and are expected to diffuse through the pores of hydrocolloid gels (Mills et al., 2011). Larger carbohydrates cannot fit through the pores and must follow a different mechanism of release. These molecules need to be broken down first, such as by amylase cleavage of starch into maltose, and then can be released from the gel (Gidley, 2013). In addition to the properties of the gelling agent and carbohydrate, many other factors contribute to the process of release and are discussed below.

2.3.1.1. Diffusional release

Small carbohydrates, such as glucose and sucrose, are able to move through the pores of most gel networks and thus follow a diffusion behaviour (Mills et al., 2011). Therefore, the primary factors which control release are gel surface area, solute concentrations, and mass transfer rates (Nishinari and Fang, 2016). Much of the literature regarding sugar release from gels is regarding sweetness perceptions of sucrose which involves chewing and short times (Nishinari and Fang, 2016). Surface area of the gel piece has been shown to be a significant driver in the speed of release (Mills et al., 2011; Nishinari and Fang, 2016). Impacts have been observed not just through the fabricated dimensions but also based on the fracture and breakup of the gels during mastication (Morris, 1994; Yang et al., 2015; Khin et al., 2021). In fact, many studies are dominated by the fracture behaviour of simulated oral processing rather than by diffusion through the gel network (Khin et al., 2021). Melting or serum release from a gel can also greatly increase the speed by quickly mixing with the saliva or solvent (Sala et al., 2010; Mills et al., 2011; Khin et al., 2021).

2.3.1.2. Enzyme triggered release

Carbohydrates larger than the network pores must be broken down before they can be released. The digestive enzyme α-amylase is present in the human saliva and small intestines which hydrolyses linear starch-based carbohydrate chains into predominantly maltose units (Dhital et al., 2017). Amylase must travel through the food matrix to reach the starch carbohydrate chains. Factors which slow the movement of amylase or change the carbohydrate arrangement can both decrease the release (Tharakan et al., 2010; Gidley, 2013; Fabek et al., 2014). Numerous recent studies have examined the effects of hydrocolloids on starch availability to amylase digestion. Generally, a lower release was measured (Koh et al., 2009; Sasaki and Kohyama, 2011; Ramírez et al., 2015; Zhang et al., 2018; Srikaeo and Paphonyanyong, 2020). These studies were very application focused and a detailed discussion of how the gel network impacts the release was missing. None have provided a comprehensive comparison of different gelling agents, different concentration, or how the microstructure impacts the release.

A hydrocolloid network was thought to slow and decrease hydrolysis by acting as a physical barrier and slowing the movement of molecules (Wee and Henry, 2020). Movement of amylase was slowed by higher viscosity fibres and resulted in slower release of glucose from starch mixtures with added amyloglucosidase (Fabek et al., 2014). A similar response was noted with guar gum in a model of the small intestine (Tharakan et al., 2010). These effects are thought to be caused by the viscosity of the hydrocolloid because the same effects were not observed for low-viscosity or insoluble fibres (McRorie Jr and McKeown, 2017). Binding between the amylase and certain hydrocolloids (such as cellulose) can also decrease the enzymatic activity (Dhital et al., 2015).

Aggregated gel structures of starch molecules can also inhibit release by decreasing the efficiency of amylase. The ability of amylase to bind to the chains is decreased by the crystallites and helices and their packing (Dhital et al., 2017). Retrograded starch is partially amylase resistant due to the irregular structure and lower enzyme affinity (Gidley et al., 1995a; Butterworth et al., 2011). Even short and medium length amylose chains from starch formed more compact aggregates structures which were more resistant to enzyme hydrolysis (Gong et al., 2019). Gels can also reduce starch gelatinization and retrogradation by holding water or sterically inhibiting swelling. An example of this has been shown by a pectin gel which decreased the readily digestible starch and increased the amount of resistant starch (Zhang et al., 2018).

2.3.1.3. Testing methodology

Human trials offer the truest measure of sugar digestion, however there are many factors which cause variability in measurements including chewing styles, amylase concentrations, hormones, and prior meals (Dhital et al., 2017). Not all sugars are absorbed equally, and the digestion rates are influenced by molecular size and required enzymes. From human trials, the highest oxidation rate (digestion rate) for carbohydrates was 1.1 g/min regardless of concentration (Jeukendrup and Jentjens, 2000). While glucose and maltose can be directly absorbed, larger molecules such as maltodextrin need to be broken down enzymatically before adsorption (Hofman et al., 2016). Therefore, changes in the amount of amylase can affect blood glucose levels and the insulin response (Dhital et al., 2017). Glycaemic responses of different individuals were significantly different even when the food particle size was controlled for (Ranawana et al., 2011). The complexity involved in human testing

has lead scientists to utilize *in vitro* testing for most experiments on the fundamental properties of carbohydrate digestion (Woolnough et al., 2008; Koh et al., 2009).

For true digestion and glycaemic index measurements, *in vivo* human tests are necessary. However, *in vitro* offers greater ease and the removal of natural human differences (Nishinari and Fang, 2021). Factors such as the amount of chewing, bolus size, enzyme concentrations, and residence times are all natural human differences that add variability with *in vivo* release measurements (Gidley, 2013; Dhital et al., 2017). Starch release experiments require the procurement of the enzyme amylase. Instead of using human saliva, many experiments use microbial produced enzyme with a known activity level (U/mg) (Koh et al., 2009; Zhang et al., 2018). The unit U is a measure of enzyme activity defined by the amount of substrate released U = µmol/min released. For example, 500 U means the maximum capacity of released glucose is 500 µmol/min. This offers decreased variation compared to human testing, however even for *in vitro* testing wide variation have been reported in literature with no standard method for glycaemic index or similar (Woolnough et al., 2008). Because there is no standard, it has been difficult to compare results between different researchers. Recently, a large group of scientists have proposed a uniform testing methodology (INFOGEST) which aims to become a worldwide standard (Minekus et al., 2014; Brodkorb et al., 2019). If generally accepted, this would allow for beneficial comparisons between research groups.

2.3.2. Swelling of gels

Polymer gels have the ability to increase in size by taking up considerable amount of water into the network (greater than their own mass). Any gel can swell if the osmotic pressure

inside the gel is greater than the elastic pressure of the network (Annaka et al., 2000; Sakai, 2020). The total pressure of gel (Π) is described by the summation of polymer-solvent mixing (Π_{mix}), chain elasticity ($\Pi_{elastic}$), and counterions (Π_{ion}) by the equation (Annaka et al., 2000; Sakai, 2020):

$$\Pi = \Pi_{mix} + \Pi_{elastic} + \Pi_{ion} \quad \text{(Eq. 2.6)}$$

The theory of Flory-Rehner describes the osmotic pressure of a gel as the sum of osmotic pressure and elastic pressure whereby crosslinks between chains limits swelling of gels by contributing to the elastic pressure counterbalancing the osmotic pressure (Van der Sman, 2015). Flory-Rehner theory uses the swollen polymer volume fraction to estimate the molecular weight between crosslinks (M_c) by the equation:

$$\frac{1}{M_c} = \frac{2}{M_n} - \frac{\left(\frac{\nu}{V_1}\right)\left[\ln(1-v_{2,s}) + v_{2,s} + \chi_1 v_{2,s}^2\right]}{v_{2,r}\left[\left(\frac{v_{2,s}}{v_{2,r}}\right)^{\frac{1}{3}} - \left(\frac{v_{2,s}}{2v_{2,r}}\right)\right]} \quad \text{(Eq. 2.7)}$$

Which includes contributions from the molecular weight (M_n), a polymer specific volume (ν), molar volume of water (V_1) at 18 mL/mol, Flory-Huggins interaction parameter (χ_1), polymer volume fraction in the relaxed state ($v_{2,r}$), and polymer volume fraction in the swollen state ($v_{2,s}$). From the M_c, a pore size (ξ) can be calculated by the equation (Lin and Metters, 2006):

$$\xi = v_{2,s}^{-1/3} l_0 \sqrt{2\, M_c\, C_n \,/\, M_r} \quad \text{(Eq. 2.8)}$$

Which includes contributions from a bond length (l_0), characteristic ratio (C_n), and molecular weight of the repeating unit (M_r). There has been some debate about the validity of using non-Gaussian chains and multiple ions in this model, but previous work has established a suitability in helix-forming hydrocolloids (Van der Sman, 2015).

Swelling is typically measured using the ratio of initial mass to final mass where M is the measured sample mass after swelling and M_0 is the initial mass (Djabourov et al., 2013):

$$\text{Swelling Ratio } (q) = M/M_0 \quad \text{(Eq. 2.9)}$$

A similar equation, but with drastically different results, is the swelling ratio of a freeze dried polymer. This swelling degree (Q) measures the final sample mass (M) in relation to the freeze-dried polymer weight ($M_{0\ dried}$) (de Souza et al., 2021):

$$\text{Swelling Degree } (Q) = (M - M_{0\ dried}) / M_{0\ dried} \quad \text{(Eq. 2.10)}$$

Many authors remove the water from a hydrogel before swelling (by freeze drying or lyophilisation) which partially destroys the structure (Cassanelli et al., 2018a). Additionally, as the swelling is reported as a ratio of the dried weight (eq. 2.10), a shift in the amount of water in the gel based on the extent of lyophilisation would widely vary the result. Some authors reported a time length of the swelling process, but others did not. LA gellan gum is known to take several hours to swell and then begin to dissociate over time (Nitta et al., 2006; Hossain and Nishinari, 2009). Clearly the length of time for measuring the swelling would affect the reported values.

Charged gels typically have largest swelling due to the associated counter ions of the charged groups which cause osmotic swelling from the Donnan effect (Sakai, 2020). Under environmental conditions with equal ions both outside and inside, the gel has much lower swelling (Annaka et al., 2000; Coutinho et al., 2010). In addition to the osmotic force, gels which swell must have a low crosslink density to allow the rearrangement (Moe et al., 1993). The crosslink density can actually been estimated by the maximum swelling volume of a gel (Moe et al., 1993; Sakai, 2020).

2.4. Maltodextrin

2.4.1 Maltodextrin structure

Maltodextrin is a widely used polymer in the food industry for applications including thickening, bulking, and encapsulation (Chronakis, 1998). Created by the hydrolysis of starch into smaller glucose chains, the resulting maltodextrin chemistry is based on both the initial starch structure and the degree of hydrolysis (Chronakis, 1998). The commonly used term to describe the chain lengths or degree of hydrolysis is the dextrose equivalent (DE) (Hofman et al., 2016). A simple measurement, the DE is calculated by the percent of reducing sugars in a sample (Hofman et al., 2016). Therefore, a pure dextrose sample would have a DE value of 100, corresponding to 100% of the molecules with an available reducing end. Lower DE values reflect the lower number of reducing ends available in samples composed of chains, since only the molecule at the end of a chain is a reducing sugar (Hofman et al., 2016). Maltodextrin can be produced using a range of degrees of hydrolysis and from various starch sources, and the resulting chemistry of these factors influences the final physical properties.

By definition, a maltodextrin has an average DE between 3 and 20 (Chronakis, 1998). However, because the DE is an average measurement, the actual size of the maltodextrin chains follow a distribution which is only centred at the DE value. Commercial maltodextrins were found to contain wide ranges of molecular weights in a single product and a binomial distribution of sizes (Wang and Wang, 2000; Castro et al., 2016). The binomial distribution consisted of a high MW and a low MW fraction (Bulpin et al., 1984; Wang and Wang, 2000; Castro et al., 2016). The fraction of high MW chains (in a DE 5-8 MD) were highly branched,

while the low MW fraction was practically all linear (Bulpin et al., 1984). Likely, the small MW fraction is comprised of the degraded amylose-portions of the starch, and the large MW fraction contains the branched amylopectin regions which were not hydrolysed (α-limit dextran) (Bulpin et al., 1984; Schierbaum et al., 1990). Products of differing DE values showed peaks at the same two MW sizes, but differences occurred in the ratios of the high and low MWs (Castro et al., 2016). Additionally, the type of hydrolysis utilized impacted the range of chain lengths. Enzyme hydrolysis resulted in a narrower range of MW chains than acid hydrolysis (Castro et al., 2016). Potato starch granules are known to be larger and not contain the pores typical of corn starch (Nishinari and Fang, 2021). Not unexpectedly, maltodextrin MW distribution varies with both brand and source (Alevisopoulos et al., 1996) in addition to the hydrolysis method.

Although commonly used within commercial maltodextrins, the DE value is not sufficient to describe the full functionality. Commercial maltodextrins have been shown to have different physical properties (specifically the viscosity) even with the same DE value (Dokic et al., 1998; Castro et al., 2016). These variations are suggested to be based on other chemical features (such as the MW or the ratio of amylose to amylopectin) which is not directly included in the DE calculation (Dokic et al., 1998; Castro et al., 2016; Hofman et al., 2016). Causing further discrepancies, Wang and Wang (2000) found that the measured DE value (determined by the Nelson method) for several manufactures' products were outside specified range (Wang and Wang, 2000). Source and DE are key factors of maltodextrin functionality, but comparison of products suggests each maltodextrin should be individually characterized for full understanding of the chemistry and material properties.

2.4.2 Maltodextrin gelation

Gelation of polymers occurs through association and junction formation between chains, creating one continuous network. For maltodextrin, the mechanism of this network formation occurs through three steps: (1) double helix associations and (2) packing of double helices into hexagonal structures and (3) aggregation into crystalized regions, with longer chains connecting helix aggregates together in a gel (Reuther et al., 1984; Schierbaum et al., 1990; Kasapis et al., 1993b; Chronakis, 1998; Loret et al., 2004b) as shown in Figure 2.3. This mechanism is identical to the structure formation observed for amylose and amylopectin (Chronakis, 1998). The key to reach a true gel point is through connection of crystalline regions by chains participating in multiple aggregation points (Figure 2.3). Thus, chain length is of major importance in gelation capabilities. Alternatively, the crystallization point (as distinguished from the gel point) has been defined by the association between two double-helix chains (4 total chains, with 3 association points) (Schierbaum et al., 1990; Loret et al., 2004b). Whereas gelation is associated with an increase in viscosity, crystallization has been attributed to the cloudiness of gels (Loret et al., 2004b). Both processes are needed during gel formation to create the necessary structures of a continuous network (Loret et al., 2004a).

Based on the gelation mechanism, the presence of sufficient concentrations of long chains to connect crystalline regions is key to network formation (Schierbaum et al., 1986; Gidley and Bulpin, 1987; Schierbaum et al., 1992). For glucose oligomers, a chain length of ten (Gidley and Bulpin, 1987) or eleven (Bulpin et al., 1984) monosaccharides was needed to crystalize, and a shorter chain length of six was able to co-crystalize (Gidley and Bulpin,

1987). In agreement with this theory, a low MW maltodextrin [approximately DE 11] did not form a gel network, but did show sedimentation characteristic of crystallization (Schierbaum et al., 1992). Likely, longer chains are needed to form associations between aggregated regions. Addition of long-chain components (amylose) to an otherwise non-gelling maltodextrin solution promoted gelation of the sample (Schierbaum et al., 1986; Schierbaum et al., 1992). The addition of amylopectin to an amylose solution also caused aggregation (German et al., 1992). Interestingly, several studies have shown that both short and long chains are needed to form a gel. When only the large MW chains were present, the mixture was not able to form a gel even at concentrations up to 45% (Bulpin et al., 1984). Thus, the shorter chains must be needed to participate in double helix formation (Loret et al., 2004b), and may also be the cause of increasing gel strength (for up to 12 days) after initial formation (Chronakis and Kasapis, 1995; Loret et al., 2004a).

In addition to chain length, the extent of branching (amylose versus amylopectin) also influenced gel structure. It has been hypothesized that amylopectin fragments reduce the size of junction zones (crystallization sites), as evidenced by gel networks with increased rigidity and viscoelasticity (Vorwerg et al., 1988). In application, replacing some DE 3 with a DE 8 maltodextrin in a low-fat margarine formulation progressively decreased the peak stress and changed from a fracture-able gel to more paste-like compression profile (Chronakis and Kasapis, 1995). Past experimentation with maltodextrin and starches has led to an understanding of the influences of size and branching of chain during network formation.

Critical gelling concentrations and times reported through literature vary with DE, source, and gelling method and are summarized in Table 2.1. Overall, higher concentrations showed strong and more solid gels with fracture properties of a brittle gel, but at low concentration appeared creamy (Schierbaum et al., 1992; Loret et al., 2004a; Loret et al., 2004b). Other factors of gel preparation, such as dispersion temperature, gelling temperature, and gelling time also impacted gel formation and these will be discussed below.

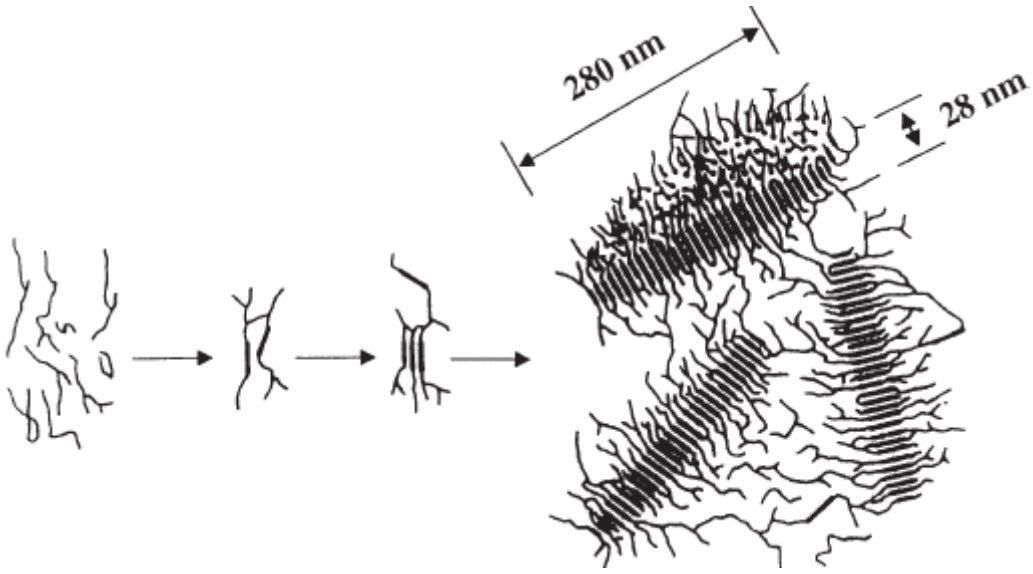

Figure 2.3. Visual representation of maltodextrin gelation through double helix association, aggregation of double helix into crystalline regions, and connection of crystalline regions by long chains (reproduced from Chronakis 1998).

Table 2.1. Parameters of critical gelling factors for maltodextrins reported in the literature

Critical Gelling Concentration (C*)	Temperature	Maltodextrin Type	Authors
17%	Below 50 °C	Avebe Paselli SA-2, DE 2 potato MD	Loret et al 2004
20% (30% for brittle gels)	20 °C	DE 5-8 MD	Bulpin et al. 1984
15% (25% for brittle gels)	10 °C	Avebe Paselli SA-2, DE 2 potato MD	Loret et al. 2004
10%	30 °C	DE 6 potato MD	Schierbaum et al. 1990
15%	20 °C	Avebe Paselli SA-2, DE 2 potato MD	Kasapis et al. 1993b
25%	20 °C	Avebe Paselli SA-6, DE 6 potato MD	Kasapis et al. 1993b

2.4.2.1. Influences of dissolution process

To form a gel, maltodextrin powders are typically hydrated in hot water and cooled for a specified time and temperature. The process of heating maltodextrin dispersions is critical in gel formation to fully hydrate the polymer chains. Insufficient heating leaves regions of dispersed crystalline material, and this decreases the effective solution concentration and even has had a seeding effect that quickened gelation (Chronakis and Kasapis, 1995). When completely dissolved (heating to 95 °C) and then cooled, the gel formed a continuous aggregate network, with a sharp, peak fracture (Chronakis and Kasapis, 1995; Loret et al., 2004a). However, heating below 85 °C and then cooling produced gels that had not

completely dissolved (25% undissolved at 75 °C by optical rotation) and above 100 °C showed signs of degradation; both extremes produced weaker gels (Chronakis and Kasapis, 1995; Loret et al., 2004a). Thus, variability in thermal treatments which do not fully dissolve the maltodextrin may be responsible for batch-to-batch variation in gel physical properties which have been observed (Chronakis and Kasapis, 1995). Additionally, the presence of nucleation sites from non-hydrated polymer has also been shown to impact gelation kinetics (Loret et al., 2004b).

2.4.2.2. Influences of gel setting method

The holding temperature of a maltodextrin dispersion after cooling impacted the kinetics of aggregation, gelation, and the resulting microstructure. Both higher concentration and lower holding temperature increased the rate of aggregation and gelling, and the lowest temperatures formed the most solid gels (Schierbaum et al., 1992). Even after raising a gel to a higher temperature, there was evidence of initial structuring (as evidenced by a difference between gels with identical ending temperature but different initial holding temperature), although this trend did not hold true for concentrations less than 25% (Schierbaum et al., 1992). Other studies have found that cooling rate and gel temperature impacted gel kinetics, but had a minimal impact on final gel strength (Loret et al., 2004a; Loret et al., 2004b). However, it is likely the range of temperatures examined (only up to 40 °C) and short time length (only up to 27 hours) reduced the potential for detecting differences. Expansion of the range of temperatures or gelation time would allow for a better understanding of kinetics and reversibility of maltodextrin gelation.

Crystallization theory states that high temperatures favour thermodynamic control of the structure formation, while at low temperatures kinetics control the structure (Zhang and Zhou, 2016). For maltodextrin, the mechanisms of gelation and crystallization are competing, and have been demonstrated to depend on cooling time and temperature (Schierbaum et al., 1992; Loret et al., 2004b). At high holding temperatures, crystallization was favoured and cloudiness was observed without formation of a gel (Loret et al., 2004a). At cooler temperatures, a stronger gel is formed than by holding at a higher temperature (Schierbaum et al., 1992). With application of crystallization theory to maltodextrin, higher temperatures seem to favour the growth of crystals with slower gelation, while cooler temperatures favour initiation of new junction points and quicker gelation. Presumably, other factors which influence gelation speed, such as concentration and chain physical chemistry, would also impact the gelation mechanism and structure formation.

2.4.3. MD mixed gels

Low DE MD has been studied in many mixed gel systems with common hydrocolloids (Table 2.2). Most researchers have reported a phase separated structure with the exception of LA gellan gum (which was thought to be an interpenetrating network, IPN). The mixed gel with gelatin has been the most widely examined because of its proposed use as a fat replacement in food products (Chronakis, 1998). The phased separated structure with gelatin has been well characterized (Kasapis et al., 1993a; Kasapis et al., 1993c; Brown et al., 1995; Lundin et al., 2000; Lorén and Hermansson, 2000; Normand et al., 2001; Butler and Heppenstall-Butler, 2003; Nickerson et al., 2006). At concentrations with a microstructure above 50% of the phase volume, MD formed the continuous phase polymer (Norton and

Frith, 2001). The polymer comprising the continuous phase vs. dispersed phase switched at the critical points of approximately 10% (w/w) DE 2 MD and 5% (w/w) gelatin up to 15% (w/w) DE 2 MD and 10% (w/w) gelatin (Norton and Frith, 2001). Properties such as cooling rates, salt content, and concentration ratios were all thought to impact the equilibrium.

Unlike a typical phase separated structure, MD is additionally thought to self-separate (or fractionate) into regions of large and small sized chains (Kasapis et al., 1993d; Loret et al., 2005). Within a mixture of agarose and MD, a higher proportion of the small MW fraction was in the same phase as agarose while the large MW fraction was in a separate phase (Loret et al., 2005). A similar behaviour was reported with gelatin (Kasapis et al., 1993d). This polydisperse nature adds complexity to defining and describing the functionality of MD.

Table 2.2. Summary of reported network type using a low DE maltodextrin at or greater than a 10% w/w concentration and above the critical gelation point of the 2nd polymer.

2nd polymer	**Network type**	**Authors**
Gelatin	Phase Separated	(Kasapis et al., 1993a; Lorén et al., 1999)
Pectin (low methoxyl)	Phase Separated	(Picout et al., 2000b)
Agarose	Phase Separated	(Loret et al., 2006b)
iota-carrageenan	Phase Separated	(Wang and Ziegler, 2009)
Locust bean gum	Phase Separated	(Annable et al., 1994)
Gum acacia	Phase Separated	(Annable et al., 1994)
Carboxymethyl cellulose	Phase Separated (high salt)	(Annable et al., 1994)
LA Gellan	IPN	(Clark et al., 1999)

2.5. Gellan gum

2.5.1. Gellan gum structure

Gellan is a polysaccharide hydrocolloid produced by the bacteria *Sphingomonas elodea* (ATCC 31461) and approved for food use in the European Union, USA, and many other countries (Sworn, 2009). Two forms are generally commercially available: the native or high acyl (HA) and the low acyl (LA) gellan. Figure 2.4 shows the chemical structure of high and low acyl gellan gum. The structure of HA gellan gum is a four-sugar repeating unit with one carboxylic acid and glycerate present in every repeating unit and an acetate every other repeating unit (Sworn, 2009; Morris et al., 2012). When quantified, the native gellan HA Kelcogel LT100 had glycerate groups on 90% of the tetrasaccharide units and acetate on 40% of the units (Kasapis et al., 1999). To produce the LA variant, acyl groups are removed from the native form using an alkaline environment (Sworn, 2009). The HA gellan polymers have a MW between 4.2 and 10 x 10^5 Da (Kang et al., 2017; Shinsho et al., 2020). It has been proposed that this range is from the aggregates of 2-10 gellan gum chains together (Shinsho et al., 2020). Commercially available gellan has salt concentrations in the range 2-4% potassium, 0.4-3.0% sodium, 0.1-0.3% calcium, and 0.1-0.2% magnesium (Miyoshi et al., 1998; Picone and Cunha, 2011; Vilela and Cunha, 2016).

Within the food industry the LA gellan is more frequently used with applications for thickening and gelation in jellies, confectionery, and dairy (Sworn, 2009). Pharmaceutical industries have also taken interest in gellan gum for applications in controlled release and wound healing (Stevens et al., 2016; Palumbo et al., 2020). The different structures of HA

and LA gellan yield completely different organization and gel textures and thus are key to controlling functionality for industrial use.

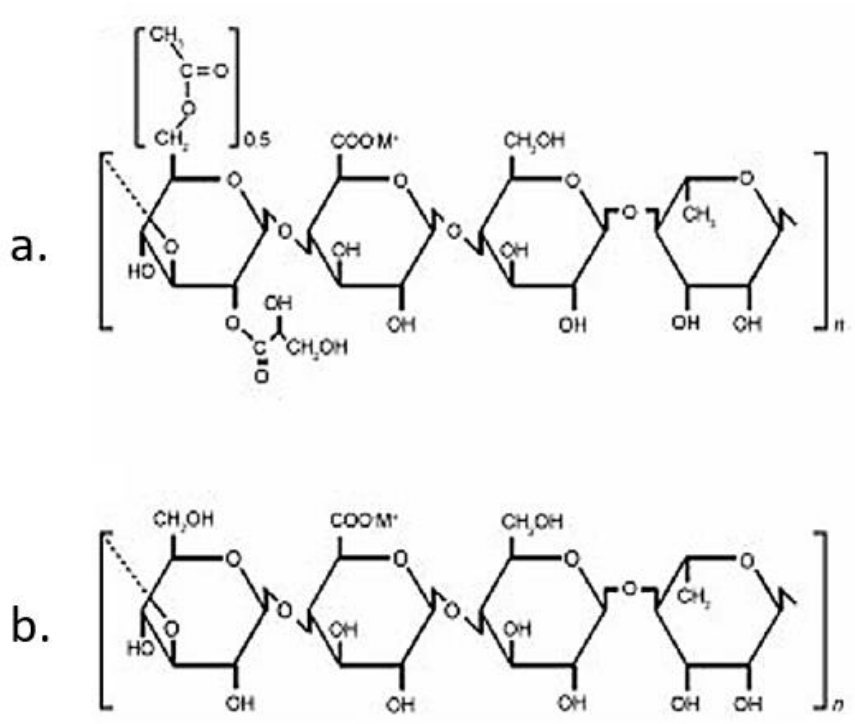

Figure 2.4. Molecular structure of (A) HA and (B) LA gellan gum adapted from Sworn (2009).

2.5.2. High acyl gellan gelation

HA gellan produces a soft and flexible gel formed by a fibrous network of double helices (Sworn, 2009). The gel network is formed by dispersing and hydrating powdered gellan in hot water (80-90 °C) and set by a coil-helix transition occurring upon cooling. Molecules in the random coil state undergo a coil-helix transition and form double helix structures by association of the two carbohydrate chains. Double helices are oriented with glyceryl groups located on the inside of the helix and the acetyl groups facing outward (Morris et al., 1996). A gel network based on a fibrous model is formed by these helices connected through branching and end-to-end associations as shown in Figure 2.5 a (Noda et al., 2008; Funami et al., 2008). The elasticity and extendibility of the gel suggests an incomplete conversion of

chains to a helical structure (Clark, 1991). Glyceryl groups increase helix stability by forming hydrogen bonds between chains (Morris et al., 1996; Morris et al., 2012) and hydrophobic interactions (Yang et al., 2019). The acetyl groups inhibit chain aggregation (Morris et al., 1996; Kasapis et al., 1999).

Critical aggregation concentrations can be as low as 0.05% (Yang et al., 2019) and critical gelation concentrations around 0.2% (Sworn, 2009; Tako et al., 2009). The fibrous network structure and small junction zones explain the soft and easily deformable gel of HA gellan. Sol-gel transition temperatures for melting and gelling are 50 °C without the presence of salts (Noda et al., 2008) and between 65 - 80 °C with increasing salt contents (Mazen et al., 1999; Kasapis et al., 1999; Huang et al., 2004; Noda et al., 2008; Flores-Huicochea et al., 2013). Heating and cooling thermograms showed a small hysteresis (0 to 5 °C) and a wide peak width (40 – 75 °C) suggesting minimal cooperation between chains which is consistent with the absence of chain aggregation (Morris et al., 1996; Mazen et al., 1999; Morris et al., 2012). The removal of acyl groups changes the mechanism of helix formation and aggregation forming very different gel properties in the LA gellan gum.

Although similar in structure and charge, the acetyl and glyceryl groups on HA gellan gum yield a greater hydrophobic behaviour (Tako et al., 2009; Cassanelli et al., 2018a; Yang et al., 2019). Hydrophobic interactions were suggested to contribute to chain associations (Tako et al., 2009). A lower water binding affinity was measured for HA gellan with a contact angle of greater than 90° (Cassanelli et al., 2018a). Yang et al. (2019) have suggested the HA gellan solution is micro-phase-separated in water while Shinsho et al. (2020) proposed these were aggregates (a result of freeze-drying during manufacturing) which had not been sufficiently

dispersed during preparation. Hydrophobic behaviour of HA gellan gum has not been fully explored, but the current literature would suggest it should be considered in characterization.

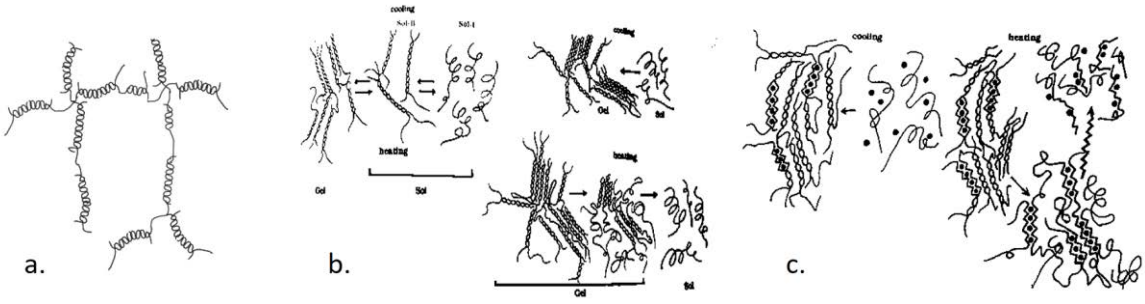

Figure 2.5. Schematic models of gelation for (a) HA gellan, (b) LA gellan with monovalent cations, and (c) LA gellan with divalent cations (Noda et al., 2008 and Miyoshi and Nishinari, 1999).

2.5.3. Low acyl gellan gelation

Gels formed of LA gellan are firm (high modulus) and brittle, in stark contrast to the HA variant (Sworn, 2009; Morris et al., 2012). The absence of acyl groups allows the helices to aggregate into ordered junction zones with the presence of monovalent or divalent cations as shown in Figure 2.5b and 2.5c, respectively (Gunning and Morris, 1990; Miyoshi and Nishinari, 1999; Morris et al., 2012). The lack of acetyl groups allows the aggregation of helices and the removal of glyceryl group means a tighter packing of the chains and less stable helix structure (lower melting point) (Morris et al., 1996). A thermal transition occurs around 30-40 °C from melting of the non-aggregated helices and another much higher (110 °C or greater) for the aggregated helices and both are salt dependant (Miyoshi and Nishinari, 1999; Morris et al., 2012). Monovalent ions complex with one carboxylic groups and assist in chain aggregation by inhibiting electrostatic repulsion (Morris et al., 1996;

Morris et al., 2012). Divalent ions bridge carboxylic groups on adjacent aggregates forming the more stable junction zones in a similar mechanism to the alginate (Morris et al., 1996; Morris et al., 2012). Aggregation of chains is also indicated by the thermal hysteresis between melting and gelling temperatures (Morris et al., 2012).

2.5.4. Functionality of gellan gum

Usage of the LA gellan gum variant is more common than the HA gellan (Morris et al., 2012). Both polymers contain carboxyl groups which conveys some similar functionality. However, the deacylation process removes most of the bulky acyl groups and changes the gel structure and material properties (Morris et al., 2012). When used together, the LA gellan and HA gellan form a phase separated mixed gel with completely separate gel networks (Kasapis et al., 1999). Characterization of mixtures with other gelling agents have predominantly focused on LA gellan gum. An IPN was proposed with maltodextrin (Clark et al., 1999) and agarose (Amici et al., 2000), while a phase separated structure was measured with kappa-carrageenan (Nishinari et al., 1996a) or gelatin (Lau et al., 2000). For HA gellan gum, the non-gelling polymers of chitosan fibres (Liu et al., 2013) and soybean fibre (Chen et al., 2020) were proposed to arrange within the pores but characterization of the network type was not the focus of the work. Behaviour of HA gellan with other polymers still needs to be examined.

Both gellan gums swell upon submersion into water if the osmotic environment is appropriate. Submersion of LA gellan gum in DI water resulted in an increased volume of 19-30% (Nitta et al., 2006; Hossain and Nishinari, 2009). Swelling of a freeze dried HA gellan gum gel increased by 192% (Cassanelli et al., 2018a). A summary of reported swelling ratios

of HA gellan is summarized in Table 2.3. Due to the osmotic driven swelling, in high salt solutions the swelling decreases for both HA and LA gellan (Annaka et al., 2000). The swelling ratio of LA gellan is much lower, and likely because the crosslink density of LA gellan is too great to allow considerable swelling (Moe et al., 1993). Lower crosslink densities yielded gels with greater swelling capacity (Coutinho et al., 2010). Chemically cross-linked LA gellan gum (which did not contain aggregation regions) yielded much higher swelling of 2,600% (Annaka et al., 2000) and 10 -1,000% (Coutinho et al., 2010). As discussed in section (2.3.2. Swelling of gels), there are different methodologies for measuring the swelling of a hydrogel. Whether the polymer was lyophilized, the time of swelling, and salt content all effect the measurement and these differences make comparing different values for gellan gum difficult (Nitta et al., 2006; Hossain and Nishinari, 2009; Cassanelli et al., 2018a).

Swelling of polymer gels is expected to decrease the modulus because of the lower density of network, unless there are changes to the network such as new bonds (Sakai, 2020). For LA gellan gum submerged in a saline solution, an increased modulus was observed (Nitta et al., 2006; Tanaka and Nishinari, 2007; Hossain and Nishinari, 2009; De Silva et al., 2013; Yu et al., 2017). It was determined that the additional cations from the solution migrated into the gel and caused further chain aggregation (Nitta et al., 2006; Tanaka and Nishinari, 2007; Hossain and Nishinari, 2009; De Silva et al., 2013; Yu et al., 2017). Interestingly, swelling of LA gellan gum in DI water (no additional cations) also led to an initial increase in modulus before dissolution (Nitta et al., 2006; Hossain and Nishinari, 2009). This behaviour was not further examined but was proposed to be caused by a “stiffening of network chains” (Hossain and Nishinari, 2009). High degrees of swelling are thought to no longer follow

Gaussian behaviour because of the extensive stretching of the polymer chains (Skouri et al., 1995; Djabourov et al., 2013).

Table 2.3. Summary of swelling behaviour for HA gellan gum gels. Reported values were either normalized to the freeze dried weight (Q) or the gel weight (q).

Gellan	**Solution**	**Swelling**	**Time**	**Authors**
2%	DI water	q = 1.92	24 hours	(Cassanelli et al., 2018a)
0.2%	DI water	Q = 50	2 hours	(Chen et al., 2020)
1.6%	PBS	Q = 11.5	83 hours	(Liu et al., 2013)
2%	PBS	Q = 83	Up to 170 days	(De Silva et al., 2013)
0.75%	PBS	Q = 50	16 and 175 hours	(Khang et al., 2015)
0.5%	pH 4	Q = 100	30 mins	(de Souza et al., 2021)
	pH 8	Q = 50		
1%	pH 4	Q = 325	30 mins	(de Souza et al., 2021)
	pH 8	Q = 60		
2%	DI water	q = 7.1	14 days	(Kanyuck et al., 2021b)

Chapter 3. Temperature influences on network formation of low DE maltodextrin gels

_____

Published article

Kanyuck, K. M., Mills, T. B., Norton, I. T., & Norton-Welch, A. B

Carbohydrate Polymers. 2019. (218), 170-178.

Abstract

Gelation of maltodextrin (DE 2) was examined over a range of temperatures to understand the behaviour within mixed-gel systems. Maltodextrin solutions were prepared at 95 °C and held at temperatures between 5 °C and 60 °C for four days. Bulk gel properties and the underlying microstructure were analysed using fracture strength, proton relaxation time, and differential scanning calorimetry (DSC). Holding at lower temperatures led to a greater gel strength with a brittle and crumbly texture. Analysis of the microstructure showed that gelation at 10 °C versus 60 °C produced a greater number of aggregates (melting enthalpy 14.5 J/g versus 3.4 J/g) and structuring of a higher melting entropy (45 mJ/g K versus 10 mJ/g K). A thermal hysteresis with signs of structure corresponding to both holding temperatures was also measured. Elevated temperature was hypothesized to decrease the amount of smaller molecular weight chains participating in aggregation by shifting from the helix to coil form.

Author Contributions

Kelsey M. Kanyuck: Conceptualization, Methodology, Formal analysis, Investigation, Writing - original draft.

Tom B. Mills: Supervision, Writing - review & editing.

Abigail B. Norton-Welch: Supervision, Funding acquisition, Writing - review & editing

Ian T. Norton: Supervision, Funding acquisition, Writing - review & editing.

3.1. Introduction

Maltodextrin is a widely used polymer in the food industry for applications including thickening, bulking, and encapsulation (Chronakis, 1998). Gelation of maltodextrin occurs at relatively high concentrations (10 to 20%) through association of double helix chains, with longer chains connecting aggregates to form the continuous network (Reuther et al., 1984; Schierbaum et al., 1990; Loret et al., 2004b). Higher concentrations lead to stronger and more solid gels with fracture properties of a brittle gel, but low concentrations have shown creamy appearances (Schierbaum et al., 1992; Loret et al., 2004a; Loret et al., 2004b). A handful of researchers have studied material properties of single maltodextrin systems and reported properties characteristic of physical gels (Bulpin et al., 1984; Schierbaum et al., 1992; Kasapis et al., 1993b; Loret et al., 2004a; Loret et al., 2004b). When included in a mixed gel system, unique fat-like properties have been observed (Chronakis, 1998). Surrounding this effect, many studies have focused on maltodextrin mixed gels with gelatin (Kasapis et al., 1993a; Kasapis et al., 1993c; Brown et al., 1995; Lundin et al., 2000; Lorén and Hermansson, 2000; Normand et al., 2001; Butler and Heppenstall-Butler, 2003; Nickerson et al., 2006), pectin (Picout et al., 2000b), and agarose (Loret et al., 2006a). Several patents have even been granted utilizing the unique creaminess of maltodextrin-gelatin mixed gel system for reduced fat food products (Cain et al., 1990; Wesdorp et al., 1995). From the findings of both single and mixed systems, gelling temperature and time were highlighted as key parameters in determining the maltodextrin gel properties.

Kinetics of gelation and the resulting microstructure have been impacted by holding time and temperature of the maltodextrin dispersion during gelation. An increasing gel strength (for up to 12 days) after initial formation is typically observed for maltodextrin (Chronakis

and Kasapis, 1995; Loret et al., 2004a). Both higher concentration and lower holding temperature increased the rate of gelation, and the lowest temperatures formed the most solid gels (Schierbaum et al., 1992). Other studies have found that cooling rate and gel temperature impacted the rate of gel formation, but had a minimal impact on final gel strength (Loret et al., 2004a; Loret et al., 2004b). However, it is likely the range of temperatures examined (only up to 40 °C) and short time length (only up to 27 hours) reduced the potential for detecting differences. A general understanding of the initial gelling parameters has been established from these articles, but not yet an analysis of the material properties of an equilibrated gel. Expansion of the range of temperatures or gelation time would allow for a better understanding of network development of maltodextrin gels.

This article will compare maltodextrin network formation at a range of gelling temperatures. Previous articles have noted differences in gelation caused by temperature, however these experiments focused on rates of gelation rather than the equilibrated gel characterization (Schierbaum et al., 1992; Kasapis et al., 1993b; Loret et al., 2004b). A strengthening of up to 14 days has been observed for maltodextrin gels (Chronakis and Kasapis, 1995; Loret et al., 2004a), so the previous work has limited application to a final gel structure. Specifically, the maximum experimental time lengths were 13 hours (Loret et al., 2004b), 40 minutes (Schierbaum et al., 1990), and 7 hours (Kasapis et al., 1993b). These short times have suggested a preliminary understanding but are unable to predict crystallization or structure development on an industry-relevant timescale. This work aims to provide a detailed characterization of the equilibrated microstructure to comprehensively assess how temperature influences network development. Additionally, even within the previously mentioned short time-scales, Schierbaum (1992) reported a

partial thermal irreversibility in maltodextrin gels. Different solid-liquid ratios were observed for gels consistently held at 20 °C than gels previously held at 4 °C or 40 °C, with a bigger differentiation at lower concentrations (time lengths not specified) (Schierbaum et al., 1992). Although a thermal hysteresis has been observed in maltodextrin gels through NMR analysis, the bulk properties were not compared nor fully characterized. It was hypothesized that the process of maltodextrin aggregation can vary in type or quantity of associations and the gelling temperature controls the mechanism and resulting gel properties. This article aims to characterize the differences in microstructure created in each of the temperatures and examine any irreversible effects of temperature on the final network and material properties of maltodextrin gels.

3.2. Materials and methods

3.2.1. Materials

Potato maltodextrin (Paselli SA-2 lot number F3332901) was purchased from Avebe, Netherlands. This maltodextrin has a reported dextrose equivalent (DE) between 2.7-2.9 (Kasapis et al., 1993d; Manoj et al., 1996) and degree of branching 3.7% (Manoj et al., 1996). Loret et al. (2004a) reported a binomial size distribution of molecular weights centred at 10,290 g/mol and 492,000 g/mol, using size exclusion chromatography. The small MW fraction is known to be the degraded amylose-portions of the starch, and the large MW fraction contains the branched amylopectin regions which were not hydrolysed (Bulpin, et al., 1984; Schierbaum, et al., 1990). Longer chains form associations between aggregated regions, while the shorter chains participate in double helix formation (Loret et al., 2004b). The deionized water (DI) used was filtered through a reverse osmosis milli-Q water system.

All materials were used with no further purification and no external preservatives or additives were used in the gel systems.

3.2.2. Preparation of gels

To prepare gels, maltodextrin was slowly dispersed in heated DI water. The mixture was stirred and heated for 4 hours at 95 °C (+/- 3 °C) to ensure full hydration of the maltodextrin, as indicated by a change in color from white to translucent and results from Chronakis and Kasapis (1995). Any water lost during heating was added back by matching the initial and final weights. The hot solution of maltodextrin was poured directly into the sampling holder for each test, and all gelation occurred within that pot. Plastic containers were used for deformation properties, aluminium for DSC, and glass for NMR. Samples were sealed or covered to prevent evaporation. To maintain gelling temperatures, samples were placed in thermostated ovens (at 60 °C, 45 °C, or 38 °C), at room temperature (for 22 °C), or in a refrigerator (at 10 °C or 5 °C). Unless otherwise stated, gels were held at the indicated temperature for 4 days. All samples were equilibrated to room temperature (22 °C) for 2 hours prior to analysis.

3.2.3. Large deformation properties

The gel strength during penetration and fracture was assessed with a texture analyser TA.XT.plus (Stable Micro Systems, UK). This instrument measured the force to move a 6 mm diameter cylindrical probe, with a speed of 2 mm/s, into the gel up to a 50% strain. All gels fractured prior to the set 50% strain value, and most fractured between 5 and 15% compressive strain. Cylindrical gels (with a diameter of 20 mm) were cut into pieces of 20 mm height and compressed from the circular face at the centre of the cross section. Measurements were repeated nine times for each sample.

3.2.4. Differential scanning calorimetry

Gel analysis with differential scanning calorimetry (DSC) was performed using a DSC25 (TA Instruments, USA). Samples were prepared by adding the heated solution to a Tzero hermetic pan (TA Instruments, USA) and allowing gelation to completely occur within the sample pan. Prior to analysis, each pan was equilibrated to room temperature. The DSC heated the samples from 20 °C to 120 °C at 5 °C/min with a matching mass of DI water in the reference chamber. Preliminary experiments showed hysteresis in samples that underwent multiple heating treatments, thus all curves are from the first heating cycle. A baseline was constructed by fitting a linear equation to the heat flow before and after the observed peak, and data is reported as the observed signal with a baseline subtraction. The onset temperature was reported as the point of deviation from the baseline, while peak temperature was calculated at the maximum heat flow. Changes in enthalpy (ΔH) during transitions were determined by integration of the area below the baseline. Changes in entropy (ΔS) were determined utilizing the Gibbs Free Energy equation ($\Delta G = \Delta H - T\Delta S$). Since ΔG is known to be zero at the midpoint of the transition, the change in entropy was calculated through the rearrangement of the equation to $\Delta S = \Delta H/T_{midpoint}$ (Cassanelli et al., 2018b). A ΔG was calculated by substituting the calculated ΔH, ΔS, $T_{gelling}$ into the Gibbs equation.

3.2.5. NMR analysis

Relaxation times (T_2) and rates ($1/T_2$) were measured on a mq20 minispec NMR instrument (Bruker, USA). This instrument operates with a set frequency of 20 mHz. A H20-10-25 AVGX probe and water bath were used to maintain a constant sample temperature of 25 ± 1 °C. A CPMG pulse sequence was used with a pulse separation (tau) of 0.25 ms, 3 dummy echoes,

and collection of 615 ms long. Gelation occurred in 8 x 45 mm glass insert tubes (Bruker, USA) covered by cling film. Prior to analysis, all tubes were brought to room temperature (22 °C) before addition to the bottom of a larger 10 mm glass tube (Bruker, USA) and then equilibrated to 25 °C in a heating block.

The relaxation time (T_2) was calculated as the exponent for the decay function, and the relaxation rate was determined by inversing the calculated relaxation time. A manual baseline subtraction was performed prior to fitting the curve. Analysis of the free induction decay suggested solid state signal was present up to 5 ms after the initial pulse, so the exponential function was fitted to the data points from 9 ms to the baseline (400 ms). Each decay function was modelled with a mono-exponential and a bi-exponential decay function and the mean sum of squares of the error was compared using SigmaPlot 12.5 (SYSTAT Software, USA). When the ratio for the bi-exponential function was greater than 5, the more complex function was considered to be a significantly better fit, and two relaxation times were reported. Relaxation curves were also visually assessed for bent appearances to confirm practical differences between relaxation rates determined through the statistical model.

3.2.6. Transmission electron microscopy

Images were obtained on a JEOL JEM-1400 (Tokyo, Japan) transmission electron microscope (TEM). Gels were fixed by placing small pieces in 2.5% aqueous glutaraldehyde for 24 hours followed by 1% osmium tetroxide for 1 hour. Next, samples were dehydrated by two subsequent 15 minute washes in each of 50%, 70%, 90%, 100% alcohol, and propylene oxide. Samples were embedded first in 50% Propylene Oxide / 50% Resin followed by 100% resin and polymerise resin at 60 °C. Thin sections were prepared initially using a microtome

and secondly a diamond knife for sections of 50-150 nm. Sections were collected onto Formvar/carbon grids and stained with uranyl acetate.

3.2.7. Statistical analysis

All measurements were completed in at least triplicate and averages are reported with the single standard deviation. Figures depict the calculated average with error bars showing the standard deviation above and below the average. Comparison of means were conducted by ANOVA analysis followed by an all pairwise multiple comparison test using the Student-Newman-Keuls Method (SigmaPlot 12.5) and significant differences ($p < 0.05$) are shown by unique lettering. Multiple linear regression (MLR) (SigmaPlot 12.5) was used to model individual data points of ΔG, while only the average and standard deviations are shown in Figure 3.5.

3.3. Results and discussion

In this article, maltodextrin gels were evaluated on the bulk level (through large deformation material properties), the molecular level (through DSC and NMR), and the microstructure visualized with TEM. Initially, the impacts of maltodextrin concentration and gelation temperature were evaluated, and subsequently the combination of multiple holding temperatures over various time segments was utilized to study the thermo-reversibility of the network.

3.3.1. Concentration of maltodextrin

As is expected with hydrocolloids, an increase in maltodextrin concentration produced gels with an increased gel strength (Figure 3.1). At 10% maltodextrin (a ratio of 0.11 of solids to water), a gel did not form within 4 days at 5, 20, or 60 °C, and the solution remained translucent with some sedimentation. At concentrations of 15% and above (a ratio of 0.18

of solids to water), a white gel formed at 5 and 20 °C. At 40% and higher, the gel was firm and crumbly, while 30% and below displayed characteristics of a weak gel. The concentration of polymer in solution clearly dictated the extent of gelation that occurred. Gelation of polymers occurs through association and junction formation between chains, for creation of one continuous network. For maltodextrin, the mechanism of this network formation occurs through two steps: (1) helical association of two strands and (2) aggregation of the double helices into crystalized regions, with longer chains connecting helix aggregates together in a gel (Reuther et al., 1984; Schierbaum et al., 1990; Loret et al., 2004b). The crystallization point (as distinguished from the gel point) has been defined as the association between two double- helix chains (4 total chains, with 3 association points) (Schierbaum et al., 1990; Loret et al., 2004b). Whereas an increase in viscosity is associated with the formation of 3D structure, cloudiness of gels is attributed to crystallization of the polymer (Loret et al., 2004b). Both processes are needed during gel formation to create the necessary structures of a continuous network (Loret et al., 2004a). The sedimentation observed in the 10% maltodextrin sample is likely a case of crystallization occurring without gelation. Enough molecules must be present to form helices and begin aggregation, but not enough long chains existed to form a self-supporting network. From 15% and above, chains formed a network with an increasing number of connections and strength. This critical concentration for gelation is higher than most hydrocolloids and is likely due to a high proportion of short or highly branched chains which do not participate in gelation. The relationship between concentration and peak force did not appear to be linear, but instead resembled a second order polynomial (Figure 3.1), as is commonly observed with biopolymers. Similarly, the storage modulus (G') of maltodextrin has typically been

modelled to a non-linear cascade equation (Kasapis et al., 1993b; Manoj et al., 1996; Chronakis et al., 1996). The relaxation rate (as determined by NMR) of these gels also followed a similar non- linear trend. Relaxation rates are a measure of the microscopic mobility of water, and the correlation between viscosity and relaxation rates has often been observed (German et al., 1989). Both the gel strength and water mobility suggested that after initial formation of a connecting network, strengthening continued with more polymer (likely through aggregation onto the existing network). Concentration of maltodextrin was shown to be an important factor in gel properties, and the next section will discuss the influence of gelling temperatures.

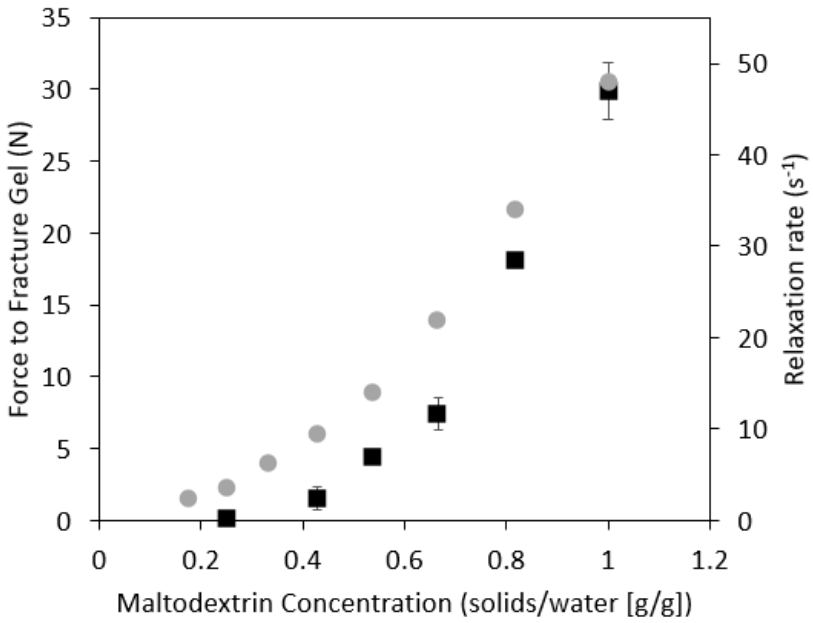

Figure 3.1. Comparison of the impact of concentration on force to fracture a gel [N] (■) and relaxation rate [s-1] (●) of maltodextrin gels. Error bars represent the average of at least 3 replicates. The force required to fracture a gel was determined by compression and is represented by the average (and standard deviation by error bars) of nine measurements. Determined using NMR, relaxation rate is the exponent for a mono-exponential T_2 decay using the CPMG pulse sequence.

3.3.2. Temperature influence on gelation

To determine the equilibrium point of gelation, gel strengthening was measured over 14 days at three temperatures. The gel strength increased over the 14 day time range for each of the temperatures (Figure 3.2). At each time point, the gels formed at 10 °C were significantly stronger than gels at 60 °C and after two days were stronger than the gels at 22 °C. At room temperature, this trend of strengthening (up to 12 days) for a maltodextrin gel has also been reported by Loret et al. (2004). All three temperatures appeared to reach a practical equilibrium between 4 and 7 days, where the change between days was less than 5 percent. To determine an experimental time point, the curves were fit to a logarithmic function. At four days, there was a change of less than 5% from the previous day (the defined practical equilibrium) and a length of four days was chosen for all future analysis unless otherwise noted. The equilibration observed at each temperature also suggested that temperature impacts the resulting aggregate structure, not just the kinetics of gel formation. After seven days, gels at each of the temperatures have mostly levelled off, without signs of increasing further (Figure 3.2). This indicates that temperature created a trapped kinetic state of aggregation and structuring. Next, the effect of temperature on gelation was directly compared using various concentrations of maltodextrin, and all were analysed at four days.

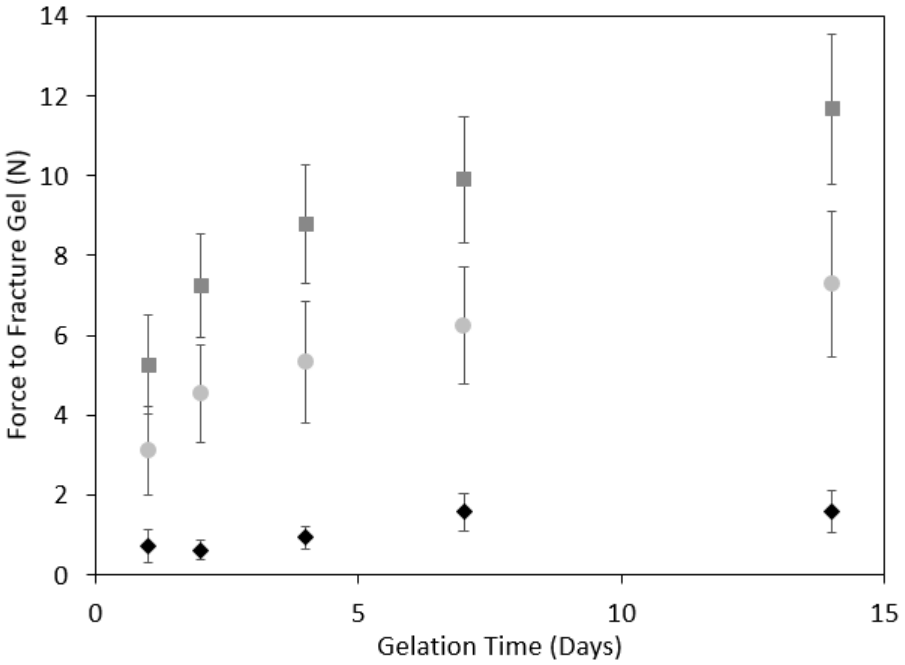

Figure 3.2. Influence of gelling time and temperature on strength of a 40% maltodextrin gel, after holding at the specified temperature (10 °C ■; 22 °C ●; 60 °C ◆) for the duration of gelation. The force required to fracture a gel was determined by compression and is represented by the average (and standard deviation by error bars) of nine measurement. All measurements took place at room temperature (22 °C) and samples were equilibrated for two hours before analysis.

3.3.2.1 Temperature influence on fracture and bulk properties

Gelation at elevated temperatures produced significantly different gel strengths, textures, and microstructures. At higher temperatures, gelation appeared slower and led to weaker gels, which was consistent at concentrations of 30%, 40%, and 50% (Figure 3.3). For all concentrations, gelation at 60 °C resulted in a significantly lower gel strength than gelation at 22 °C, 10 °C, or 5 °C. In addition to strength, gels formed at higher temperatures (45 °C and 60 °C) were paste-like, while gels formed at lower temperatures (5 °C and 10 °C) were brittle and crumbly (image inserts in Figure 3.3 which represent the material after fracture). The strain to fracture the gels were very similar (7-8% for 10 °C but 9-10% for 60 °C) while the mechanisms following fracture demonstrated differences in gel behaviour. The brittle

gels broke into pieces and fell away upon fracture (exhibiting a sharp drop in the distance vs. force diagram), while the paste-like gels retained cohesive forces and maintained contact with the probe. Temperature dependence is common for materials measured over a range of temperatures, so all measurements were performed at room temperature and after thermal equilibration, such that variability was reflective only of structural differences. The effect of temperature at the selected concentrations was even shown to be as impactful as concentration. Extremes in the gelling temperature, for the 40% maltodextrin, caused a shift in fracture force from 15 N to 1.7 N (at 5 °C and 60°C respectively). The following comparisons (Figure 3.3) further highlight the importance of gelling temperature: a 30% solution held at 10 °C formed a stronger gel then 40% held at 60 °C (2.5 N vs. 1.7 N), and a 40% solution held at 5 °C was stronger than a 50% gel formed at 60 °C (15 N vs. 11 N). These differences in bulk properties presumably originate from different types or extents of network structure, and thus the development of maltodextrin microstructure is temperature dependent. Further tests examined the underlying microstructure to explain these differences.

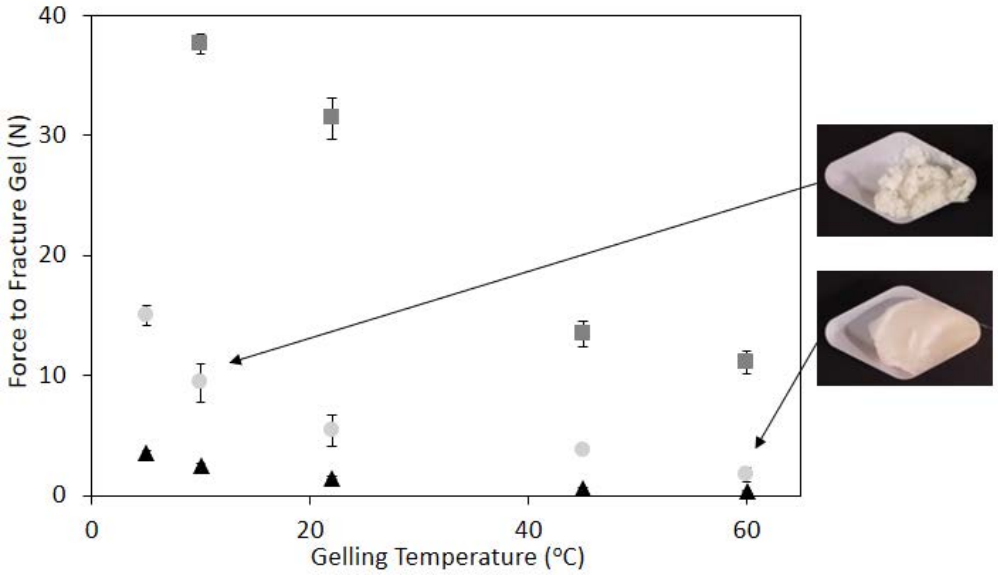

Figure 3.3. Influence of gelation temperature on gel strength for three concentration levels (50% ■; 40% ●; 30% ▲) of maltodextrin, after holding at the selected temperature for 4 days. Error bars represent the average of at least 3 replicates. The force required to fracture a gel was determined by compression and is represented by the average (and standard deviation by error bars) of nine measurement. All measurements took place at room temperature (22 °C) and samples were equilibrated for two hours before analysis. Image insets display the texture observed after fracture of 40% maltodextrin held at 10 °C and 60 °C.

3.3.2.2 Temperature influence on water distribution within network

Water mobility within each of the gels was measured through the determination of NMR relaxation rates (the inverse of the relaxation time, T_2). For concentrations of 30% and 40% maltodextrin, there was an observed increase in relaxation rate for structures formed at lower temperatures (Table 3.1). For each concentration, the sample preparation and measurement temperature of these gels are identical, and thus the changing relaxation rate is clearly an indication of differing microstructures created at the holding temperatures. The faster relaxation rates observed in the samples held at lower temperatures are indicative of less mobile protons. Within gels, faster relaxation rates suggest a stronger and more gelled polymer network with smaller sizes of water pockets (Lillford et al., 1980; Lillford, 1988).

This trend is consistent with the greater fracture force (Section 3.3.2.1) and greater enthalpy (Section 3.3.2.3) measured for gels held at lower gelling temperatures. Previous utilization of H-NMR to assess maltodextrin gels also observed a more solid gel at 4 °C than 25 °C for a DE 6 maltodextrin (Schierbaum et al., 1992). However, these experiments preformed measurements at the gelling temperature and thus could not separate the effect of temperature on sample structuring from the holding temperature (Schierbaum et al., 1992). For the current experiments, all measurements took place at 25 °C and thus are true reflections of differences in the aggregate structure. At a concentration of 50%, only gelation at 60 °C produced a different relaxation rate from the other temperatures, which is probably due to the high solid and low water content. The 50% solid content is approaching the predicted saturation of 71% from the non-freezable water content of 0.4g per 1g of maltodextrin (Radosta and Schierbaum, 1990). As the measured relaxation rate is a weighted average of protons, the high proportion of the bound water appears to be dominating the proton relaxation behaviour.

A few gels exhibited a bi-exponential decay which resulted in two reported relaxation rates. At the temperature extremes (5 °C and 60 °C) two relaxation rates were observed in the 40% sample (at 25.1 s^{-1} and 6.6 s^{-1} for 5 °C and 16.7 s^{-1} and 50.9 for s^{-1} for the 60 °C sample) (Table 3.1). Two relaxation rates are consistent with a heterogeneous distribution within the gel, and likely from micro-scale syneresis or aggregation of polymer (Lillford et al., 1980). In each case, the rate comprising a majority of the signal follows the expected trend set by the other temperatures, while the second rates fall above and below. The slowest predominant relaxation rate (measured for the sample from 60 °C) also had a minority percentage of

very-fast relaxing protons, while the fastest predominant rate had a small proportion of very-slow relaxing protons.

These should be reflective of the proton environment of the micro-heterogeneities formed at these extremes. The slow rate (6.6 s^{-1}) is closer to that of pure water and is probably the result of the presence of protons within comparatively large water pockets in the 5 °C sample. Alternatively, the fast relaxation rate (50.9 s^{-1}) of the 60 °C sample originates from a portion of the gel with fast-relaxing protons. It may have been caused by either water molecules within a highly-structured crystalline-like material or polymer protons still in solution, but further NMR analysis would be necessary to confirm the identity. Based on the entropy of the structures, which will be discussed next, the fast relaxation rate present at 60 °C is hypothesized to be from a crystalline-like formation. Consistent with the 40% concentration, the 50% sample held at 60 °C also showed a heterogeneous water distribution. The aggregation structures of maltodextrin were shown to vary with temperature, with micro-heterogeneities observed at both temperature extremes.

Table 3.1. Measured relaxation rates at 25 °C for 30 %, 40%, and 50% maltodextrin gels, after holding at the indicated temperature for 4 days.

Maltodextrin Concentration	Gelation Temperature (4 days)	$1/T_2$ (1st) Relaxation Rate (s^{-1})	$1/T_2$ (1st) Amplitude %	$1/T_2$ (2nd) Relaxation Rate (s^{-1})	$1/T_2$ (2nd) Amplitude %
50 %	60 °C	51.9 ± 5.4	82 %	37.0 ± 2.3	18 %
	45 °C	44.3 ± 0.3	100 %		
	22 °C	45.1 ± 0.5	100 %		
	10 °C	45.3 ± 0.9	100 %		
	5 °C	44.9 ± 0.0	100 %		
40 %	60 °C	16.7 ± 0.7	83 %	50.9 ± 3.3	17 %
	45 °C	16.6 ± 0.2	100 %		
	22 °C	20.6 ± 0.3	100 %		
	10 °C	22.3 ± 0.1	100 %		
	5 °C	25.1 ± 0.1	98 %	6.6 ± 0.5	2 %
30 %	60 °C	7.2 ± 0.5	100 %		
	45 °C	7.7 ± 0.3	100 %		
	22 °C	10.5 ± 0.5	100 %		
	10 °C	12.0 ± 0.5	100 %		

3.3.2.3 Temperature influence on aggregation enthalpy, entropy, and free energy

Impact of temperature on the energy and amount of bonds was explored further with DSC analysis. Due to time limitations, only the concentrations of 30% and 40% were analysed. Melting curves of maltodextrin gels set at five temperatures are compared in Figure 3.4 with calculations of melting temperatures, enthalpy, entropy, and free energy changes compiled in Table 3.2**.** The curves from 30% and 40% were similar in appearance so only the 40% MD data is shown for simplicity. High variability was seen in the enthalpy of the 60° samples but with a similar peak temperature; individual curves are displayed so the similarity can be seen. Onset melting temperatures of the networks ranged from 33° to 76° C at a

concentration of 40% maltodextrin. Within this temperature range**,** Reuther et al. (1984) confirmed the presence of type-B crystallinity in maltodextrin gels with a melting onset at 56 °C after holding at room temperature (Reuther et al., 1983). From the DSC curves (Figure 3.4), energies of network formation were examined to determine the mechanism of ordering. Aggregation of maltodextrin chains occurs through hydrogen bonds, and both the enthalpy and entropy of the network were affected by the holding temperature. The higher enthalpy changes (ΔH) measured at lower holding temperatures indicated a greater amount of hydrogen bonds, through more extensive helix formation and aggregation. The lowest enthalpy was observed at high holding temperatures, which was also consistent with the results of a lower gel strength and slower relaxation rates. Although more bonds were formed at low gelling temperatures, a higher melt point was observed in gels formed at higher temperatures. The onset melting temperature was always higher than the temperature used to form the network. Independently, the enthalpy change cannot describe the size of aggregates, but calculation of the entropy leads to an understanding of the size. The shift in melting temperature is a reflection of the increased entropy (ΔS) of the structure, as calculated by the Gibbs Free Energy balance equation ($\Delta G = \Delta H - T\Delta S$) (Cassanelli et al., 2018b). Lower entropy structures are reflective of larger aggregate regions with greater compactness and chain lengths. Alternatively, the higher entropy structures formed at low temperatures indicate a more amorphous network with smaller aggregates. DSC analysis allows for the general interpretation that the network formed at high temperature was characterized by higher entropy structures with fewer aggregates, while the low gelling temperature produced a greater number of helices but within less ordered domains.

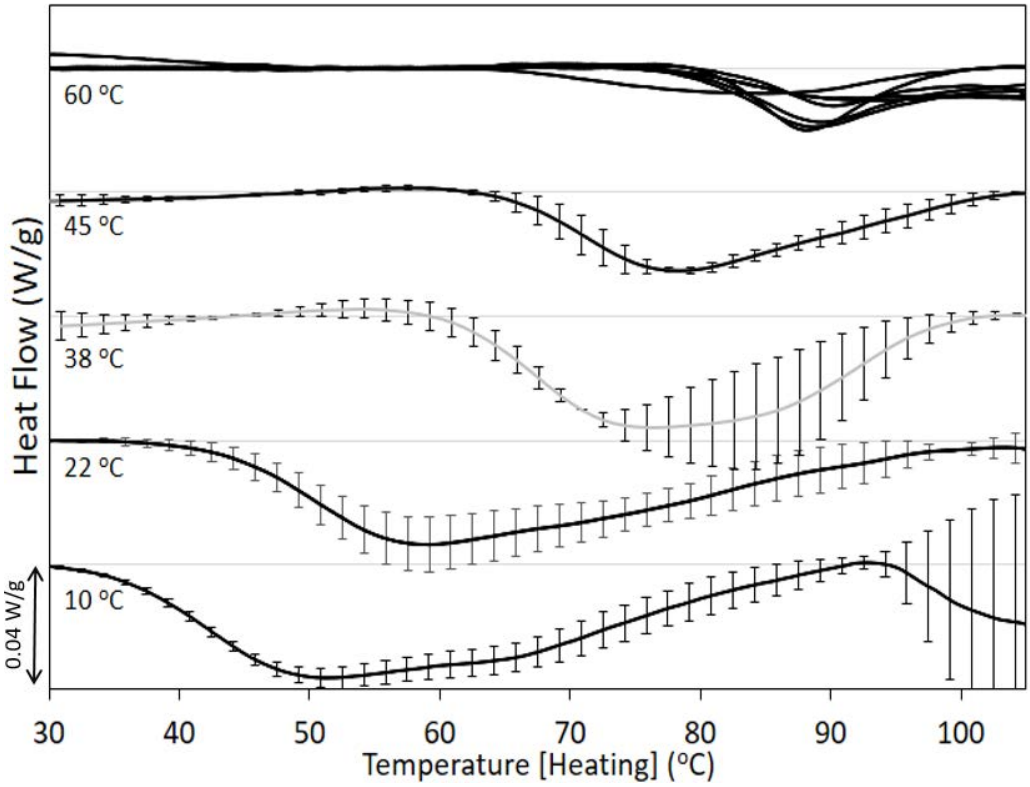

Figure 3.4. Melting DSC endotherm of 40% maltodextrin gels set for four days at the indicated temperature. A heating rate of 5 °C/min was utilized with a reference cell of water. Error bars represent the standard deviation of three replicates. Individual curves for 60 °C are shown so that the curve shape can be seen even with the high variation in enthalpy.

For comparison of structures of differing entropy and enthalpy, the total energy associated with the networks were compared by calculation of Gibbs Free Energy (ΔG) at each gelling temperature. The relationship between changes in free energy of melting and holding temperature are plotted in Figure 3.5. A multiple linear regression (MLR) model was fitted using parameters of temperature (in °C) and concentration (as a percent) yielding the equation $\Delta G = 1.31 - 0.034*\text{Temperature} + 0.023*\text{Concentration}$ with an R^2 of 0.87. The calculated free energy changes are overlaid with the MLR fit for concentration of 40% (●) and 30 % (▲) in Figure 3.5. Extending protein folding-unfolding theory to maltodextrin gelation suggests the zero-intercepts of the free energy represent the chemical equilibrium

between aggregation and remaining in solution (Santoro and Bolen, 1992). Extrapolation to a zero free energy value resulted in critical aggregation temperatures of 66 °C and 59 °C for 40% and 30% respectively. At 60 °C, no gel network was detectable by DSC for the 30% maltodextrin sample. The zero enthalpy temperature of 30% falls below 60 °C, and as would be predicted, no bonds were detectable in these samples. High variability seen in replicates of Figure 3.4 for 60 °C further suggested these bonds are likely near the critical temperature for formation of helix and aggregates so the number in each replicate is highly variable. These critical temperatures represent the chemical equilibrium shifting from ordered and aggregated chains to non-aggregated random coils. At low temperatures, the enthalpy of helix formation leads to the most network development and the greatest energy potential. Increasing temperature progressively favors the increasing energy contribution from entropy of polymers within the random coil form. This trend is not expected to hold below the temperature of 0 °C due to the complexity of water freezing in competition with chain aggregation.

Compared to the sharp peaks typical of many melting hydrocolloids, the thermograms of maltodextrin showed the gels melted over a relatively wide temperature range. The most notable range was observed at the low gelling temperatures, with the gel formed at 10 °C melting from 30 °C to 90 °C (Figure 3.4). A wide melting peak is also consistent with previous DSC analysis of maltodextrin gels (Schierbaum et al., 1992). The broad melting temperature range, indicative of heterogeneity in structure, is consistent with the gelation mechanism of aggregation and the wide dispersion of chain lengths of a maltodextrin product. Chain length variability and differences in ordering mechanisms are then the likely cause of this

wide range. This range is likely also a factor in the observed difference in aggregation at each of the temperatures.

The progressive increase in melting temperature (and subsequent decreasing of entropy) suggests a shifting equilibrium of aggregation with holding temperature. The larger number of bonds and higher entropy is proposed to be caused by the effect of temperature on helix-coil transition (solubility) of the maltodextrin chains. Gelation occurs between molecules in the more-structured helix form. Low temperatures favoured the aggregation of amylose chains (German et al., 1992), likely through a greater proportion of chains in the helix form. However, increased temperature decreases the proportion of chains in the helix versus coil state (Moates et al., 1997). As insolubility of the helix form is a driver for gelation, a greater proportion of chains in the coil form at elevated temperatures would decrease the extent of gelation. This is consistent with the observed decreasing enthalpy. Based on the higher melting temperature for gelation at 45 °C and 60 °C, the shorter chains appear to not have participated in gelation. These smaller polymers are proposed to be in the random coil state at these temperatures and subsequently stay within the aqueous phase. Instead, the larger branched chains which are in the helix state contributed to network formation. Participation by the larger molecular weight fraction at higher temperatures is consistent with the lower entropy measured for these structures, previously described as consisting of larger and more ordered aggregates of larger MW. In summary, the smaller enthalpy and entropy at high temperatures was proposed to be a reflection of decreasing contribution of the smaller molecular weight fraction to the aggregation network.

Table 3.2. Calculated melting temperatures, enthalpy, and entropy values from DSC heating endotherms of maltodextrin gels set for four days at the indicated temperature. A heating rate of 5 °C/min was utilized with a reference cell of water. Averages are reported with one standard deviation (of three replicates except 40% at 60 °C which is the average of seven replicates). Letters signify samples that have significantly different means through all pairwise comparisons (Student-Newman-Keuls Method).

Maltodextrin Concentration	Gelation Temperature	Calculations from DSC heating endotherms				
		Onset (°C)	Midpoint (°C)	ΔH (J/g)	ΔS (mJ/g·K)	ΔG (J/g)
40 %	60 °C	76.0 ± 4.3	89.0 ± 1.6	3.4 ± 0.6 ^{A}	9.5 ± 1.5 ^{A}	0.27 ± 0.05 ^{A}
	45 °C	64.3 ± 2.9	77.7 ± 1.5	5.3 ± 0.9 ^{A}	15.1 ± 2.5 ^{A}	0.49 ± 0.06 ^{A}
	38 °C	58.0 ± 2.0	77.3 ± 5.1	10.4 ± 3.1 ^{B}	29.6 ± 8.2 ^{B}	1.2 ± 0.5 ^{B}
	22 °C	42.7 ± 3.2	59.3 ± 0.58	13.1 ± 3.3 ^{B}	39.5 ± 9.8 ^{BC}	1.5 ± 0.4 ^{BC}
	10 °C	33.0 ± 2.6	51.3 ± 0.58	14.5 ± 2.7 ^{B}	44.8 ± 8.0 ^{C}	1.8 ± 0.3 ^{C}
30 %	60 °C	- **	- **	- **	N/A	N/A
	45 °C	66.3 ± 2.1	81.3 ± 1.5	4.0 ± 0.6 ^{A}	11.4 ± 1.7 ^{A}	0.41 ± 0.06 ^{A}
	38 °C	59.0 ± 3.6	79.7 ± 0.6	5.4 ± 0.9 ^{A}	15.2 ± 2.6 ^{A}	0.63 ± 0.1 ^{A}
	22 °C	39.0 ± 1.0	63.0 ± 2.6	11.4 ± 0.5 ^{B}	34.0 ± 1.2 ^{B}	1.4 ± 0.1 ^{B}
	10 °C	37.0 ± 2.6	53.0 ± 1.0	12.8 ± 2.7 ^{B}	39.1 ± 8.3 ^{B}	1.7 ± 0.2 ^{B}

**Peaks could not be resolved from baseline

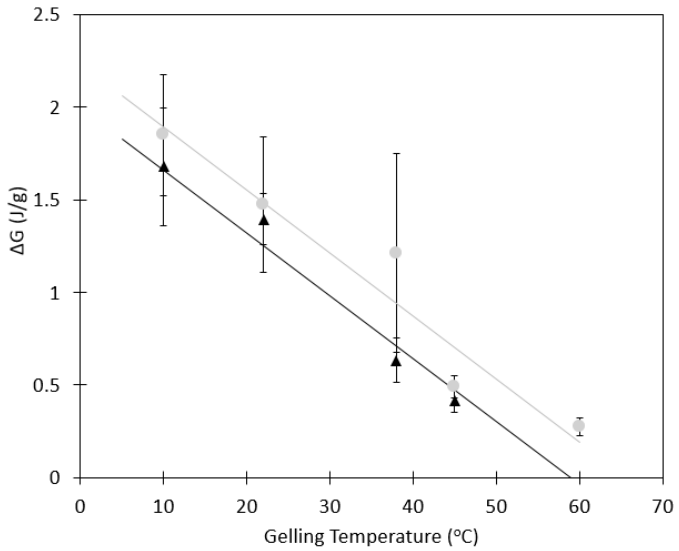

Figure 3.5. Holding temperature influence on Free Energy (Δ G) calculated from DSC thermograms. A multiple linear regression (MLR) was fitted to concentration [40% (●) and 30 % (▲)] and holding temperature. The resulting equation was ΔG = 1.31 - 0.034*Temperature + 0.023*Concentration with an R^2 of 0.87.

3.3.2.4 Temperature influence on aggregate structure

To visualize the aggregation structures, transmission electron microscopy (TEM) images were obtained. The first step of sample preparation consisted of adding small sections of sample to an aqueous glutaraldehyde solution. Thus, the images represent the non-dissolvable content of each sample as some material was expect to disperse in the solution. From the observed network, the size of crystallites was largest in the 60 °C sample (2-4 µm) compared to 22 °C (2 µm) or 10°C sample (1-2 µm) (Figure 3.6). A greater crystallinity was also seen in the 60 °C than either the 22 °C or 10 °C, indicated by more blurry images at 10 °C caused by diffusion of electrons passing through amorphous regions. These images support the previous claims of larger aggregate zones and a more crystalline-like network when held at 60 °C. The presence of larger crystalline regions is also consistent with the small proportion of fast-relaxing protons only observed for the sample held at 60 °C. Although the gels have equilibrated at the selected temperature, moving the gel to a different temperature may modify the equilibrium point. To examine this concept, the thermal reversibility of the structure was analysed to determine if these bonds remained after moving to a different temperature.

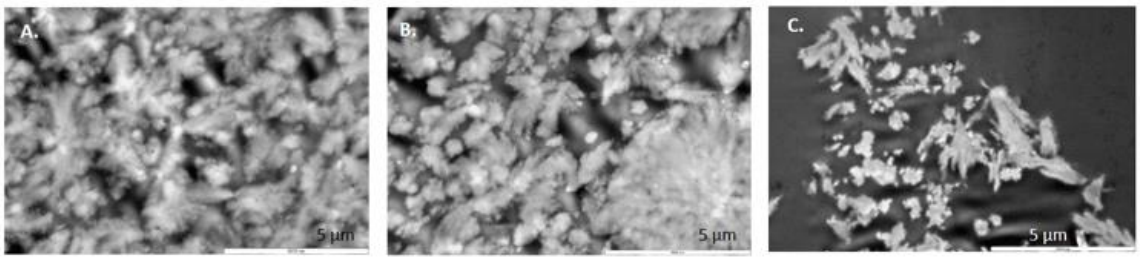

Figure 3.6. TEM images of maltodextrin networks (at 40%) held for four days at (A) 10 ^{o}C, (B) 22 ^{o}C and (C) 60 ^{o}C. Each image is 12 x 8 µm.

3.3.3. Thermal hysteresis of gel network

In the previous section, the gelling temperature was shown to impact structure formation. A constant temperature created a gel network approaching an apparent equilibrium. Next, hysteresis of the gel network was examined by holding samples of 40% maltodextrin at multiple temperatures to assess whether these structures were thermally reversible. After an initial gelation period of 4 days, samples were moved to a second gelation temperature for 2 days (Figure 3.7A) and 6 days (Figure 3.7B). Consistent with work reported in the previous section, all samples were equilibrated to room temperature (22 °C) for two hours prior to analysis. Points along the dotted grey line represent the control samples which were kept at the same temperature during both gelling periods. Deviation from this control line show the influence of the second temperature. A lower (colder) second gelling temperature generally increased the gel strength, while a higher temperate decreased the strength (Figure 3.7). The strength of gels held at a second temperature of 10 °C and 22 °C were higher than the control gel at 60 °C (peak forces of 13 N, 8 N, and 2 N respectively). Following a second holding period of 6 days at 10 °C, none of the samples initially held at other temperatures were significantly different in gel strength than a gel continuously held at 10 °C. However, a second gelling temperature of 60 °C showed hysteresis. A gel formed at 10 °C or 22 °C did not (after 2 or 6 days) adjust to the strength of a gel at 60 °C. Some of the network formed at 10 °C or 22 °C is preserved, even if the temperature is changed, indicating the irreversibility of some associations. To further analyse this partially reversible network, the relaxation rates of water within the gel were compared using NMR.

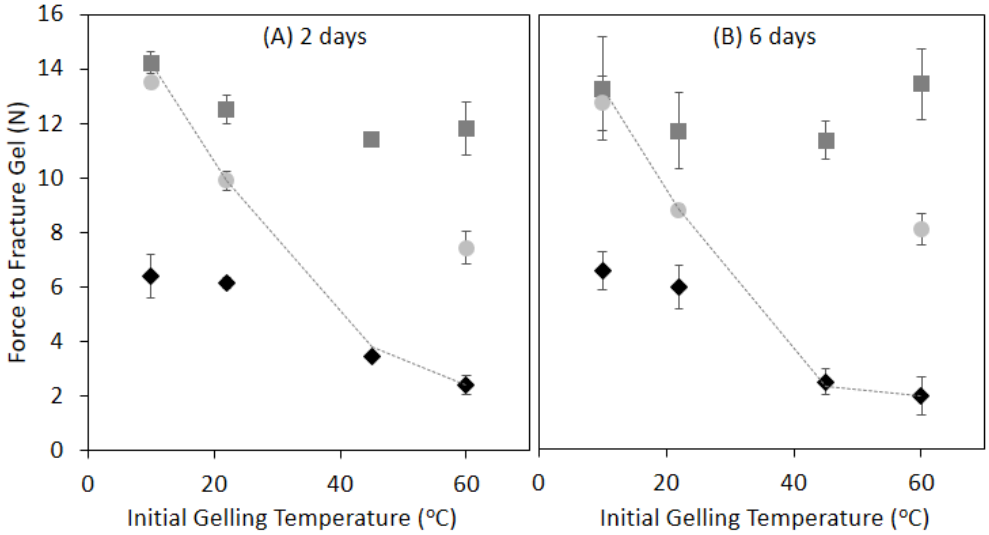

Figure 3.7. Reversibility of gel structure for a 40% maltodextrin, after holding at the initial temperature for 4 days and the secondary temperature (10 °C ■ ; 22 °C ●; 60 °C ◆) for (A) 2 days and (B) 6 days . The dotted line represents the control samples which were maintained at a constant temperature.

In agreement with analysis of the fracture properties, the water relaxation also displayed a hysteresis when subjected to multiple temperature holds. For all four of the initial gelling temperatures, a second hold at 10 °C formed a gel with the fastest relaxation rate and 60 °C at the slowest relaxation rate (Table 3.3). Moving to a cooler second temperature increased the solidity of the network (faster relaxation rate), while a warmer second temperature formed a more mobile network. Interestingly, gels initially held at 60 °C all showed two relaxation times, consistent with a heterogeneous material. As previously discussed, the appearance of a minor portion of protons relaxing with a faster rate was predicted to be indicative of crystalline-like regions. The presence of highly-ordered structures in all samples that initially gelled at 60 °C suggests an irreversible formation at this temperature.

Table 3.3. Water relaxation rates, measured at 25 °C, for 40% maltodextrin gels, after holding at the initial temperature for 4 days and the secondary temperature for 6 days.

1st Gelation Temperature (4 days)	2nd Gelation Temperature (6 days)	T_2 (1st)		T_2 (2nd)	
		Relaxation Rate (s^{-1})	Amplitude %	Relaxation Rate (s^{-1})	Amplitude %
10 °C	10 °C	24.7 ± 0.1	96 %	10.7 ± 0.1	4 %
	22 °C	23.2 ± 0.0	100 %		
	60 °C	19.4 ± 0.1	100 %		
22 °C	10 °C	23.1 ± 0.0	100 %		
	22 °C	21.7 ± 0.1	100 %		
	60 °C	18.9 ± 0.1	100 %		
45 °C	10 °C	25.6 ± 0.4	94 %	13.9 ± 2.9	6 %
	45 °C	17.9 ± 0.2	100 %		
	60 °C	17.0 ± 0.1	100 %		
60 °C	10 °C	29.4 ± 0.7	70 %	21.1 ± 0.7	30 %
	22 °C	22.2 ± 0.2	74 %	34.6 ± 0.7	26 %
	60 °C	20.0 ± 0.1	89 %	54.0 ± 3.6	11 %

Previously described as highly ordered aggregation regions, these seem to be of high stability and only formed at 60 °C. Shifts over time and at other temperatures could be using these junction zones as a seed point for further growth. Comparing the magnitude of the second relaxation rates, the ordering is probably a reflection of the average size of the regions. Interestingly, the fracture strength of these three samples did not show signs of hysteresis, but the relaxation rates indicate the microstructure is different. Further analysis of the microstructure investigated the bond energies of the networks using DSC.

The network remaining after multiple temperature holds was investigated to detect any type of irreversible structures. As indicated previously (section 3.3.2), the associations formed at 10 °C have a melting onset of 30 - 35 °C and peak of 50 - 55 °C, while the network formed at 60 °C has a melting onset of 70 - 80 °C with a peak of 90 - 95 °C (Figure 3.4). When

gels were held at two temperatures, melting peaks were observed at temperatures reflective of a combination of each gelling condition (Figure 3.8 and Table 3.4). Bimodal DSC melting peaks have also been observed in gelatin gels, and two types of structure (formed at each of the holding temperatures) was similarly proposed (Busnel et al., 1988). Based on corresponding enthalpy values (Table 3.4), the amount of gel structuring was more reflective of the secondary gelling temperature than the initial temperature. Moving a gel set at 10 °C to an environment at 60 °C, only 2 J/g of bond energy remained at the expected 10 °C position, while 8 J/g of new bonds were formed reflective of the secondary gelling temperature (60 °C). Similarly, with an initial gelling temperature of 60 °C and secondary hold at 10 °C, 1 J/g of bond energy (of the 3 J/g) remained at the expected 60 °C position, while 9 J/g were formed at the 10 °C location. For each of these switches, the enthalpy values created in the second holding temperature were also different than a single temperature hold. With an initial hold of 10 °C, more associations formed at the 60 °C location (8 J/g versus 3 J/g without another temperature hold). Thus, the bonds formed during the 10 °C hold enhanced aggregation at the second temperature hold of 60 °C. This disparity is likely due to a seeding effect of the high entropy bonds formed at the first temperature that initiated lower entropy associations. At 10 °C, there were minimal bonds melting near 90 °C, so any residual bonding from the first hold does not account for the difference. Previously, the low entropy bonds formed at 60 °C were proposed to be near the critical gelling point due to the high variability and low enthalpy (section 3.3.2). This apparent influence of seeding to increase gelation supports the previous hypothesis that gelation at 60 °C is near the edge of stability. Examining the opposite transition, from 60 °C to 10 °C, there was alternatively a decrease in the number of bonds formed at the second

gelling temperature (8 J/g versus 14 J/g without another temperature hold). In this transition, the bonds formed at 60 °C appeared to inhibit aggregation and bond formation at the second holding temperature. The low entropy bonds characteristic of gelation at 60 °C were proposed to lead to larger junction zones, and it may be these bulky structures sterically inhibit high entropy bonds. Some of the structuring formed at 60 °C (with a melting point between 80 - 95 °C) breaks apart while holding at a second temperature, as seen in the decreased in the enthalpy from 3 J/g to 1 J/g (switching to 10 °C). The sample was never at a temperature high enough to melt, so the low entropy configuration must not be stable at 10 °C. A minor proportion of the maltodextrin aggregation shows thermal irreversibility, although the resulting network is more reflective of the ending thermal influence.

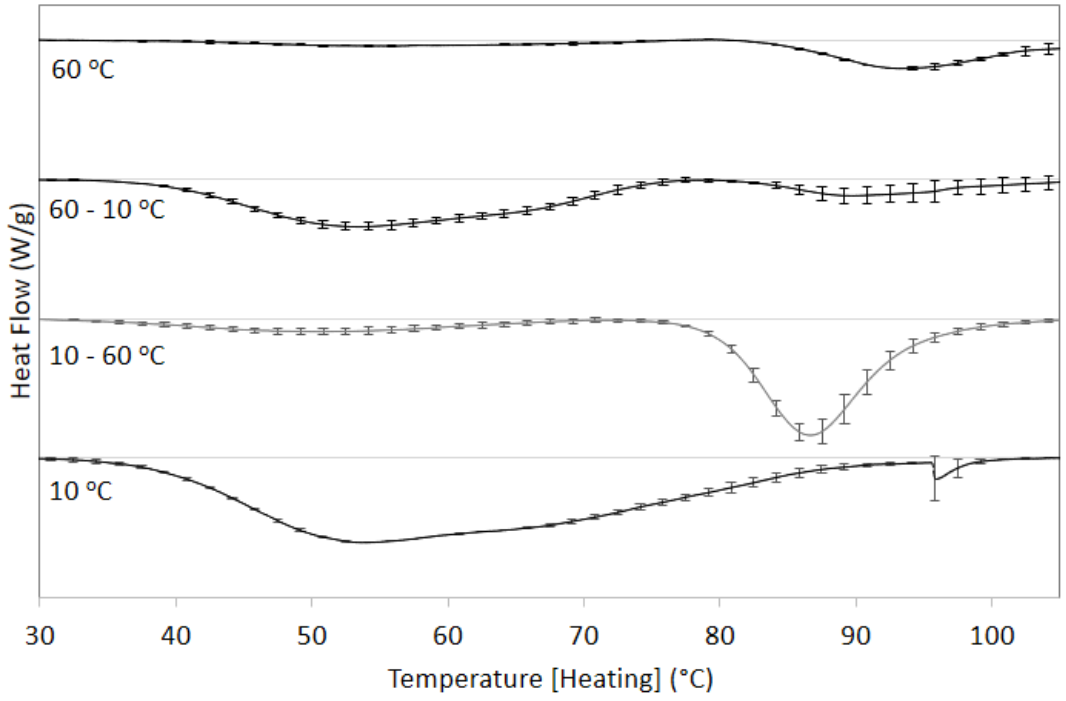

Figure 3.8. Melting DSC endotherm of 40% maltodextrin gels set for four days first temperature, and another 6 days at the second temperature. A heating rate of 5 °C/min was utilized with a reference cell of water.

Table 3.4. Calculated melting onset temperatures, enthalpy of melting values, and entropy from DSC curves after holding at the initial temperature for 4 days and the secondary temperature for 6 days. Letters signify samples that are significantly different means through all pairwise comparisons (Student-Newman-Keuls Method).

				1st Peak			2nd Peak		
1st Temp (4 days)	2nd Temp (6 days)	Total ΔH (J/g)	Total ΔG at 22 (J/g)	Midpoint (°C)	ΔH (J/g)	ΔS (mJ/g·K)	Midpoint (°C)	ΔH (J/g)	ΔS (mJ/g·K)
60 °C	60 °C	2.9 A	0.56 A	- **	- **	- **	94.0 ± 1.4	2.9 ± 0.3	7.8 ± 0.7
60 °C	10 °C	9.2 B	0.99 B	53.3 ± 0.6	7.6 ± 0.8	23.3 ± 2.6	91.3 ± 3.2	1.5 ± 0.9	4.1 ± 2.4
45 °C	10 °C	11.3 B	1.5 C	- *	-*	- *	- *	-*	-*
22 °C	60 °C	10.1 B	1.6 C	49.8 ± 1.0	2.3 ± 0.4	7.0 ± 1.3	88.3 ± 0.5	7.8 ± 1.0	21.6 ± 2.7
10 °C	60 °C	10.1 B	1.6 C	49.8 ± 2.1	2.0 ± 0.6	6.2 ± 1.7	86.5 ± 0.6	8.1 ± 0.7	22.4 ± 2.0
10 °C	10 °C	13.9 C	1.3 BC	52.5 ± 0.7	13.9 ± 0.1	42.8 ± 0.4	- **	- **	- **

*Peaks could not be resolved from each other
**Peaks could not be resolved from baseline

3.4. Conclusion

Temperature was shown to impact which chains participated in the helix formation and the organization of helices during network development, and thus the hypothesis was supported. Previous work had focused on temperature's effect on gelation speeds, but the novelty of this work examined the impacts on the near-equilibrated gel microstructure and fracture properties. Importantly, all analysis was completed at identical temperatures, so results are a true reflection of the underlying structure differences formed at the gelling temperatures. Gels formed at lower temperatures (10 °C) were stronger and more brittle which corresponded to a higher entropy network with a greater number of aggregates. Higher holding temperatures (up to 60 °C) resulted in less network formation and lower entropy creating the appearance of a weak gel. An exploration of the spontaneity of

aggregation through shifting entropic and enthalpic contributions demonstrated the importance of temperature in controlling molecular ordering. Holding temperature was proposed to influence the amount of smaller molecular weight chains participating in aggregating by remaining in the coil form at higher temperatures. The low entropy structure formed at high temperatures is of particular interest as it could impart digestion properties similar to resistant or slowly digestible starch to the maltodextrin gels. This demonstrated control of gelation mechanism through temperature allows for selection of ideal properties to use in food applications such as mixed gel preparation.

Chapter 4. Structural characterization of interpenetrating network of high acyl gellan and maltodextrin mixed gels

---

Published article

Kanyuck, K. M., Norton-Welch, A. B., Mills, T. B., & Norton, I. T.

Food Hydrocolloids. 2021. (112), 106295.

Abstract

A mixed-gel of high acyl (HA) gellan gum and maltodextrin (MD) (potato DE2) demonstrated a range of physical properties with a proposed interpenetrating network. Mixed hydrocolloid gels allow for the development of novel properties that neither polymer alone could create allowing unique functionality in textures or controlled release. The aim of this work was to identify the type of network formation by examining material properties and the contribution from of each polymer. Material properties of quiescently set composite gels were characterized through bulk fracture, small deformation rheology, DSC, and microscopy. A continuous shift in fracture strain and modulus were created through mixed gels of the soft and flexible HA gellan with the firm and brittle MD. By adding MD (from 0 to 40%) at a constant 0.5% gellan, the gel true strain at fracture decreased from 0.50 to 0.18 while the Young's Modulus increased from 3 to 1780 kPa. No indication of phase separation or chemical complexation was measured. Analysis of the time-dependant MD contribution and composite material properties hypothesized a gelation mechanism in which HA gellan forms a network first and MD aggregates within the pores without phase separation. MD dominated the small deformation rheology while HA gellan appeared to dominate the fracture point. Material properties were indicative of the type of structural organization in the HA gellan MD mixed gel network.

Author Contributions

Kelsey M. Kanyuck: Conceptualization, Methodology, Formal analysis, Investigation, Writing - original draft.

Abigail B. Norton-Welch: Supervision, Funding acquisition, Writing - review & editing

Tom B. Mills: Supervision, Writing - review & editing.

Ian T. Norton: Supervision, Funding acquisition, Writing - review & editing.

4.1. Introduction

Mixed biopolymer gel systems have become popular to achieve a wider and more controllable range of properties than any single gelling system. Applications in the food industry include creation of novel textures, mimicking of traditional foods with improved nutritional profiles (low and no-fat), and controlled release functionality. The key to understanding the properties of composite gels lies in a microstructural understanding of the gel network formation (Norton and Frith, 2001). Mixed gel networks are divided into three idealized types: phase separated, interpenetrating (IPN), and coupled (Morris, 1986; Kasapis, 1995; Norton et al., 2014a). Interactions between two polymers may either be segregative or associative based on the enthalpy of interaction of between similar versus dissimilar polymers (Morris, 2009). A phase separated network originates from segregative interactions and is often observed as a water-in-water dispersion in which one polymer forms droplets within a continuous network of the second polymer (Morris 2009, Norton 2014). Both IPN and coupled are types of associative interactions between polymers. For an IPN gel, both polymers form networks spanning the gel in one phase and without direct interaction of the polymers (Kasapis, 1995; Norton et al., 2014a). A coupled network additionally involves an electrostatic bond between the two types of polymer, and this type has only been observed in a few systems (Morris, 1995; Kasapis, 1995; Morris, 2009).

A key distinction between these types for polymers that gel by forming aggregates, which may appear as phase separated, is whether phase separation occurs prior to gelation (true phase separated by segregative interactions) or the gelation mechanism simply leads to regions rich in one polymer (micro-phase separated or interpenetrating) (Clark et al., 1999;

Djabourov et al., 2013). Phase separated systems are common because frequently the enthalpic contribution from like-to-like polymer interactions outweighs the association of dissimilar polymers and small entropic contribution of staying mixed (Kasapis et al., 1993d; Clark, 1996; Morris, 2009). Interpenetrating networks occur when the enthalpic contribution of separation is low (such as with a charged and an uncharged polymer). This work will examine the network formation between high acyl (HA) gellan and maltodextrin. The first section will examine the type and mechanism of network formation and the second will examine contributions of each polymer to composite modulus and fracture behaviour.

Maltodextrin (MD) gels are formed by dense aggregate regions which form strong brittle gels at high concentrations (Schierbaum et al., 1992; Chronakis, 1998; Loret et al., 2004b; Kanyuck et al., 2019). This polymer is a carbohydrate created through the hydrolysis of starch into shorter chains (Chronakis, 1998). A low dextrose equivalent (DE) MD has a lower degree of hydrolysis, and it is the larger MW of these MDs which exhibit gelling abilities. Gelation occurs by aggregation of double helix chains of polymer strands and the presence of sufficiently long strands that are able to connect multiple aggregate regions (Reuther et al., 1984; Radosta and Schierbaum, 1990). For the DE 2 potato MD used, critical gelling concentration are reported between 15 and 20% by weight (Kasapis et al., 1993b; Loret et al., 2004b; Kanyuck et al., 2019).

High acyl (HA) gellan gum forms a soft and flexible gel with a high strain to fracture caused by a fibrous gel network (Sanderson et al., 1988; Funami et al., 2008). Gelation occurs through double helix formation of individual chains (Chandrasekaran et al., 1992), and helices are connected by branching and end-to-end associations (Morris et al., 1999; Noda et al., 2008; Funami et al., 2008). Unlike many hydrocolloids, there is limited helix

aggregation due to the steric hindrance of the acetyl groups (Noda et al., 2008; Funami et al., 2008). The microbial fermented hydrocolloid is an acidic carbohydrate comprising of a four-sugar repeated unit with 0.9 glycerate and 0.4 acetate groups on the first sugar unit and one carboxyl group on the second unit (Kasapis et al., 1999; Sworn, 2009). The more commonly studied variant low acyl (LA) gellan gum has the same carboxyl groups but the deacetylation process removed most of the bulky acyl groups, thus changing the gel structure and material properties (Morris et al., 2012).

MD has been studied in mixed gelling systems previously, and most often for applications in fat reduction due to the creaminess mimicking abilities of MDs (Chronakis, 1998). Most literature has proposed phase separated mixed gels between a low DE MD and gelatin (Kasapis et al., 1993a; Lorén and Hermansson, 2000), low methoxy pectin (Picout et al., 2000a), agarose (Loret et al., 2006b), iota carrageenan (Wang and Ziegler, 2009), milk protein (Chronakis et al., 1996), locust bean gum, gum acacia, and high salt carboxymethyl cellulose (Annable et al., 1994). For charged polymers, phase separation was either not observed with high methoxy pectin (Evageliou et al., 2000) or was only observed at sufficient levels of added salts with carboxymethyl cellulose (Annable et al., 1994). One study has suggested the presence of an IPN formed with MD in combination with low acyl (LA) gellan (Clark et al., 1999). Experimentation with HA gellan is limited, although the non-gelling polymers of chitosan fibers (Liu et al., 2013) and soybean fiber (Chen et al., 2020) have been proposed to arrange within the pores without phase separation. No published work has examined the mixed gel of HA gellan and MD, and there is only limited knowledge of the interactions between HA gellan with other hydrocolloids.

The large disparity between the material properties of MD and HA gellan gum allowed a rheological analysis of the microstructure contribution of each polymer to the mixed gel. This work proposes the structural organization of the mixed gel is reflective in the physical and chemical properties of the composite. Materials properties, microscopy, DSC, and modelling of composite gels will be used to characterize the mixed gel of MD with HA gellan gum. Contributions of each polymer to specific material properties will also be discussed to examine the structural influence of individual gel networks.

4.2. Materials and methods

4.2.1. Materials and gel preparation

HA gellan gum (KELCOGEL LT100 lot # 5B1259A) was obtained from CP Kelco (UK). MD (Paselli SA-2) was purchased from Avebe (Netherlands) produced from potato with a dextrose equivalent (DE) between 2.7 and 2.9 (Kasapis et al., 1993b; Manoj et al., 1996). The salt content of HA gellan was 19473 ppm potassium, 3615 ppm sodium, 2187 ppm calcium, and 29 ppm magnesium as measured by ICP-OES (Optima 8000 by PerkinElmer). The DE 10 MD (Paselli SA-10) was purchased from Avebe (Netherlands), the modified MD originated from waxy corn starch and was modified to increased branching and lower the molecular weight (Agenanova from Agrana, Austria), and the glucose was purchased from Sigma Aldrich (UK). DI water was purified with a reverse osmosis milli-Q water system.

Prior to mixing, each polymer was dispersed individually to ensure complete hydration. HA gellan was mixed into DI water at 90 °C and hydrated for 2 hours with stirring to reach a stock concentration between 4 and 5% (Cassanelli et al., 2018a). MD was slowly dispersed in DI water at 95 °C and stirred for 4 hours to hydrate at stock concentrations ranging from

40% to 60% (Kanyuck et al., 2019). Glucose and the other MDs (DE 10 and modified) were prepared identically by fulling hydrating in heated water prior to mixing. Water loss was accounted for by replacing any lost mass to the sample during heating. Gels were prepared by mixing these heated stock solutions together with the required amount of heated DI water to achieve the range of concentrations utilized in this work. Hot solutions were stirred until homogenous (approximately 5 minutes) and quiescently set in plastic cylindrical molds (20 mm diameter) excluding the samples for DSC which were prepared in specific vessels. Gels for time-dependent measurements were prepared from a single solution to produce five samples, and at each of the time points one sample was measured and destroyed.

4.2.2. Compression and fracture of gels

Bulk material properties were assessed by compression of gels with a squeeze-flow setup using a TA.XT.plus texture analyser (Stable Micro Systems, UK). Samples were prepared using a 20 mm diameter cylindrical mold and cut to a 20 mm height. Gels were compressed with a speed of 2 mm/s between parallel surfaces of a flat probe (40 mm diameter) and a stationary stage until fracture (up to a 90% reduction of the initial sample height). Further deformation was not possible with the instrument and would have resulted in gel material squeezing outside the geometry and loosing contact with the upper plate. From the instrumental measurement of force (F) and distance (ℓ), the strain (ε), stress (σ), Young's Modulus (E), true strain (ε_T), and true stress (σ_T) were calculated:

$$E = \sigma/\varepsilon \text{ from } \varepsilon = 0.01 \text{ to } \varepsilon = 0.05 \quad \text{(Eq. 4.1)}$$

$$\varepsilon_T = \ln((\ell_0 + (\ell_0 - \ell) / \ell_0) \quad \text{(Eq. 4.2)}$$

$$\sigma_T = (F/A_0) (1 + \varepsilon) \quad \text{(Eq. 4.3)}$$

Where 'ℓ_0' is the initial sample height and A_0 the initial contact area of 314 mm^2.

4.2.3. Differential scanning calorimetry

A µDSC3evo (Seteram Instrumentation, France) was used with a temperature range of 20 to 95 °C with a heating and cooling rate of 0.2 °C/min with 10 minute isothermal holds at each extreme. A second heating and cooling step was performed immediately following the first. Only the first heating and cooling are shown graphically but calculated enthalpies are reported for all steps. Integration and curve smoothing was preformed using CALISTO software (Seteram Instrumentation, France). Enthalpies were normalized to grams of total sample and curves were compiled after a manual linear baseline subtraction. Prior to data collection, gels were pre-melted in the DSC by heating and cooling at 1 °C/min from 20° to 95° C with a 10 minute hold at 95° to ensure a homogenous sample over the bottom of the vessel. For adequate measurement of the MD contribution to the gel, all samples were held at room temperature for 4 days prior to the reported DSC analysis (Kanyuck et al., 2019). Gels were added hot with a mass of 0.8 ± 0.1 g and a matching mass of DI water. Sample and reference cells had a volumetric capacity of ~ 0.9 mL and were sealed vessels of Hastelloy material.

4.2.4. Modelling by polymer blending laws

The isostress and isostrain equations are often used to model physical properties of phase separated gel systems based on a composite of the individual polymers. Theory and models were adapted from Morris (1992). The equations predict the composite gel modulus (G_C), using the phase volume of HA gellan gum (ϕ_{HAG}) and MD (ϕ_{MD}) and calculated moduli

at the effective concentration of HA gellan gum (G_{HAG}) and MD (G_{MD}):

$$\text{Isostrain } G_c^{=} \phi_{HAG}G_{HAG} + \phi_{MD}G_{MD} \quad \text{(Eq. 4.4)}$$

$$\text{Isostress } 1/G_c^{=} \phi_{HAG}/G_{HAG} + \phi_{MD}/G_{MD} \quad \text{(Eq. 4.5)}$$

Application of these models to biopolymer gels relied on several assumptions that required modification; no polymer volume, complete phase separation, and a mathematically model-able modulus (Morris, 1992). Firstly, the assumption of no polymer volume is invalid in this system with MD concentrations up to 40% (Manoj et al., 1996). To account for this, effective concentrations of each polymer were expressed as polymer per water (w/w) ($Mass_{polymer}$ / $Mass_{water}$) to calculate the modulus. This modification allows consideration to the concentrating effect that a 30% MD solution would have on the effective HA gellan gum concentration through a reduction in the amount of water in the total mixture. For example, a 1% HA gellan gum with 30% MD would be calculated using the water amount of 69% and the effective concentration becomes 1.4%. Secondly, the concept of calculating phase volumes (ϕ) became difficult without observation of any separation so typical methods of measuring volume of each water phase were not applicable to this system. Relaxation rates ($1/T_2$) of single polymer gels and mixed gels were used to approximate the proportional water binding by shifts in the composite relaxation rates. Addition of 1% HA gellan caused a shift along the entire curve approximately equal to 10% MD, and thus a 1% HA gellan to 10% MD equivalence point was estimated (Appendix A). Previous effective concentration measurements for LA gellan and MD were modelled non-linearly but values were of a similar ratio (Clark et al., 1999). Variations above and below this ratio were tested in the models, but similar fits to the reported values were obtained. We acknowledge many

assumptions were made from this simplification, and this value merely represents the closest possible approximation of a value we propose is meaningless in the mixture. Effective concentration models (Figures 4.4C and 4.4D) did not utilize the assumption of phase volumes. Concentration curves of individual polymers were used to estimate the contribution of each individual polymer. Polynomial equations from predictive models were written for calculations of modulus at any effective concentration (G_{HAG} and G_{MD}).

4.2.5 Scanning electron microscopy (SEM)

SEM measurements were acquired using a JEOL 6060LV (Tokyo, Japan). Samples were cut into 1.5 x 1.5 mm cubes and suspended 1 cm above liquid nitrogen for one minute and then immersed in liquid nitrogen for one minute. An aluminium sample stage and carbon tab were cooled via immersion in liquid nitrogen for one minute. Images were acquired using back scatter electrons (BSE), a low vacuum of 50 Pa, an accelerating voltage of 10 kV, and a 10 mm working distance.

4.2.6 Statistical analysis

Figures show the average of at least three samples and error bars represent the standard deviation. Statistical lettering was used in Table 4.2 to distinguish statistically different ($p < 0.05$) samples after using an ANOVA and all pairwise comparison test with the Student-Newman-Keuls method (SigmaPlot 12.5). In reference to the discussion of Figure 4.9 and Table 4.1, the claim of “no change with time” was based on a comparison of means for each concentration of MD and a p-value of 0.01 to account for the number of pairwise comparisons.

4.3. Results and discussion

4.3.1 Network characterization

Fracture mechanics, lack of continuous phase discontinuity, disagreement with phase-separated models, cumulative bond energies, and microscopy will be discussed to support the proposition of an interpenetrating network of HA gellan and MD. Above critical gelling concentrations of both polymers, a true IPN network was suggested and was consistent with the mechanism proposed for LA gellan and MD by Clark et al. (1999) whereby the MD aggregated within a porous gellan network without phase separation. Below the gelling concentration of MD (approximately 20%), a non-segregative gel was comprised of MD aggregates within a continuous HA gellan network.

4.3.1.1 Material properties

Material properties of the gels were measured by compression of cylindrical shaped samples using a texture analyzer. The compression curves were measured as force over distance and converted to true stress and true strain using equations 4.1 and 4.2 (Section 4.2.2) with examples of representative curves in Figure 4.1. Arrows point out the fracture point for each sample. Strain at fracture, stress at fracture, and modulus were observably different by examining the shape of compression profiles between individual gels of MD and gellan (solid lines). MD alone at a concentration of 30% formed a firm gel with a large modulus and showed brittle fracture at 0.13 true strain (Figure 4.1). Conversely, the 1% HA gellan was soft and flexible with fracture only at 0.56 true strain. The composite gels resulted in intermediate strain at fracture and modulus (Figure 4.1). For the composite gels, only one fracture point was observed.

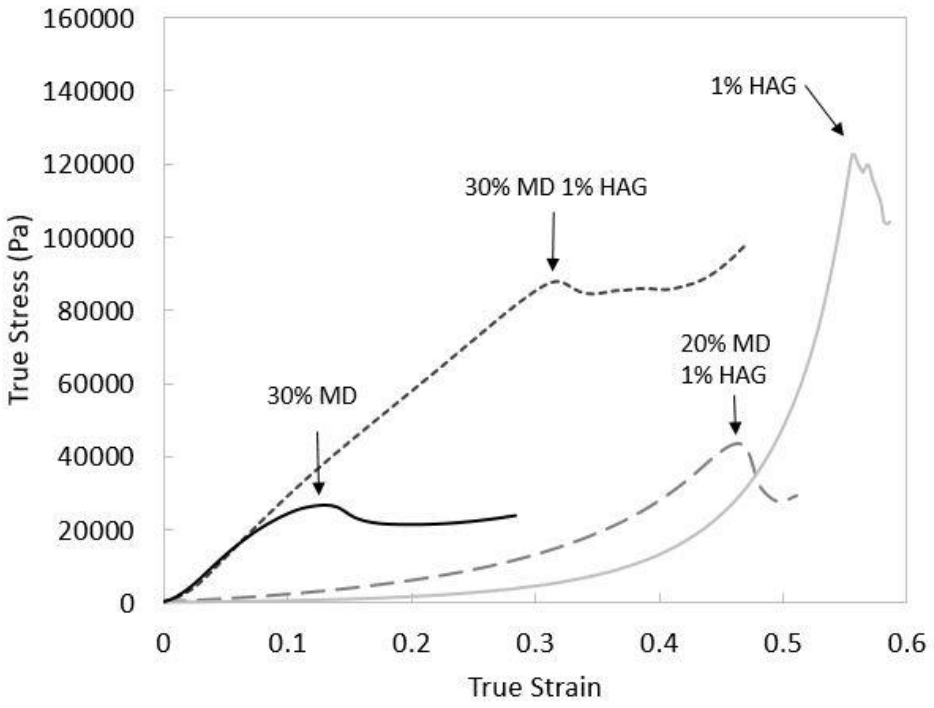

Figure 4.1. Compression curves for 30% MD and 1% HA gellan (HAG) (- - - -) with comparison to 30% MD (—), 1% HA gellan (—), 20% MD and 1 % HA gellan (HAG) (— —) using calculated true stress and true strain values. Arrows show the points of fracture for each gel.

Fracture points of the composite material and the contribution of polymer concentrations are displayed in Figure 4.2. HA gellan gum was very flexible with high strains to fracture (0.49 to 0.59) while MD alone fractured at low strains (0.14-0.18). Mixtures showed fracture points varying between the two individual polymer values. A common indication of a phase separated gel is a large shift in behaviour (discontinuous) from switching between continuous phases (Norton and Firth, 2001). A phase separated system would be expected to show strain values determined by the continuous polymer (with some modification from the interface) and a large shift when the continuous phase changed (Norton and Frith, 2001). This was not observed and the incremental change in fracture strain of the composite gel (non-discontinuous) suggests there is not bulk phase separation. Increasing

levels of MD also increased the Young's Modulus of the mixed gel (Figure 4.3). All samples of HA gellan without the inclusion of MD resulted in comparatively low moduli (2500 – 5000 Pa). The curve shapes of the Young's Modulus of mixed gel closely followed the MD curve (□) with a small increase from greater HA gellan concentrations (Figure 4.3). HA gellan had a much smaller modulus than MD, by one to two orders of magnitude, so the minimal contribution was not unexpected.

MD independently did not form a gel below 20%, and at 15% the solution was still pourable with visibly increased light scattering from chain aggregation (Kasapis et al., 1993b; Loret et al., 2004b; Kanyuck et al., 2019). Below the gelling concentration, aggregates are proposed to be adding inhomogeneity to the HA gellan network as well as overall rigidity to the composite by acting as filler particles. The formation of aggregated regions of MD within a rearranged HA gellan network are consistent with the deswelling and "elongated configurations" proposed when co-gelling with LA gellan (Kasapis et al., 1999). Below the gelation point of MD, the decreased strain to failure is suggested to have originated from inhomogeneities in the HA gellan network created by the MD. For most food gels, the fracture point occurs when the applied force becomes greater than the cohesive bonds and the concentration of polymer does not actually effect the strain at fracture (Zhang et al., 2005).The failure point is expected to be characterized by the microstructure defects and energy dissipation mechanism, which initiate and propagate fracture respectively (van Vliet and Walstra, 1995). Aggregation of MD into large dense regions within the HA gellan network is feasible to have created cracks or inhomogeneities. This aggregation is proposed to modify the loose HA gellan network into less flexible regions. These heterogeneities within the network act as cracks and focus the stresses to cause a more brittle fracture (van

Vliet and Walstra, 1995). Above the gelling concentration (20%) which coincides with the largest changes in strain, MD is proposed to reach a critical number of aggregates to form a second continuous network. Only at this point is the mixed gel network hypothesized to create two interpenetrating networks. Below the gelation point of MD (20%), MD appeared to act as a filler particle without formation of a secondary gel network. Bulky aggregates appeared to have sterically hindered compression by decreasing mobility of the HA gellan network in the mixed gel.

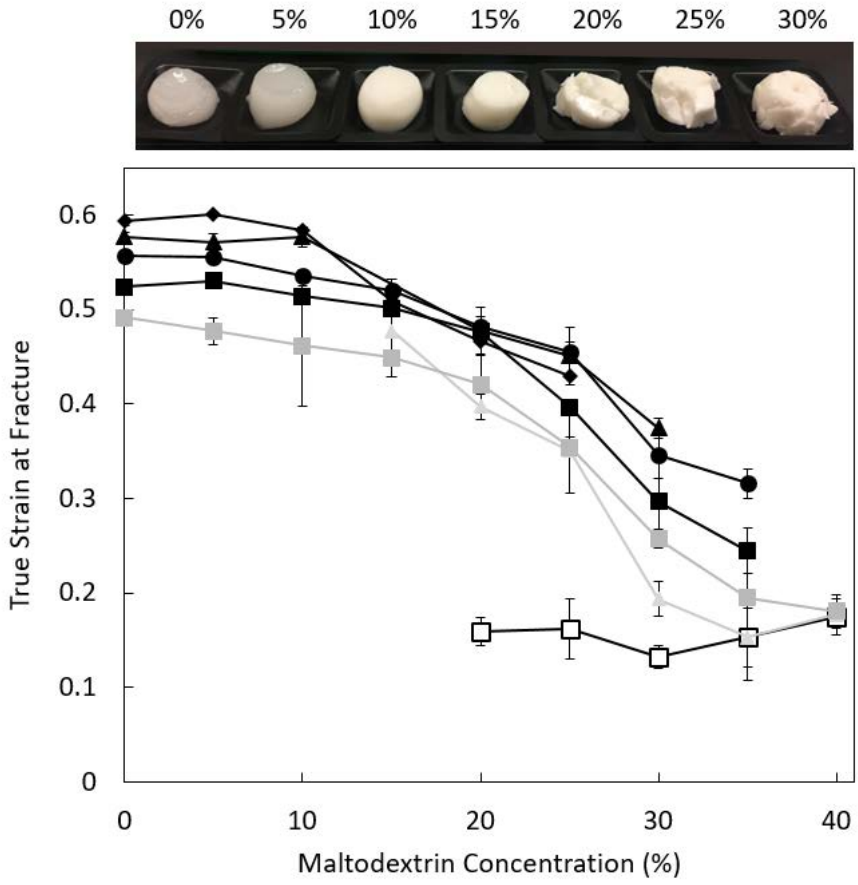

Figure 4.2. Comparison of the strain at failure for increasing levels of MD with HA gellan concentrations of 0 % (□), 0.25% (▲), 0.5% (■), 0.75% (■), 1% (●), 1.5% (▲), and 2% (◆). Images show the appearance of 1% HA gellan with maltodextrin after compression.

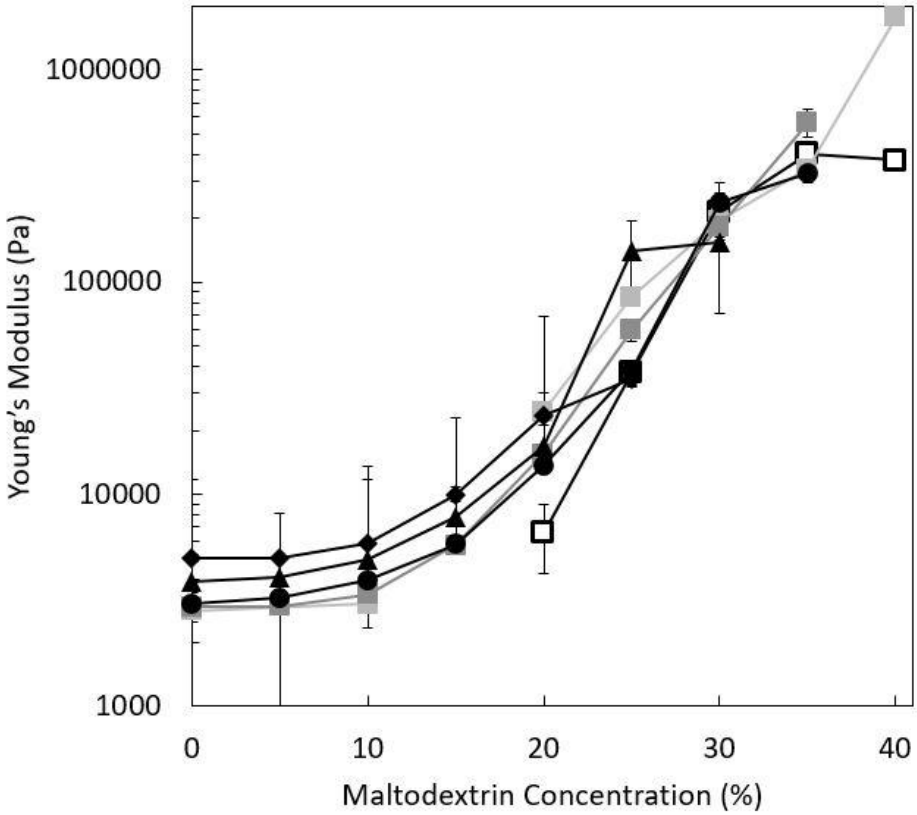

Figure 4.3. Small deformation mechanics before failure as indicated by the Young's Modulus for HA gellan concentrations from 0 % (□), 0.25% (▲), 0.5% (■), 0.75% (■), 1% (●), 1.5% (▲), and 2% (◆) at increasing levels of MD.

4.3.1.2. Microstructure analysis

Theoretical models can be utilized to analyse the relationship between microstructure and function. Phase separated biopolymers have commonly been understood by modelling individual contributions to isostrain and isostress models by considering effective concentrations and assuming complete phase separation. A phase separated system is suggested when predicted values from these models are similar to the measured values, although minor deviation is always expected (Kasapis, 2008). Utilizing the models refined by Morris (1992), the equations were modelled for 0.5%, 1% and 1.5% HA gellan with

increasing concentrations of MD (Figure 4.4). Due to the high levels of maltodextrin (up to 40%) which replace water in the system, changes in effective concentrations of HA gellan gum should be expected (Clark et al., 1999). All estimates have been modified to effective concentrations (considered a percentage of the water mass in the sample) to account for the high solid content of MD, comparable to the method of Manoj et al. (1996). True Isostrain and isostress predications are shown in Figure 4A, 4B, and 4C which takes into account the effective concentrations after an assumed phase separation of the polymers. Alternatively, Figure 4.4D, 4.4E, and 4.4F only adjusts the concentration based on the total water within a sample and assumes no liquid-liquid demixing. Both models utilize the in-series model (isostress) and the in-parallel (isostrain) models for the contribution of each polymer (equations 4.4 and 4.5). Other concentrations of HA gellan were also modelled and showed equivalent trends and quality of fit and thus are not included for redundancy.

The phase-separated models (Figure 4.4A-C) were not a good fit for the observed composite moduli. At most concentrations of MD (below 25%), the measured modulus was weaker than predicted. When liquid-liquid mixing occurs, higher effective concentrations of each polymer occur in both phases. In this system, no indication of phase separation by increases in modulus from higher effective concentrations was observed. Additionally, at higher MD concentrations neither phase-separating model could predict the measured composite modulus effectively. The prediction from the non-phase separating models (Figure 4.4D-F) were closer to the measured values. At low concentrations (0-10% MD), none of the models predict a deviation far from that of HA gellan alone and was consistent with measured values (Figure 4.4D-F). The rise in modulus with increasing MD was best accounted in the single phase isostrain model, which is consistent with the compositional theory of two

networks spanning the length of the gel (Ross-Murphy, 1995). Similarity of models in Figure 4D-F to the measured values suggested a lack of phase separation which could be consistent with either an IPN or coupled network.

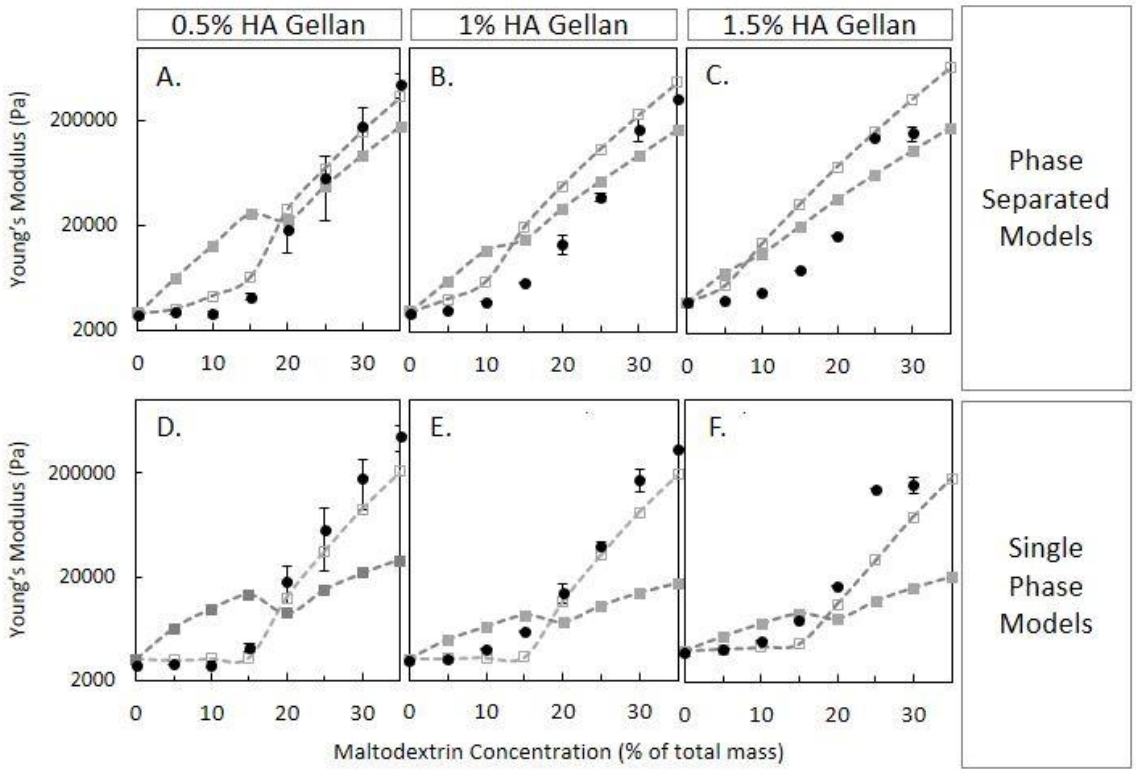

Figure 4.4. Comparison of measured network modulus of (A) 0.5% HA gellan, (B) 1% HA gellan and (C) 1.5% HA gellan with added MD (●) to calculated moduli from the isostrain (□) and isostress (■) phase separation models and (D) 0.5% HA gellan, (E) 1% HA gellan and (F) 1.5% HA gellan for models utilizing one phase concentrations.

Glucose-based polymers of various sizes were substituted at equivalent concentrations with 1% HA gellan in an attempt to separate the aggregation (solid filler) and solvent quality effects of MD from the network effects. Material properties of these gels are summarized in Table 4.1. The DE 2 MD is the one used throughout this paper. The DE 10 MD is also from potato and further hydrolysed so that it can form aggregates but is unable to form a gel network. The modified MD (with increased branching) and glucose are unable to form aggregates or a gel network. Comparison of these three analogues to the DE 2 MD allowed for determination of the influence of network formation specifically. Changes in solvent quality or water of hydration (mimicked by glucose or the modified MD) only showed a small (less than 10%) change in composite modulus at fracture strain and highlighted the importance of DE 2 gelation on composite fracture and modulus (an increase of 6,000 %). The contribution of MD to the mixed gel originates in network structure formation beyond just a small influence from changes to the solvent. Fracture strain was only decreased with the DE 2 and DE 10 MDs (Table 4.1) which both form aggregates (Kasapis et al., 1993b). The DE 10 MD is able to form aggregates but is thought to not have enough long chains to gel, although the composite flexibility was still decreased. Aggregation of these MDs can also be seen in the time dependence (a change in modulus over 14 days, which is discussed in section 4.3.2) while no effect was seen for the modified MD nor the glucose. In these mixed gels, aggregates appear to have created enough structural inhomogeneities in the HA gellan to increase brittleness of the composite gel. A network formation by the DE 2 MD was indicated by the large increase in modulus that not even the non-aggregating MD exhibited.

Table 4.1. Comparison of material properties of 1% HA gellan gels with 30% carbohydrate additives. Time dependence refers to a significant change ($p < 0.05$) in Young's Modulus or true strain at fracture over the period of 1 and 14 days.

Carbohydrate Type	**Young's Modulus (Pa)**	**Strain at Fracture**	**Stress at Fracture (kPa)**	**Time Dependence**
MD DE 2	235,707 ± 42,000	0.32 ± 0.01	122 ± 3	Yes
MD DE 10	3,300 ± 200	0.47 ± 0.01	25 ± 2	Yes
Modified MD (non-aggregating)	3,300 ± 250	0.57 ± 0.01	207 ± 16	No
Glucose	3,600 ± 90	0.57 ± 0.01	184 ± 11	No
No Additive (1.5%)	3,870 ± 82	0.58 ± 0.01	283 ± 29	No
No Additive (1.0%)	3,200 ± 100	0.56 ± 0.01	114 ± 18	No

Gel networks were further compared by differential scanning calorimetry (DSC) to check for associations between polymers indicative of a coupled network. Thermograms of gels melting (A) and cooling (B) are shown in Figure 4.5. The range of melting temperatures (between peak onset and offset) from both polymers was quite broad and has been attributed to low cooperation between aggregates (Morris et al., 1996; Mazen et al., 1999). Individually, the 1% HA gellan showed gelling and melting temperatures of 63 °C and 60 °C respectively (Figure 4.5) and was consistent with the small hysteresis usually reported because of the minimal aggregation of helices (Morris et al., 1996; Kasapis et al., 1999; Mazen et al., 1999; Morris et al., 2012). Heating curves for MD showed a broad breaking of the network during melting, but no observable bonds were measured during the cooling process (Figure 4.5B). Although unusual for most hydrocolloids, this is consistent with the long gelling time of multiple days for MD (Loret et al., 2004b; Kanyuck et al., 2019). The slight upward movement of the MD curve approaching 25 °C could be from the beginning of detection of MD aggregation. There was indication that some bonds slowly reformed evidenced by the melting enthalpy of 27% of the original during the second heating cycle (Table 4.2).

Melting endotherms and enthalpy were additive without indication of increased enthalpy or bonds between polymers. Enthalpy values were not different than a pure summation of the two polymers (Table 2) and no new bonds were suggested by new peaks at different melting temperatures (Kasapis, 2008). The first melting cycle includes both MD aggregates and HA gellan gel helices melting as samples were held for 4 days prior to analysis. In cooling, only the HA gellan was observed to gel within the experimental timeframe (which is consistent with the proposed mechanism of slow MD gelation). A slight increase in gelling

temperature between HA gellan with or without MD can be attributed to an increase in effective concentration of the HA gellan component. Due to the 20% MD in the formation, less water resulted in an effective concentration of 1.25% which was consistent with a melting temperature of 66 °C (Figure 4.6). The enthalpy respective to gelation of the HA gellan was unchanged by the MD ($p > 0.05$). Additive bond energies were consistent with an IPN or phase separated gel, and inconsistent with a coupled network. Preceding analysis has eliminated the phase separated model and jointly the results are only consistent with an IPN.

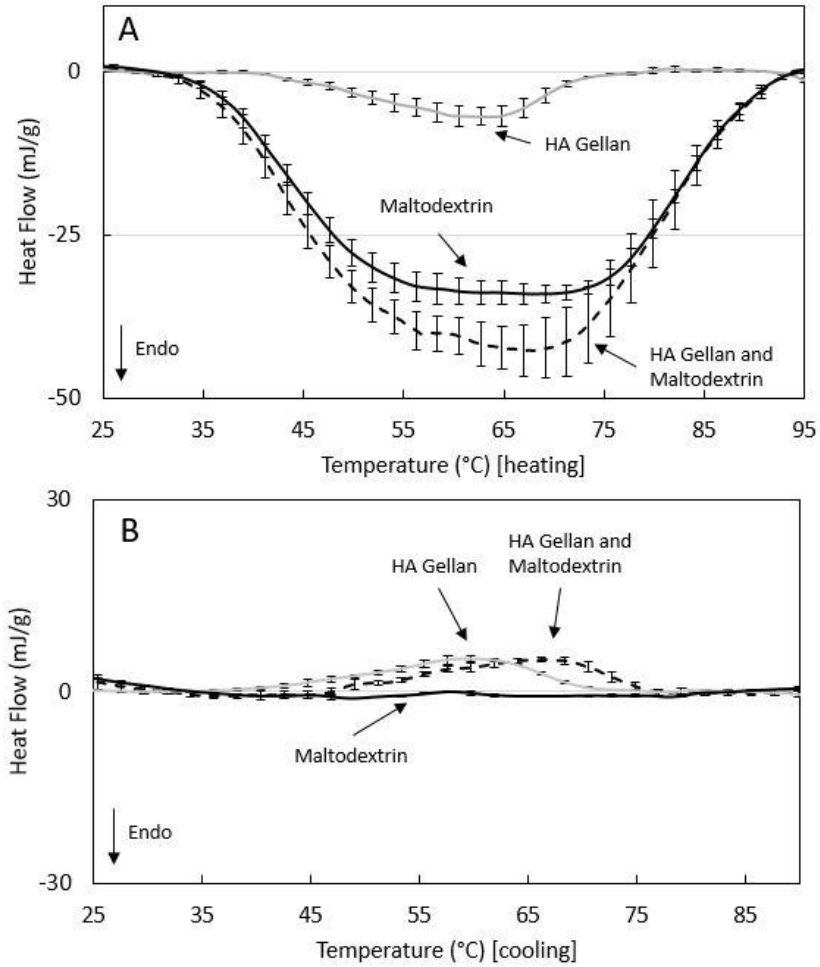

Figure 4.5. DSC heating (A) and cooling (B) curves for gels of 1% HA gellan (—), 20% MD (–), and 1% HA gellan with 20% MD (- - -) after four days of gelation. After baseline subtraction, the error bars represent a standard deviation of triplicate samples.

Table 4.2. Calculated enthalpy values (J/g) from DSC heating and cooling cycles based on grams of total sample. Values are reported as the average with one standard deviation for three replicates. Different letters indicate significantly different sample means.

	1st Cycle (4 day gelation)		2nd Cycle	
	Heating	Cooling	Heating	Cooling
HA gellan (1%)	$0.13^{A} \pm 0.04$	$0.12^{A} \pm 0.04$	$0.10^{A} \pm 0.01$	$0.09^{A} \pm 0.01$
MD (20%)	$1.74^{D} \pm 0.09$	**	$0.47^{B} \pm 0.07$	**
Measured HA gellan (1%) + MD (20%)	$1.92^{E} \pm 0.16$	$0.12^{A} \pm 0.01$	$0.59^{C} \pm 0.12$	$0.13^{A} \pm 0.01$
Summation of HA gellan (1%) + MD (20%)	1.87 ± 0.1	0.12 ± 0.04	0.57 ± 0.07	0.09 ± 0.01

** peaks could not be resolved from baseline

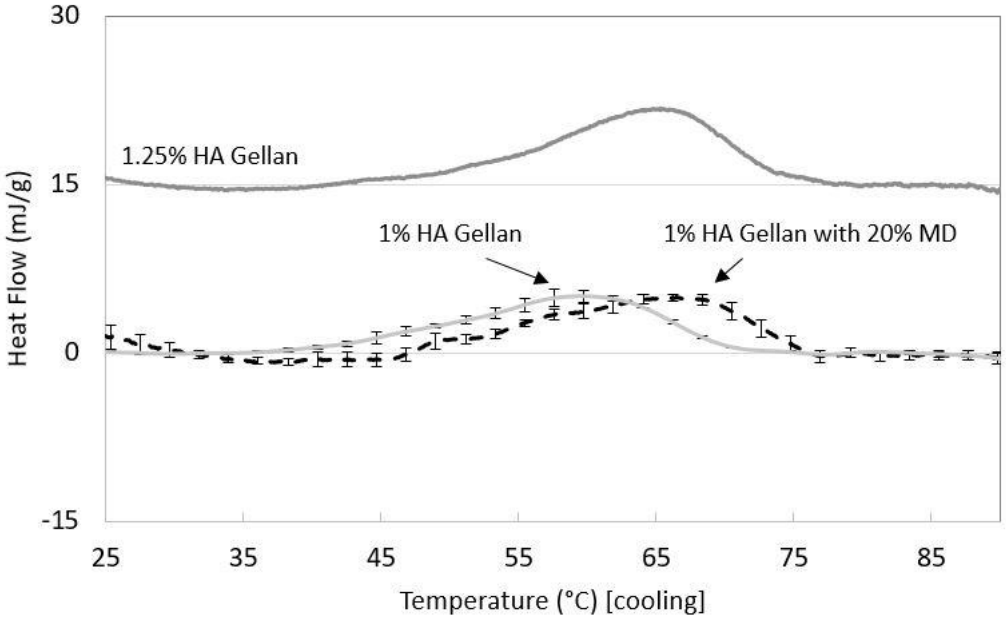

Figure 4.6. DSC curves comparing melting temperature of 1% HA gellan gum with and without 20% MD to 1.25% HA gellan gum.

Microscopy images of a 30% MD gel and a mixed gel of 25% MD and 1% HA gellan are shown in Figure 4.7. Images were representative of the entire gel that was viewed and no signs of macroscopic phase separation were observed. It was not possible to image the HA gellan component due to visible cracking from evaporating/melting at low magnification in a 1% HA gellan sample. Additionally, the lack of aggregation of double helix strands means the gel structure would be very fine and therefore difficult to observe. MD gelation occurs through the formation of large crystalline regions of aggregated double helices (Chronakis, 1998). The gelation mechanism can appear as phase separated with a microscopy technique, but the lack of demixing prior to gelation excludes the applicability of phase-separated descriptions (Clark et al., 1999). TEM images of MD aggregate networks have shown microspheres of 20-30 μm (Schierbaum et al., 1984) made of smaller comb-like structures of 1-4 nm (Schierbaum et al., 1984; Clark et al., 1999; Kanyuck et al., 2019). Evidence of the smaller aggregates were seen in gels with or without HA gellan (Figure 4.7A and 4.7B). The arrangement of the microcrystalite aggregates showed differences with the presence of HA gellan, but continuous networks were observed in each. Smaller and more regular microcrystalites were observed in the mixed gel, while larger rod-like structures were formed of the aggregates for MD alone (Figure 4.7C and 4.7D). As the MD aggregated within the pores of the HA gellan network, it appears that formation of very large aggregates were prevented. This is also consistent with the images of MD with LA gellan observed by Clark et al. (1999). Although the HA gellan strands could not be seen, the modification to the MD network were consistent with an interpenetrating network.

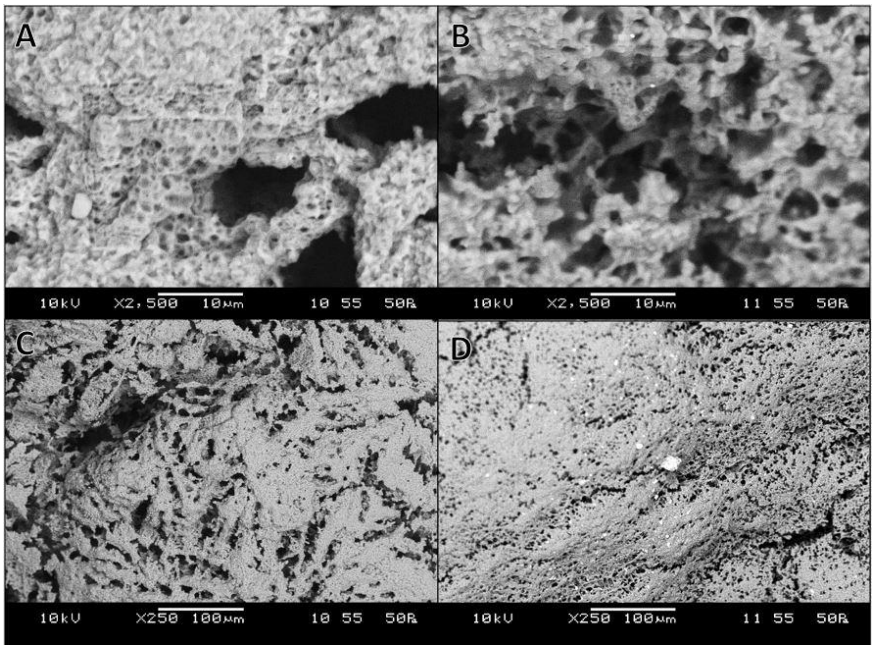

Figure 4.7. SEM images of 30% MD (A and C) and 1% HA gellan with 25% MD (B and D).

4.3.2. Polymer contributions

Compression profiles and microstructure analysis have suggested interpenetrating networks. The presence of two continuous networks naturally leads to a questioning of the specific contribution of each polymer. Utilization of the time dependence of MD aggregation allowed measurement of the direct contribution of this aggregation. The small deformation behaviour of the composite appeared most similar to the MD while the HA gellan network appeared dominant in the fracture. This was consistent with the relative magnitudes of individual properties. Composite material properties were not simply additive and showed an interaction between components during network formation. The presence of another polymer was proposed to affect the distribution and microstructure of each respective network but not the actual chemistry of the network (consistent with no changes in the enthalpy, Table 4.2).

Previous experiments (Figure 4.3) showed the concentration dependence of the composite Young's Modulus to be more strongly effected by MD than HA gellan. Considering the modulus of individual components, this was not surprising as the modulus of MD is almost a hundred times higher than that of HA gellan. It was of interest to understand the effects of MD aggregation on the composite modulus. A unique behaviour of low DE MDs is increasing gel strength, following a logarithmic function, over the time frame of weeks, (Loret et al., 2004b; Kanyuck et al., 2019) and shown by in Figure 4.8. For gels containing MD at concentrations above (30 and 25%) and below (20, 15, and 10%) the gelation point, an increase in Young's Modulus followed a natural log function (Figure 4.8). HA gellan alone had the lowest Young's Modulus and was unchanged over the measured time period of 1 to 14 days. Lack of change in the HA gellan sample and the characteristic natural log curve shape suggested the increase was caused by aggregation of MD. Thus, the direct influence of MD aggregation was able to be observed. MD concentrations below the critical gelation level resulted in a modulus at an order of magnitude lower. However, both above and below the expected gelation point of MD the aggregation kinetics were the same (natural log curve shape). Aggregates of MD thus influenced the composite gel firmness even at points when a true network had not formed. As initially proposed in section 4.3.1.1, the aggregates added bulk and resistance to deformation. At concentrations sufficient to form a MD gel network, MD is the major contributor to the resistance in small deformations as seen from the similarity in modulus with or without HA gellan (Figure 4.8 and Figure 4.3).

While MD aggregation caused an increase in the Young's Modulus of the composite gel, the strain and stresses at fracture exhibited behaviour more similar to HA gellan. The next experiment examined the change in fracture strain by the aggregation of MD through

utilization of the time-dependence discussed previously. Concentrations of each polymer expected to form two continuous interpenetrating networks were selected for this study. The fracture of the composite is caused by breakage of the HA gellan network, while the MD is thought to modify the stress propagation (section 3.1). At the composite fracture point the MD network had already fractured. A decrease in the strain at fracture for all three concentrations of HA gellan tested corresponded to an increasingly brittle gel with aggregation of MD (Figure 4.9). For comparison, a 30% MD alone is also shown with fracture at a low strain (0.14 true strain). Alone a 1% HA gellan did not fracture until 0.56 true strain (Figure 4.2). The shifting in stain at fracture between these two extremes is proposed as an indication of inhomogeneities forming and growing in the HA gellan network by aggregation of MD. The stress at fracture was not changed ($p > 0.01$) over the 14 days (data not included). Decreasing in fracture strain was indicative of the changing distribution of HA gellan aggregates and consistent with the proposed mechanism of network heterogeneities (distribution of polymer chains and junction zone size) (van Vliet and Walstra, 1995) and microscopy images (Figure 4.7). As the MD aggregates grew larger, the HA gellan bends to allow the large and bulky aggregates which decreased stress propagation during compression. The influence on composite fracture also supports the proposal of MD aggregating within the pores of the HA gellan network without phase separation (IPN model). If phase separation had occurred, a continued aggregation within an excluded MD phase should not have an impact on the continuous HA gellan phase.

Due to the great difference in individual properties, each polymer was a major contributor to different composite properties. With a brittle gel and large Young's Modulus from many dense aggregates, the MD dominated the small deformation behaviour. The flexible and

soft network from HA gellan dominated the fracture behaviour of the composite. Importantly, each polymer impacted the distribution (microstructure) of the other but not the chemistry of associations. The aggregation of MD made the composite stronger from the bulky aggregates and also more brittle by introducing heterogeneities into the HA gellan network.

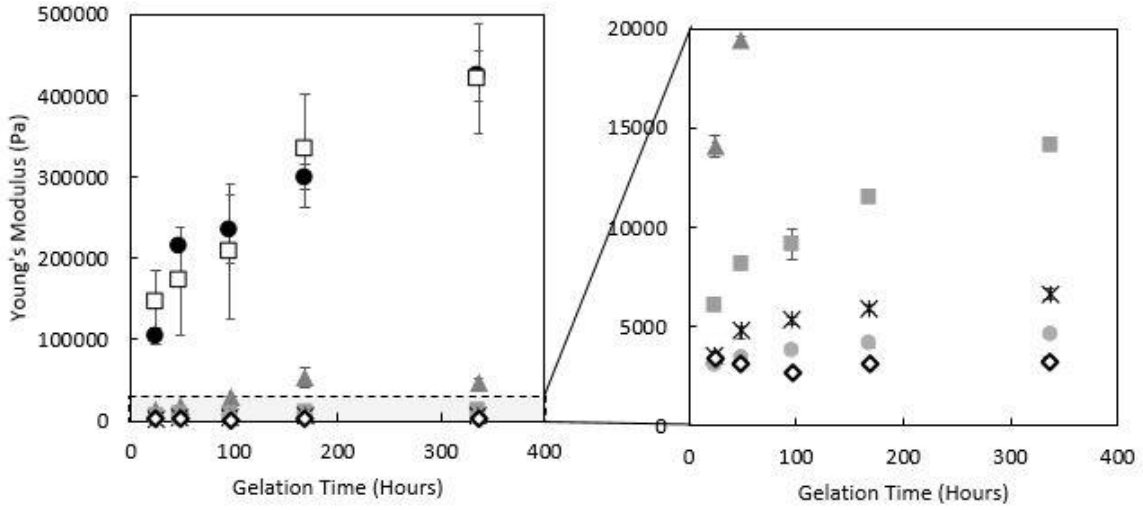

Figure 4.8. Contribution of MD aggregation to the composite Young's Modulus at 0 % (◇), 10% (●), 15% (X), 20% (■), 25% (▲), and of 30 % (●) to a 1% HA Gellan network and 30% MD without HA gellan (□) from 24 hours to 14 days.

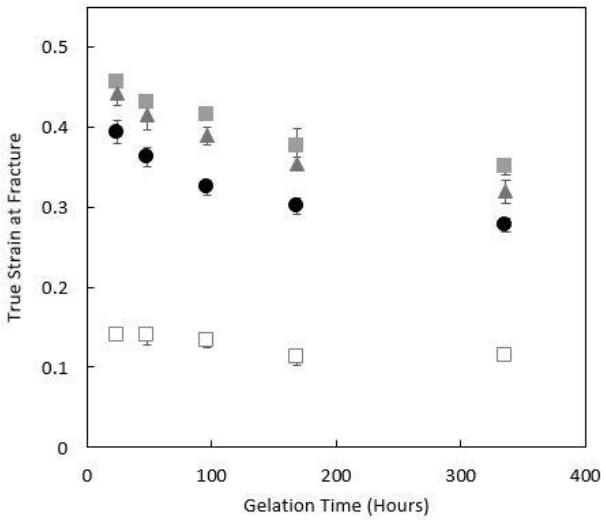

Figure 4.9. Contribution of MD aggregation to the true strain at fracture for mixed gels with 30% MD and 1% (●), 0.75% (■), 0.5% (▲), and 0% (□) HA gellan from 24 hours to 14 days.

4.3.3. Gelation mechanism

The following mechanism is proposed for development of the interpenetrated networks and is illustrated in Figure 4.10. Initially upon cooling, HA gellan forms a network with negligible impacts from the presence of MD in solution. As the gelation is very quick, the HA gellan network has been set prior to aggregation of MD (which is consistent with DSC cooling curves). As the slow gelation of MD begins, aggregates form within pores of the HA gellan network. Growth of these regions condenses and introduces structural defects in the formerly loose and flexible HA gellan chains. Formation of these MD aggregates within the pores of HA gellan inhibits the growth of very large microcrystallites, but not the smaller helix aggregate structure. The distribution of the gellan network was also impacted by the MD, while on molecular level the helix and aggregate formation remained unchanged (DSC confirmed the enthalpy stays the same for both polymers). Aggregates of the MD network contribute a resistance to deformation to the flexible HA gellan network. The more flexible HA gellan network was responsible for the ultimate fracture of the gel. Both polymers thus contribute to the composite physical properties and complex interactions between the networks resulted in a broad range of physical properties.

Formation of this IPN is likely caused by an associative interaction from a thermodynamic unfavourability of separation. Self-association of gellan would need to overcome the charge repulsion of the carboxylic acid groups and entropy of counterions. Concentrating similar charges into one phase is thermodynamically unfavourable and the charge repulsion theory has been proposed for other interpenetrating networks (Amici, 2002). In similar cases with one ionic polymer, single phase mixtures are favoured from the higher entropy of

counterions within a concentrated system (Piculell et al., 1995).The IPN suggested between MD and LA gellan supports the charge repulsion theory also occurs for the HA variant (Clark et al., 1999). It is possible that gelation of HA gellan could kinetically trap the mixed system before separation, but no indication of segregative interactions was observed in this work. Many phase separated polymers are thought to have a thermodynamic equilibrium in complete phase separation, but the gelation kinetically traps into smaller regions of separation (Kasapis et al., 1993d; Lorén et al., 1999). Future work should investigate whether segregative interactions could occur in other regimes such as controlling the rate of gelation or effects of salt or pH to neutralize charge repulsion and would allow a better understanding of mechanism, but is outside the scope of this paper. Similar experiments on the gelatin maltodextrin system showed the extent of phase separation could be controlled (Lorén et al., 2000).

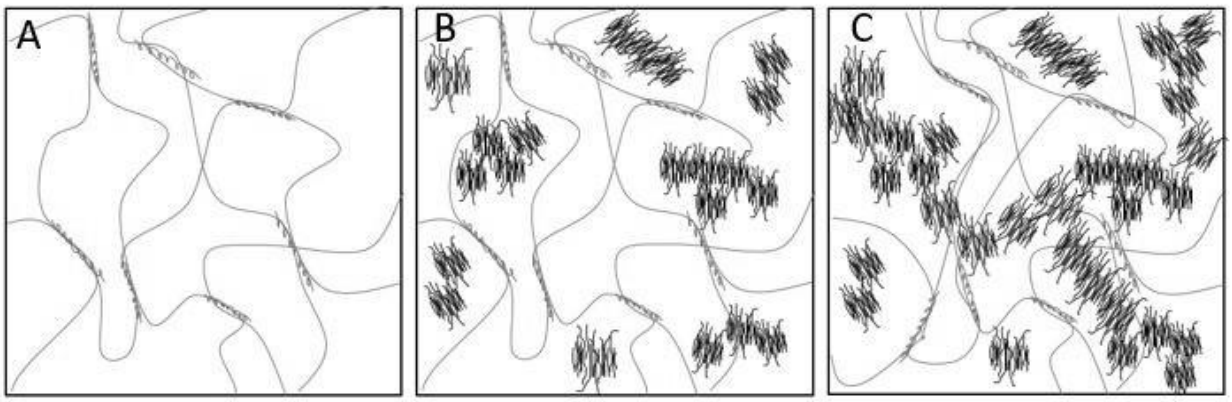

Figure 4.10. Proposed schematic for HA gellan network alone (A) and contributing to an interpenetrating network with MD (aggregates) below (B) and above (C) the critical gelation concentrations of MD.

4.4. Conclusion

An IPN of MD and HA gellan has been characterized. The mixed gel showed complex interactions between the polymers based on modification to microstructural distribution and crack propagation to fracture. Opposite textures of individual polymers have allowed an understanding of the contribution of each through analysis of the composite properties. Through microstructure modification, material properties of the composite gel shifted over a continuous range from the firm and brittle MD to the soft and flexible HA gellan. The time-influence of MD aggregation was shown to increase the modulus of the composite, but did not change the fracture stress. MD aggregation showed signs of increasing brittleness through introduction of stiffness and inhomogeneities to the HA gellan network. The quick gelation and charge repulsion of HA gellan provide a thermodynamic justification for an associative interaction. The Young's Modulus, appearing almost entirely dependent on the MD contribution, supports previous claims of the limited utility of small deformation to predict texture of mixed biopolymer gels (Van den Berg et al., 2007). Both small deformations and bulk fracture measurements were needed to describe the physical properties of this IPN gel. Characterization of mixed gels from these polymers have brought a greater understanding of the physical property to microstructure relationships for multicomponent systems.

Chapter 5. Release of glucose and maltodextrin DE 2 from gellan gum gels and the impacts of gel structure

---

Submitted article

Kanyuck, K. M., Norton-Welch, A. B., Mills, T. B., & Norton, I. T.

Food Hydrocolloids. 2022. (122), 107090.

Abstract

Structural influences of hydrocolloids gels on the release of carbohydrates was examined with a focus on structure-function relationships. This understanding will guide formulation of food gels for targeted sugar release in populations such as diabetics and athletes. Hydrocolloid gels with well characterised structures, with a focus on high acyl (HA) and low acyl (LA) gellan gum, were formulated with glucose, maltose, DE 10 maltodextrin (MD) and DE 2 MD. Gel structure did not significantly affect glucose release, but mixed gel type had a significant effect on MD availability. A DE 2 MD required amylase to release more than 10% of the carbohydrates but still had 38% retained in a gel formulated with 30% MD. Formulation with any non-melting gelling hydrocolloid decreased the amount of released MD and phase separated networks released more than interpenetrating networks. Differential scanning calorimetry was used to compare helix formation of MD gels and the number of helices was inversely correlated with carbohydrate release. These results demonstrated a range of sugar release profiles achievable from formulation from specific gelling agent structures and carbohydrates.

Author Contributions

Kelsey M. Kanyuck: Conceptualization, Methodology, Formal analysis, Investigation, Writing - original draft.

Tom B. Mills: Supervision, Writing - review & editing.

Ian T. Norton: Supervision, Funding acquisition, Writing - review & editing.

Abigail B. Norton-Welch: Supervision, Funding acquisition, Writing - review & editing

5.1. Introduction

Hydrocolloids can control the release, digestion, or adsorption of various nutrients ranging from starches to vitamins by controlling their network structure and response to known digestive stimuli (Norton et al., 2014b; McClements, 2021). Controlling carbohydrate digestion is crucial in formulation of foods when considering specific populations which require a sustained energy release or low glycaemic index such as diabetics and athletes (Gidley, 2013; Norton et al., 2014b). Carbohydrates, a major source of energy for humans, come in many sizes ranging from monomers (glucose) and dimers (maltose) and up to 30-150 saccharide units (maltodextrin (MD)) and 100-1,800 saccharide units (starches). Smaller molecules are able to diffuse through viscous solutions or gel networks (Mills et al., 2011). Larger molecules need to be broken into smaller units which can then move into the chyme where they can be absorbed (Tharakan et al., 2010; Gidley, 2013; Fabek et al., 2014). To formulate products with controlled sugar release, the relationships between carbohydrate size and hydrocolloid gel structure must be understood.

For most hydrocolloid gels, small molecules such as mono and disaccharides, salts, and artificial sweeteners, are all smaller than the pores of the gel network and are able to diffuse through the gel. Thus, the network mostly acts to prevent mixing (a faster mass transfer) and only a small deviation from diffusion coefficients has been measured (Jönsson et al., 1986; Lorén et al., 2009a; Lorén et al., 2009b). In one study, a 14% - 30% decrease in diffusion coefficient of salt was measured for hydrocolloids between 1 and 4% mass (Mills et al., 2011). Larger molecules (3 vs 8 nm) showed a greater decrease in diffusion coefficients with increasing polymer concentration (Lorén et al., 2009b). Differences

between gelling agent and concentration were not significant with an exception major structural changes such as melting (Mills et al., 2011). It is well known that surface area of a gel has a large influence on the rate of release, so that brittleness or a tendency to fracture causes a quicker release (Morris, 1994; Mills et al., 2011). Texture, breakdown, and serum release of the gel during mastication thus plays a major role in differentiation between hydrocolloids gels (Khin et al., 2021).

Release of larger carbohydrates (those not able to diffuse through the pores) is more complex. The digestive enzyme α-amylase cleaves maltose units from starch (Butterworth et al., 2011; Dhital et al., 2017) which is then small enough to diffuse out of the gel. Small amounts of glucose, maltotriose, and dextrin are also created (Butterworth et al., 2011; Dhital et al., 2017). An increased viscosity or a gel network impedes the mass transfer of the enzyme and slows the rate of digestion (Tharakan et al., 2010; Gidley, 2013; Fabek et al., 2014). Gel surface area, packing density, and subsequent entrapment impact the ability of α-amylase to reach the carbohydrate and thus the rate of digestion (Wee and Henry, 2020; McClements, 2021). In addition to the physical inhibition, chemical binding can also occur. For example, cellulose was found to inhibit α-amylase activity by binding with the enzyme (Dhital et al., 2017). Studies examining the effects of gelling hydrocolloids on the digestion of starch have typically found a decreased rate of digestion and total digestion (Butler et al., 2008; Koh et al., 2009; Sasaki and Kohyama, 2011; Ramírez et al., 2015; Zhang et al., 2018; Srikaeo and Paphonyanyong, 2020). Gelatinization, retrogradation, and steric hindrance of starch are all expected to play a role making differentiation of the separate mechanisms impossible (Zhang et al., 2018). Comparisons to MD may give insight into the contribution of network effects on retrogradation because gelatinization does not occur.

An understanding of the effects of gel structure on carbohydrate release, as a function of molecular weight (MW), is important for the formulation of products with controlled carbohydrate release. Most work has focused on either high MW carbohydrates (specifically starches) (Koh et al., 2009; Sasaki and Kohyama, 2011; Ramírez et al., 2015; Zhang et al., 2018; Srikaeo and Paphonyanyong, 2020) or very low MW, such as glucose, maltose, and sucrose (Morris, 1994; Wang et al., 2014; Yang et al., 2015; Nishinari and Fang, 2016; Khin et al., 2021), but left out intermediate MW carbohydrates like MD. The mechanism of release for the digestion of MDs has not yet been determined and was thought to be slowed by incorporation of hydrocolloids. Gellan gum has been shown to form an interpenetrating network with MD (Clark et al., 1999; Kanyuck et al., 2021a) and high acyl (HA) gellan gum variant was capable of forming a wide variety of material properties (Kanyuck et al., 2021a). Therefore, this gelling agent has considerable potential for use in customizable carbohydrate release systems.

The objective of the present investigation was to examine the role of gelling agents on carbohydrate release by comparing carbohydrates of different MW trapped within hydrocolloid gels with well-characterized properties. It was hypothesized that the MW of the carbohydrate, the gel network structure, and the response to environmental conditions (a stimuli-response) can predict release behaviour from hydrocolloids gels. MW of a carbohydrate is known to determine the path of release and digestion from gels. Although there are certainly other structural factors such as branching and linkages in carbohydrates, molar mass is just as important and is sometimes overlooked (Nishinari and Fang, 2021). Some gel networks display a response to stimuli such as melting, dissolution, or swelling which typically have large impacts on release (McClements, 2021). After determining the

pathway for MD release, a structural comparison will examine the influence of mixed gel network type and MD helix formation. Exploring these fundamental relationships between carbohydrate MW and gelling agent structure will facilitate strategic formulation of products to achieve desired release profiles.

5.2. Materials and Methods

5.2.1 Materials

Both MDs were derived from potato and acquired from Avebe (Veendam, Netherlands) with a dextrose equivalent (DE) of 2 (Paselli SA 2, batch H3362903) and 10 (Paselli MD 10, batch H4852902). The HA (LT100) and LA (F) gellan gum were acquired from CP Kelco (Atlanta, USA). The following hydrocolloids were purchased from Sigma Aldrich (St. Louis, USA): Gelatin type A with a bloom strength of 300, kappa-carrageenan, iota-carrageenan, agarose type A9539, and sodium alginate. Maltose, KCl, and $CaCl_2$ were also purchased from Sigma Aldrich. The α-amylase was from Aspergillus oryzae (10065 Sigma-Aldrich) with an activity of 32 U/mg. Glucose was purchased from Fisher Chemical (Loughborough, UK).

5.2.2. Sample preparation

All gels were prepared by dispersing the hydrocolloids in heated deionized (DI) water with stirring to fully hydrate the polymers individually in stock solutions. A summary of the formulations is shown in Table 5.1. MD and the glucose or maltose solutions were heated at 90 °C for 4 hours. Gellan gums were heated at 90 °C for 2 hours, the carrageenan, agarose, and alginate heated at 90 °C for 30 minutes, and gelatin heated at 50 °C for 30 minutes. After the individual hydrocolloids were hydrated, a hot solution (90 °C) of a stock concentration of the carbohydrate (glucose, maltose, MD DE2, or MD DE10 as indicated)

was mixed with the hydrocolloids for 5 minutes to combine. These mixtures were poured into 20mm diameter cylindrical plastic moulds and set at room temperature for at least 48 hours before analysis. Samples with MD were analysed after 4 days to give sufficient time for helix aggregation (Kanyuck et al., 2019). Kappa-carrageenan and iota-carrageenan contained an added 2.68 mM KCl to reach gelation. Sodium alginate was gelled by the diffusion method (Draget, 2009) with 91 mM $CaCl_2$ and formulated at a higher glucose concentration (40%) to account for loss during the gelation preparation.

Table 5.1. A summary of the hydrocolloids used in formulation of the carbohydrate gels.

Gelling agent	**Source**	**Conc.**	**Gel preparation**
Agarose	Type A9539, Sigma Aldrich	2%	Powder was dispersed and heated in water at 90 °C for 30 minutes
Alginate	Sodium type, Sigma Aldrich	2%	Powder was dispersed and heated in water at 90 °C for 30 minutes and then gelled by diffusion method in a 91 mM $CaCl_2$ solution
Gelatin	Type A, Sigma Aldrich	2%	Powder was dispersed and heated in water at 50 °C for 30 minutes
High acyl gellan gum	CP Kelco LT100	0.25-3%	Powder was dispersed and heated in water at 90 °C for 2 hours
iota-carrageenan	Sigma Aldrich	2%	Powder was dispersed and heated in water at 90 °C for 30 minutes and then 2.68 mM KCl was added and immediately poured into moulds
kappa-carrageenan	Sigma Aldrich	2%	Powder was dispersed and heated in water at 90 °C for 30 minutes and then 2.68 mM KCl was added and immediately poured into moulds
Low acyl gellan gum	CP Kelco F	0.25-3%	Powder was dispersed and heated in water at 90 °C for 2 hours

5.2.3. Release measurements

The method for measuring release of carbohydrates from gels followed the procedure by Koh et al. (2009) with some modification. Gels were cut into 4 pieces of ~1 cm^3 each (5 g ± 1 g). To prevent amylase from interfering with the refractive index measurement, gel pieces were placed within a dialysis tubing membrane of molecular weight cut-off 14 kDa (MEMBRA-CEL MD44-14). Amylase isolated from Aspergillus oryzae has been found to have molecular weights of 51 kDa (sedimentation and diffusion) and 49 kDa (gel filtration) and thus is too large to cross the membrane. Membrane clips were used to seal the gel sample and 5mL of amylase solution (or water when amylase was not used) within the dialysis tubing. The sample pouch was added to a volume of 150 mL of DI water pre-warmed to 37 °C inside plastic bottles with lids. The apparatus was held in a shaker (Sciquip, Newtown, UK) at 37 °C with rotation of 200 RPM for the duration of the experiment. A schematic of the experimental setup is shown in Figure 5.1. At each time point, 0.5 mL from the bulk was removed for measurement by refractive index (Rudolph research J357 automatic refractometer from Hackettstown, USA) and was returned to the bulk phase. Refractive index is a measure of the relative speed of light in a solution and is linearly related to sugar concentration. Calibration curves for glucose and maltose were used to calculate the sugar concentration in each sample by the refractive index measurement.

Measurements were normalized to the 'percent of total carbohydrates released' by dividing by the amount of carbohydrate known from the sample mass. A 'total release' value was measured after 48 hours. Initial experiments showed the sugar concentration did not increase after the 48 hour time point. A 90 minute time point is compared between samples

as an indication of the relative rate of digestion. This time point has also been shown to have the highest correlation with glycemic index (r=0.909) (Goñi et al., 1997).

Samples containing MD utilized a triggered release by addition of α-amylase to mimic human digestion. The enzyme α-amylase cleaves linear carbohydrate chains into maltose units (Butterworth et al., 2011). A stock solution of 100 U/mL amylase was prepared by dispersing the powder in DI water at room temperature for 30 minutes. 5 mL of the amylase solution was added to the dialysis tubing to reach an activity of 500U. The dialysis tubing was then sealed with a clip and placed into the bulk water phase at 37 °C within 5 minutes. Amylase concentrations in human saliva have wide variability based on time of day, most recent meal, and also the individual. The value of 500 U was chosen because it is within the range of human salivary enzyme activity (Mandel et al., 2010) and similar to the concentration used by Koh et al. (2009) and (Janssen et al., 2009).

It should be acknowledged that *in vitro* tests such as this can only approximate differences between samples. Amylase sourced from porcine or *Aspergillus oryzae* have shown minor differences to human amylase, but their use allows for consistent comparison between experiments. Some deviations should be expected, so for true glycemic index human tests should be used. However, true human experiments also have natural variability in oral processing, enzyme concentrations, hormones, and residence times in the stomach and intestine (Dhital et al., 2017). For comparison between different samples, the use of any of the amylases has shown to be effective.

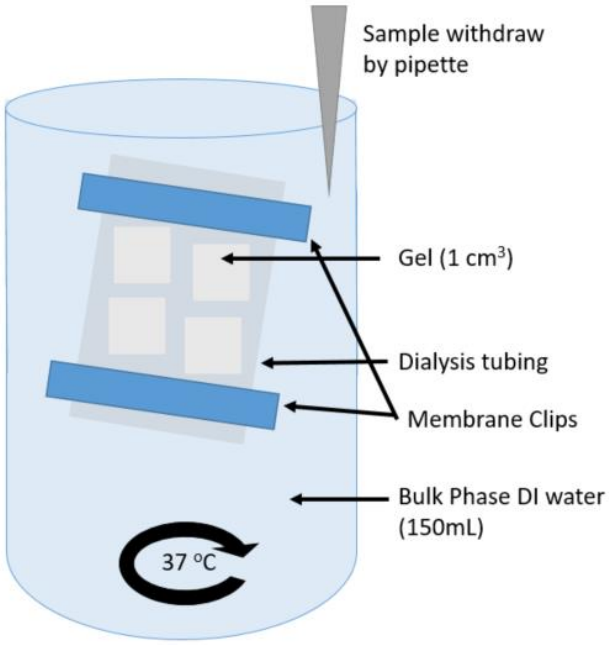

Figure 5.1. Diagram of release experimental setup showing the gels within dialysis tubing and inside of a larger bulk phase (150 mL) which was shaken at 200 rpm at 37 °C. Method was adapted from Koh et al. (2009).

5.2.4. Modelling of glucose release

Glucose concentrations measured after 24 hours had reached the predicted value (with ± 5% error) and were thus normalized to account for natural sample variability with the equation:

$$\text{Released Glucose} = M_t/M_\infty \qquad \text{(Eq. 5.1)}$$

Where M_t is the measured concentration at time 't' and M_∞ the final maximum concentration. The only sample with greater than 5% error was sodium alginate which was expected to lose some glucose during the gelation methodology (diffusion of calcium ions into the alginate solution along with diffusion of glucose out). The collected data was then fitted to a power law model and the Peppas-Sahlin Model. As the models are not able to

account for the lowering difference in concentration gradient over time, data was only fitted below 60 % of the release (the model assumes steady-state). These were then compared to a COMSOL fit of Fickian diffusion within the gel which was able to account for changing concentrations.

Power law model: A simple exponential model was fit using Microsoft Excel:

$$M_t/M_\infty = k*t^n \quad \text{(Eq. 5.2)}$$

Where 'k' is the rate constant specific to the gel formula and 'n' the diffusional exponent (Siepmann and Peppas, 2011).

Peppas-Sahlin model: Release curves were also fit to the model proposed by Peppas and Sahlin (1989). An equation with the following form was fit to the release profiles:

$$M_t/M_\infty = k_1*t^{0.45} + k_2 *t^{0.9} \quad \text{(Eq. 5.3)}$$

Where k is the rate constant where $k_1*t^{0.45}$ represents the Fickian diffusion and $k_2 *t^{0.9}$ the case II transport contributions for a cylindrical shape (Peppas and Sahlin, 1989; Siepmann and Peppas, 2011). Fickian diffusional describes the release of an active caused by a concentration gradient while the case II transport mechanism is dictated by a transition of the polymer which changes the release rate of the active (Peppas and Sahlin, 1989; Siepmann and Peppas, 2011). Similar to the single exponential model, the model is only valid for the initial 60% of glucose release to avoid the effects of lowering differences in concentration gradients. The biexponential regression was fit using SigmaPlot (Version 12.5 SYSTAT Software, USA). Proportional contributions were calculated using the equations

proposed by Peppas and Sahlin (1989). The percentage of release corresponding to Fickian release (F) is calculated by the equation:

$$F = 1/ (1 + (k_2/k_1)*t^{0.45}) \quad \text{(Eq. 5.4)}$$

and contribution of the relaxation component (R) was calculated by the equation:

$$R = (k_2/k_1)*t^{0.45}*F \quad \text{(Eq. 5.5)}$$

The percent contribution was calculated by the ratio of each coefficient for each time point.

COMSOL model: The engineering software COMSOL (COMSOL Inc. Burlington, MA, USA), was used to predict diffusion of glucose using the experimental dimensions and concentration gradients. The flux of glucose from within the gel (into the water) was calculated by Ficks' law of diffusion using the dimensions of the objects (shown in Figure 5.1) and an initial concentration of 2.38 M (2381 moles/m^3) in the gel and 0 in the water. Gels were surrounded by a water region of 150 mL with a diffusivity of (1 m^3/s) meaning practically that mixing was instantaneous. A thin mesh was drawn around the gel to ensure release only occurred at the surface of the gel and diffusion was modelled to the edges of the gel. The model was fit for a single cube of gel (1 mL) with the measured values adjusted by a factor of 0.25 for simplicity. A diffusion coefficient of glucose in water was 6.0 x 10^{-10} m^2/sec was obtained from literature (Stein and Litman, 2014). The model accounted for changes in flux with the changing concentration gradients (which the other models do not

5.2.5. Swelling

Swelling of gellan gum gels was measured by increases in mass after soaking in aqueous solutions. Gels were cut into ~20 mm height pieces from the cylindrical moulds and the

mass weighed to 7.5 ± 1 g. The gel was then placed into 150 mL of DI water at room temperature. At each time point, the gel was removed using a strainer, patted dry to remove surface water, and weighed. The amount of swelling was determined from the ratio of initial mass to final mass by the equation:

$$\text{Swelling Ratio} = M/M_0 \quad \text{(Eq. 5.6)}$$

where M is the measured sample mass after swelling and M_0 is the initial mass. These parameters were chosen to mimic the values used during release studies.

5.2.6. DSC

Gelation of maltodextrin was studied by measuring the enthalpy and entropy using a μDSC3 evo (Setaram Instrumentation, France). Samples were added in the sol phase (hot) to the sample vessels and held for 4 days at room temperature prior to analysis to allow sufficient gelation of the MD component (Kanyuck et al., 2019). A heating and cooling cycle began with a hold at 5 °C for 10 minutes and then increased at 1°C/min up to 95 °C. After a 10 minute hold at 95°C, the temperature was cooled at 1°C/min down to 5 °C.

5.2.7. Statistical Analysis

All samples were measured in at least triplicate and data are presented as means ± standard deviation. Release curves were repeated four times for each sample. Error bars show one standard deviation above and below the mean value. On the bar charts, different letters suggest significantly different mean values. A t-test with a p-value of 0.05 was used to determine which samples were significantly different.

5.3. Results and discussion

Of the many factors to consider in predicting the release, the carbohydrate MW is of crucial importance (Nishinari and Fang, 2021). To examine this effect, carbohydrates of varying molecular weight (MW) were compared by release profiles from HA gellan gel (Figure 5.2A) and LA gellan gum (Figure 5.2C). Small molecules were represented by glucose (180 Da) and maltose (342 Da) and showed complete release from the gel within 48 hours. The rate of release was slower for maltose because it is a larger molecule than glucose. Larger molecules are expected to have slower diffusion coefficients due to the greater hydrodynamic radius (Nishinari and Fang, 2021). MDs are known to contain a wide range of different molecular sizes with a bimodal distribution and the distribution of the DE 2 MD is centred at 10,000 Da and 492,000 Da (Loret et al., 2004a). Both MDs used (DE 2 and DE 10) led to a slower and incomplete release of carbohydrates from the gels. Molecules smaller than the pores are able to diffuse out of the gel network while larger molecules are trapped (Lin and Metters, 2006; McClements, 2017). The small amount of carbohydrates measured without addition of an enzyme (10% and 17% for DE 2 and 10, respectively) reflect the proportion of molecules which were small enough to diffuse out of the gellan gum gel network. Addition of amylase, the enzyme which cleaves maltose units from a larger carbohydrate chain, considerably increased the amount (to 44% and 63% for DE 2 and 10, respectively). Based on the work of (Dhital et al., 2017), amylase was thought to enter the gel network and break the MD into maltose molecules which were then small enough to diffuse out of the gel. Starch, a much larger carbohydrate, is well known to need this enzyme to break into saccharides that can be released from a gel (Koh et al., 2009; Butterworth et al., 2011; Dhital et al., 2017).

Two clear pathways of release were established based on the size of the carbohydrate; diffusion based release of the small molecules, and an amylase-triggered release for large molecules that cannot diffuse out of the gel network. The following work will be split into subsequent sections to examine effects of gel network type on the release of small (5.3.1) and medium sized aggregated (5.3.3) carbohydrates. Glucose was selected to be representative of small carbohydrates and DE 2 MD chosen for the enzyme-triggered release.

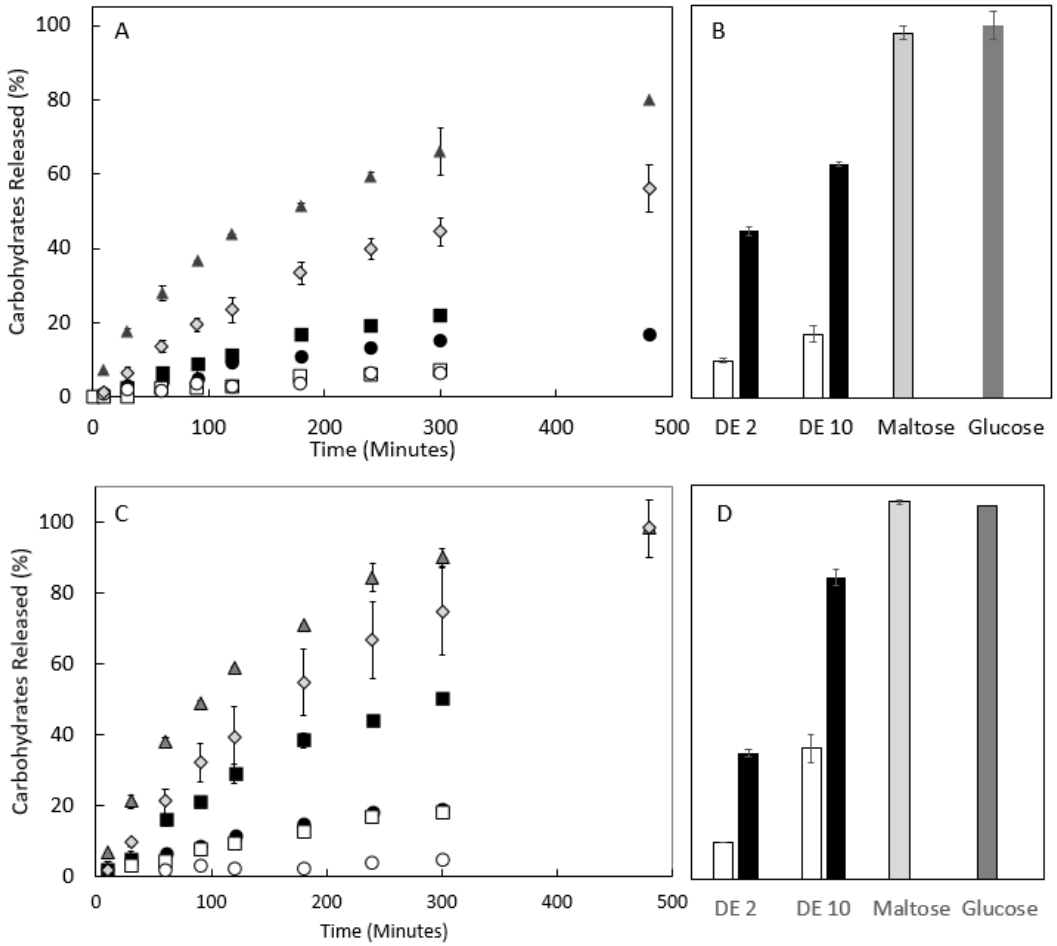

Figure 5.2. Release of carbohydrates from 1% HA gellan (A) and 2% LA gellan (C) gels formulated with 30% glucose (▲), maltose (◊), and with MD DE 2 (●) and DE 10 (■) with amylase (black) and without (white). Total release from the gels at 48 hours shown for 1% HA gellan (B) and 2% LA gellan (D).

5.3.1. Diffusion based release of small MW carbohydrates

Glucose was chosen as a model for small molecule carbohydrates and the release from different gel structures (polymer types and concentration) were compared. All samples reached 100 ± 5% after 24 hours and are shown normalized in the graph to decrease the impact of variability in the gel formulation. Changes in gellan concentration led to significant differences in the release speed ($p < 0.05$), however the differences of a few percentage points had minimal practical differences (Figure 5.3). Increases in concentration of polymer are known to decrease the release rates of small molecules, but this is typically quite a small shift (10-20%). This trend was observed for sucrose from agar gels (Wang et al., 2014; Yang et al., 2015), salt from LA gellan and gelatin (Mills et al., 2011), and dendrimers of 3 and 8 nm from kappa-carrageenan (Lorén et al., 2009b). Higher polymer concentrations are expected to decrease the pore size within gels and provides a greater physical barrier. For glucose this is minimally important because the pores are already much larger and the hydrocolloid such a small proportion of the mass (Mills et al., 2011). Larger actives (3 and 8 nm) showed progressively a greater slowing from a kappa-carrageenan gel network (Lorén et al., 2009b).

A comparison of LA and HA however shows a difference between these two polymer types, irrespective of the concentration (Figure 5.3). Both HA and LA gellan gum form physical gels by double helix formation upon cold-setting and do not melt at 37 °C or below (Morris et al., 2012). Removal of acyl groups for the LA gellan yields a completely different gel texture than HA gellan due to differences in helix aggregation which may have been a factor. The surface area for each gel was matched in these experiments (controlled in the sample

preparation). After 24 hours, all of the glucose (within a reasonable standard deviation of +/- 5%) had been released which suggested there was no significant binding between HA gellan and glucose to cause the lower diffusion rates and therefore the difference appeared to be kinetic in nature.

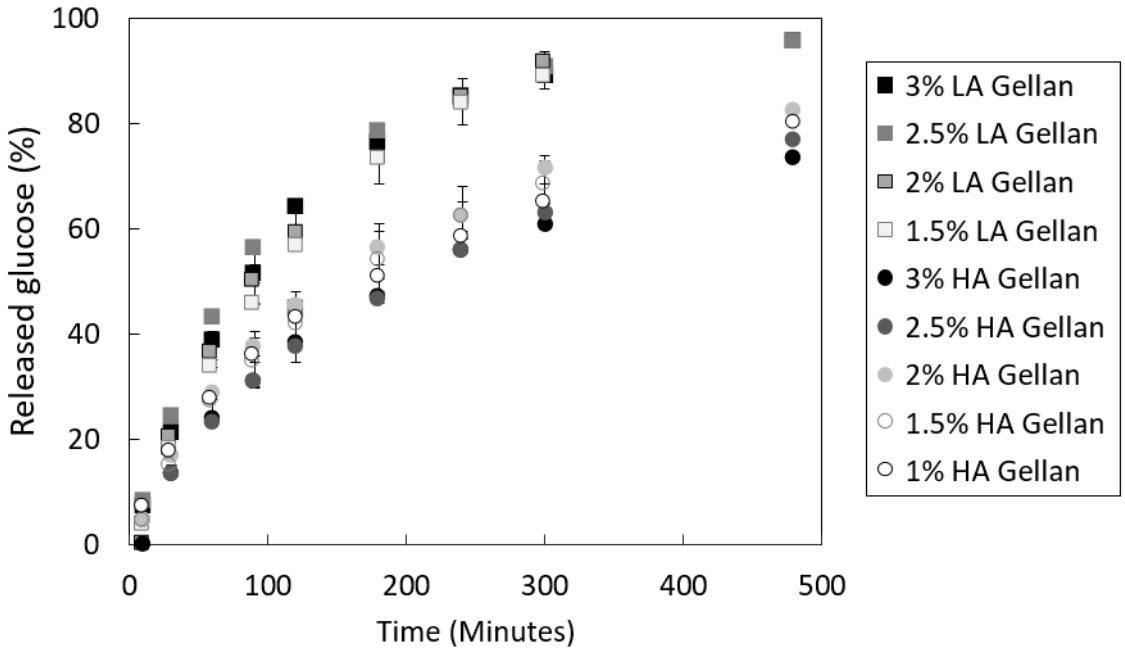

Figure 5.3. Concentration dependence of release profiles from LA gellan (squares) and HA gellan (circles) formulated with 30% glucose.

Mathematical modelling of release profiles has become a popular method for understanding the mechanisms of release from gels (Lin and Metters, 2006). Comparison of models for HA and LA gellan gum release were used to elucidate the origin or mechanism of the difference. Quality of fit for the models is shown in Figure 5.4 and the equations displayed in Table 5.2. The commonly used Peppas-Sahlin equation (Eq 5.3) models the release of an active as a summation of the Fickian diffusion ($k_1 * t^{0.45}$) and case II release ($k_2 * t^{0.9}$). As the model cannot account for changes in concentration, analysis should only be

conducted on the initial 60% of the release profile. This was reflected in the curves of Figure 5.4 which end at the 60% release point.

Comparing the importance of each coefficient (k_1 for the Fickian contribution and k_2 for relaxational case II contribution) was used to give evidence of the type of release (Siepmann and Peppas, 2011). According to this model, the Fickian or case II contribution can be modelled over time to show any changes in type of release. Relative contributions of each type, and how that shifts over the release profile, are shown in (Figure 5.5). For LA gellan gum, the release was suggested to be largely case II driven (Figure 5.5) which could also be predicted from the diffusional exponent (n) value of the single power exponent of 0.92 which is near to that of 'pure relaxation' of a 0.9 value. Alternatively, the single n for HA gellan (0.76) was between that of Fickian and case II and was reflected in the relative greater Fickian contribution (Figure 5.5).

The Peppas-Sahlin model suggested the HA gellan release profile was more similar to a Fickian release while the LA gellan was predominately dictated by case II release. Case II release is typically indicative of gel swelling which alters the release kinetics of the active (Peppas and Sahlin, 1989). In Chapter 6, the swelling of the LA gellan was found to equilibrate after ~180 minutes with a swelling ratio of 1.2 while HA gellan gum equilibrated after ~ 48 hours with a swelling ratio of 5.0 (Kanyuck et al. 2021b). The quicker equilibration of LA gellan gum swelling could be reflected in the dominance of the case II profile. However the higher magnitude of swelling for HA gellan gum (swelling ratio of 1.2 vs 2.1 at 180 minutes) was not reflected. Mathematically, the release from HA gellan was more similar to Fickian diffusion. It is possible that swelling of LA gellan effected the release

kinetics while the swelling of HA gellan did not affect the release kinetics. Further examination and a comparison to other gelling agents was necessary.

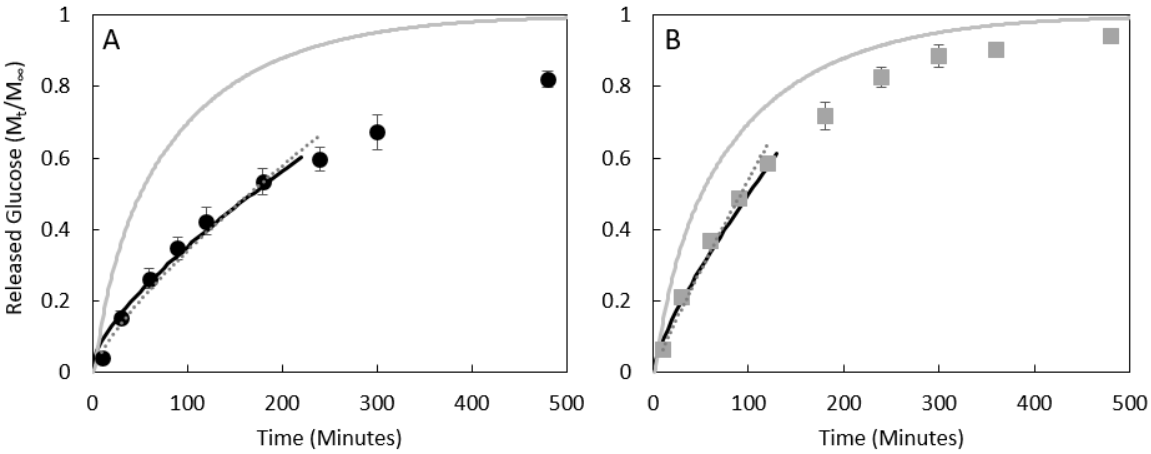

Figure 5.4. Modelling glucose release for 2% HA gellan gum (A) and LA gellan gum (B) comparing the Peppas-Sahlin Model (solid black line), single exponential (dashed grey line), and COMSOL mass transfer model (grey line). Equations are shown in Table 5.2.

Table 5.2. Equations modelled to the release of glucose shown in Figure 5.4.

Model	HA Gellan	LA Gellan
Peppas-Sahlin	$M_t/M_\infty = 0.028*t^{0.45} + 0.002*t^{0.9}$	$M_t/M_\infty = 0.017*t^{0.45} + 0.007*t^{0.9}$
Single Exponential	$M_t/M_\infty = 0.010*t^{0.76}$ $R^2 = 0.98$	$M_t/M_\infty = 0.008*t^{0.92}$ $R^2 = 0.99$

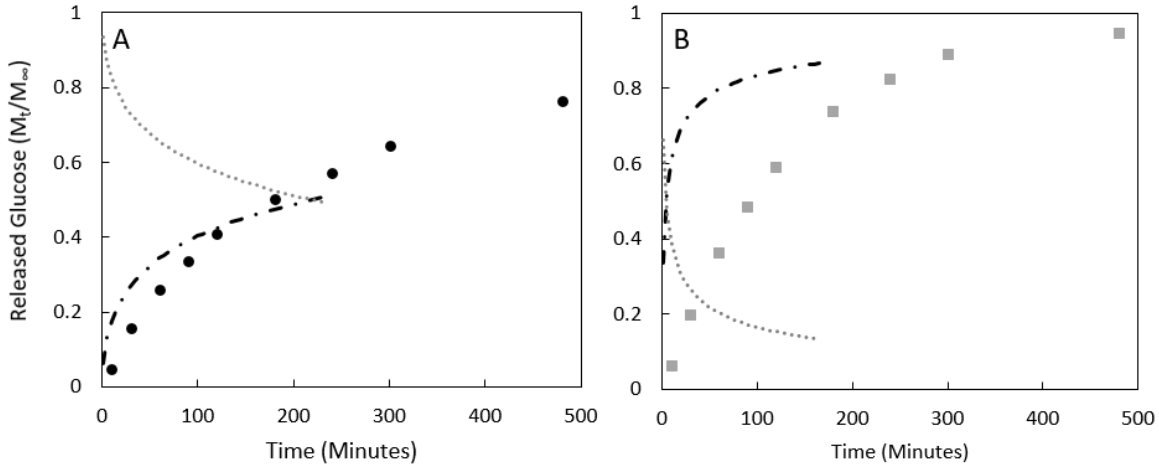

Figure 5.5. Proportional contributions of Fickian diffusion (·····) and case II transport (– · – · –) mass transfer based on the Peppas-Sahlin Model for 2% HA gellan gum (A) and 2% LA gellan gum (B).

Using a chemical engineering modelling software (COMSOL) and considering dimensions, initial concentrations, and changes during release a curve from 'pure diffusion' through the gel can be predicted for this specific system. The software was able to account for non-steady state behaviour and used the literature diffusion coefficient (D) of 6.0 x 10^{10} m^2/s (Stein and Litman, 2014). Higher similarity was observed between the expected pure diffusion and LA gellan, while the release from HA gellan was clearly slower. A marginal slower release from a hydrogel was expected due to the steric obstacle of the network by 14-30% (Mills et al., 2011). A shift farther from pure diffusion for the HA gellan gel suggested a stimuli-driven change to the gel was responsible for the slower release behaviour.

With evidence from modelling that LA gellan was closer to a 'typical' diffusion pattern, glucose release from other gelling agents were compared to give context to the different gel network structures. Release profiles from gelatin, alginate, and kappa-carrageenan are compared to that of HA and LA gellan gum in Figure 5.6. Release from alginate and kappa-

carrageenan were similar to LA gellan gum. An alginate gel network is held together by chemical crosslinks (calcium bridges) between chains (Draget, 2009) while kappa-carrageenan forms a gel network through potassium induced aggregation of double helices (Morris et al., 1980). These three different gel structures did not appear to affect the release of glucose. At the measurement temperature (37 °C) the gelatin network melted and caused a quicker release profile than any of the other gelling agents. The other gelling agents did not melt. In comparison, the behaviour of HA gellan was unprecedently slower than any of the other gelling agents. Recent work has shown that swelling of HA gellan was responsible for the slower release of glucose compared to LA gellan (Kanyuck et al., 2021b). This stimuli-driven swelling was proposed to be the cause of the slower release from HA gellan gum and will be discussed in the following section (5.3.2). For diffusion-based release, network structure of the hydrocolloid was of minor importance and differences were only observed from stimuli-driven changes to the gel, specifically melting and swelling.

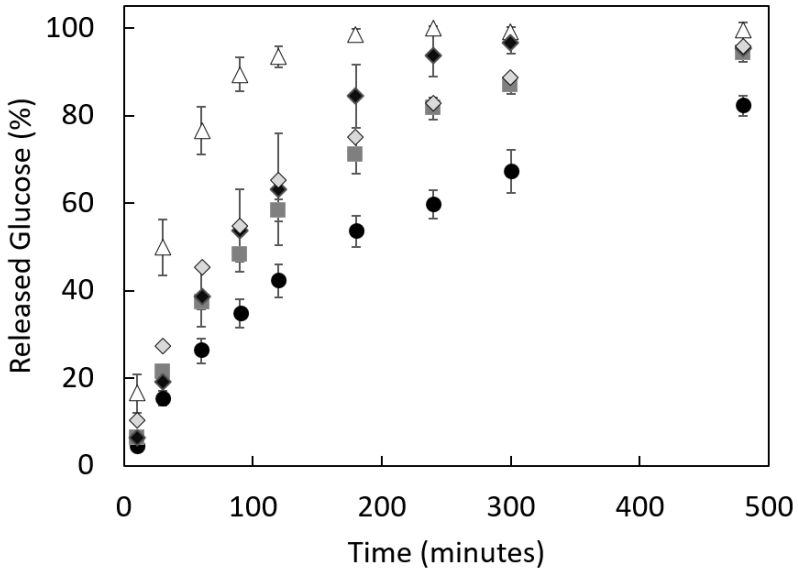

Figure 5.6. Release of glucose from 2% HA gellan gum (●), LA gellan gum (■), alginate (◆), kappa-carrageenan (◆), and gelatin (△) at 37 °C.

5.3.2. Impacts of gel stimuli-driven structural changes on release

Melting: Stimuli from the environment which cause structural changes to a hydrocolloid gel, such as swelling, dissolution, and erosion can modify the release profile (McClements, 2017). The quicker release of glucose from gelatin was hypothesized to have been caused by the melting at the analysis temperature of 37 °C. The experimental procedure was repeated at 25 °C which is below the melting temperature of gelatin. When gelatin did not melt, the release was similar to LA gellan gum (Figure 5.7). Thus the inherent structure of gelatin did not distinguish from the other gels but instead the temperature-driven structural change. Previous work has also confirmed that environmental temperatures which cause melting of a gelatin gel showed much faster release of salt than release at a temperature that did not cause melting (Mills et al., 2011). Melting of hydrocolloids gels was a stimuli-driven structural change that impacts release from gelatin.

Swelling: In many cases, swelling of a polymer increases the release rate of a small molecule due to the increased pore size of the hydrocolloid (McClements, 2017). In the case of HA gellan, swelling actually slowed the release of glucose (Kanyuck et al., 2021b) and has the potential to impact larger carbohydrates. Swelling kinetics of HA gellan is shown in Figure 5.8 for formulations with glucose, maltose, DE 10 MD, and DE 2 MD. There was significantly less swelling with inclusion of glucose or DE 10 MD, but the mass had still doubled after 180 minutes. The aggregates formed by the DE 10 MD decreased the swelling more than glucose or maltose (Figure 5.8). Very clearly the network formed by DE 2 MD inhibited the swelling of the mixed gel. This MD (DE 2) is known to form large and bulky aggregates within the HA gellan gum network (Kanyuck et al., 2021a). Not surprisingly, these appeared to have

prevented much of the typical swelling for HA gellan. Slower release of glucose, maltose, and DE 10 MD was subsequently suspected for HA gellan due to a decreased mass transfer caused by swelling (Kanyuck et al., 2021b). Swelling of a gel causes a greater volume and larger dimensions, and subsequently the slower release was thought to have been caused by a lower effective concentration inside the gel and a greater distance for the active to travel (Kanyuck et al., 2021b). This effect was observed by comparing HA gellan and LA gellan gum release (Figure 5.2). A slower release from these carbohydrate sources (glucose, maltose, and DE 10 MD) was measured for HA gellan and emphasised the importance of this stimuli-response. Just as the environmental temperature dictated melting of gelatin, the osmotic environment dictated HA gellan swelling (Kanyuck et al., 2021b). These stimuli-responsive changes were shown to be crucial for predicting release profiles and specific conditions were of critical importance.

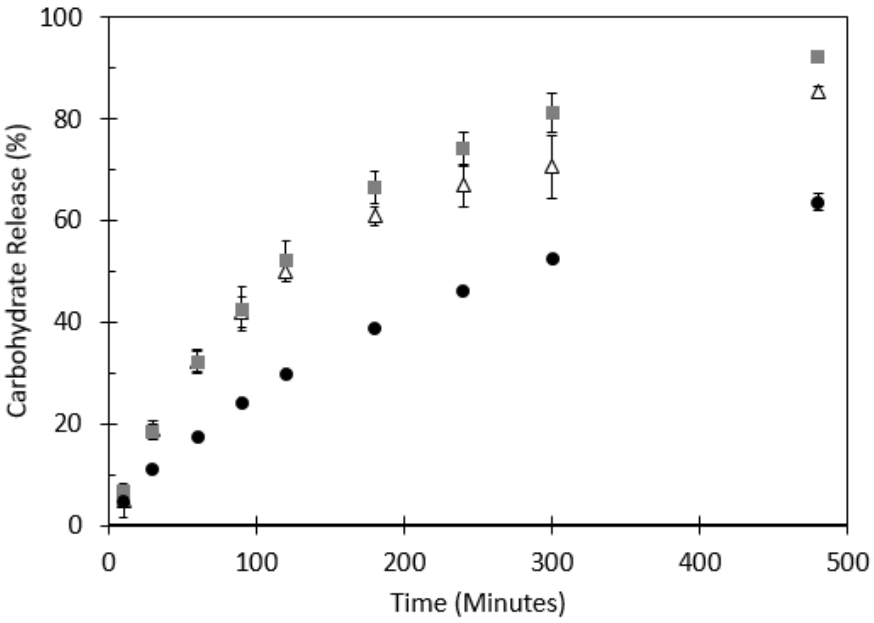

Figure 5.7. Release of glucose from gelling agents at 25 °C to compare the non-melting 2% gelatin (△) to 2% LA gellan (■) and HA gellan (●) gum.

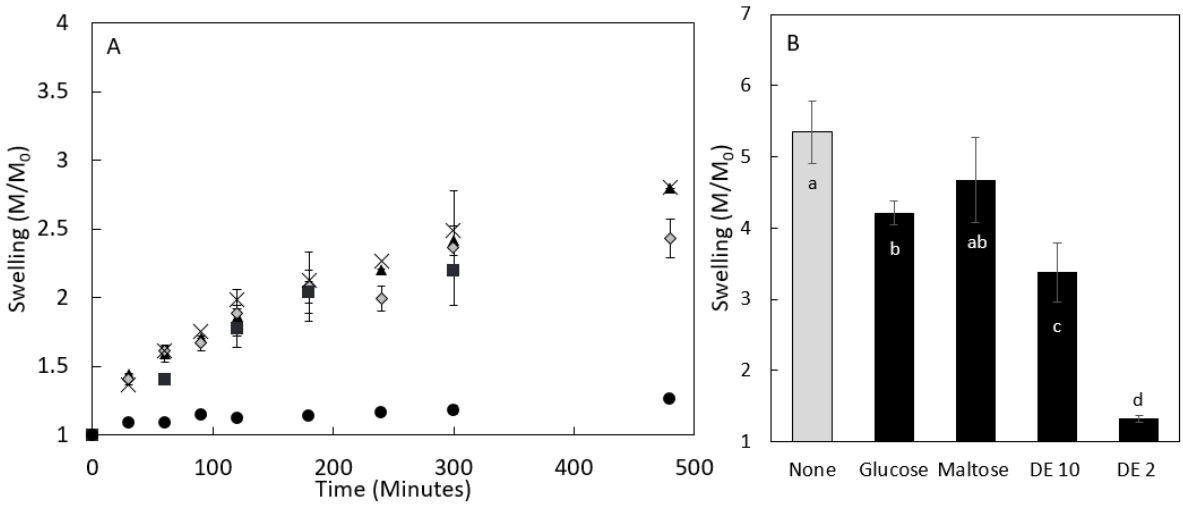

Figure 5.8. Swelling of 1% HA gellan during the timeframe of release experiments (X) compared to formulations with 30% glucose (▲), maltose (◊), and with MD DE 2 (●) and DE 10 (■). Part B displays the swelling after 48 hours.

5.3.3. Amylase-triggered release of MD

Addition of the digestive enzyme amylase was essential for the release of MD from gellan gum gels. Only 10% of the DE 2 MD chains were small enough to diffuse out of the 1% HA gellan gum gel, while addition of the hydrolysing enzyme allowed 44% of the carbohydrates to be release from the gel (Figure 5.2). Similarly for 1% LA gellan gum, 40% was released with amylase but only 10% without. The ability of amylase to enter the gel network and reach the MD to begin cleavage was of chief importance (Dhital et al., 2017). However, even with addition of amylase more than half of the carbohydrate was resistant in the experiment. Aggregates of MD were hypothesized to be the source of enzyme resistance and will be explored. Impacts of hydrocolloid gel structure on the availability of these MD aggregates will then be explored with amylase-triggered release.

5.3.3.1. MD aggregation

Self-aggregation of MD was hypothesized to play a role in the carbohydrate availability. This MD (DE 2) is well characterized in literature and known to form aggregates of double helix that form a gel at high enough concentrations (15-20%) by connection of these dense aggregates (Kasapis et al., 1993a; Loret et al., 2004a; Kanyuck et al., 2019). Holding temperature during gelation is known to affect the size and enthalpy of the aggregates formed (Kanyuck et al., 2019). Exploiting that knowledge, the impacts of MD aggregation on availability for amylase cleavage were determined by varying the gelation temperature. Higher temperatures formed fewer aggregates but at a higher entropy which was thought to be from the participation of longer chains in aggregate formation and connectivity (Kanyuck et al., 2019). Release of 30% and 40% MD gels formed at different temperatures is shown in Figure 5.9. For both concentrations of MD, lower carbohydrate release was measured for gels formed at lower temperatures. Correlation between enthalpy (Kanyuck et al., 2019) and carbohydrates released (R^2 = 0.82) suggested the helices contributed to the enzyme resistance. Structural composition was the same between gels (linkages and branch points) and all release experiments were conducted at the same temperature (37 °C) so the differences showed how aggregation impacted the accessibility of carbohydrates to amylase. Aggregation of MD was thought to function similarly to retrograded starch. Recrystallization and retrogradation of starch resulted in amorphous structures with inhibited enzyme affinity because of the irregular structure (Gidley et al., 1995b; Butterworth et al., 2011; Dhital et al., 2017).

An aggregation effect was also seen in mixed gels of MD with HA gellan gum. Higher gelling temperatures resulted in greater percentages of released carbohydrates (Figure 5.9). The presence of the HA gellan gum network also decreased the amount of available carbohydrates, and at lower temperatures there was a greater inhibitory effect. At 60 °C the HA gellan network decreased availability by 11% while at 5 °C the difference was 24%. Based on the 90-minute values which were lower than either concentration of MD alone, the HA gellan network slowed amylase diffusion through the gel irrespective of the gelling temperature. At lower temperatures the gel network was more inhibitory and possibly due to a greater steric inhibition from more MD aggregates. The structure of this mixed gel consists of MD aggregates within pores of the HA gellan network (Kanyuck et al., 2021a). More MD aggregates would add considerable bulk within the HA gellan network that appeared to have blocked and prevented amylase from reaching as many aggregates in the mixed gel. These factors emphasise the contributions of MD aggregation and a gel network exclusion effect in the release of carbohydrates from mixed gel formulations.

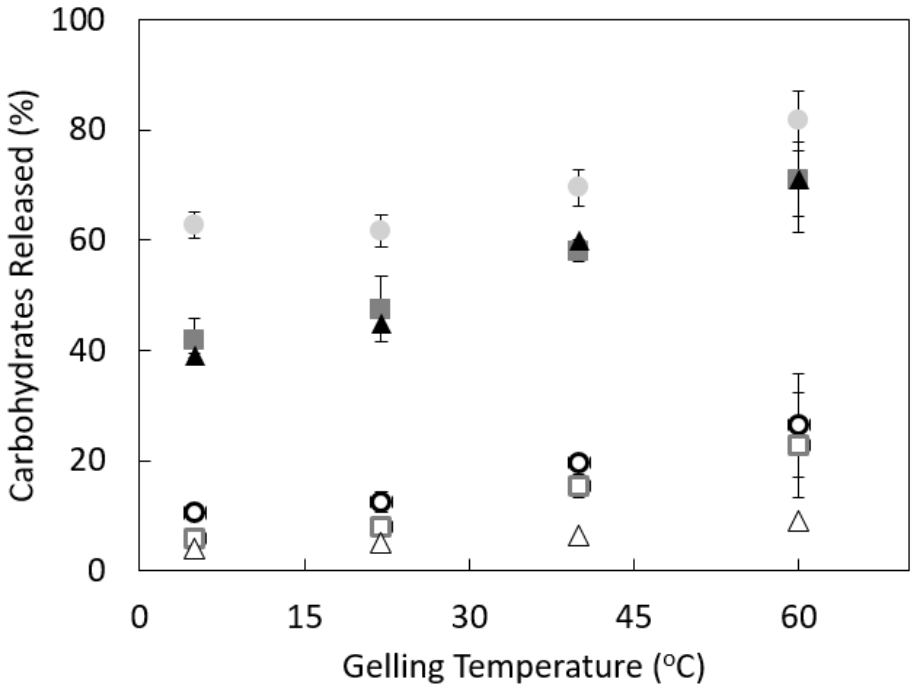

Figure 5.9. Carbohydrate release by amylase hydrolysis compared by gelling temperature for DE 2 MD at 30% (●), 40% (■), and 30% with 1% HA gellan gum (▲). Percentage released at 90 minutes shown by open symbols and final release shown by filled symbols. Samples were held at the indicated gelling temperature for 4 days prior to measurements and release experiments were all conducted at the same temperature (37 °C).

5.3.3.2. Gelling agents

MD gels were formulated with various gelling hydrocolloids to examine their structural effects on MD availability. Different concentrations of HA and LA gellan gum at a constant 30% MD and the release profiles are shown in Figure 5.10. Addition of either HA or LA gellan gum decreased the speed of carbohydrate release as well as the total availability compared to a MD-only gel. Higher concentrations also decreased the total carbohydrate availability (Figure 5.10B). Unlike the similarity observed for glucose release, a smaller pore size from greater concentrations of polymer decreased the speed of release. The slower release from HA gellan gum was likely due to swelling from the greater distance amylase needed to travel into the gel (Figure 5.8). Additionally, a lower amount of total carbohydrate was released

with higher concentrations of gellan gum. Even at concentrations below gelation of gellan (0.5% for LA and 0.25% for HA) the gel network caused a decrease in availability compared to MD alone (Figure 5.10). Higher concentrations of gelling agents produce gels which have a higher modulus, more helices, and a smaller pore size (Djabourov et al., 2013). As shown previously (section 5.3.1), this change in gel network density had no significant effect on the diffusional release of glucose because it was much smaller than the pores. However, the behaviour of MD was different. Release was likely prevented because of entrapment of MD aggregates within these pores and a network density that limited the accessibility of amylase to reach all parts of the gel. For gels that slow the release, typically the polymer slows the movement of critical lyzing enzymes into the gel (McClements and Xiao, 2014). A comparison to other gelling agents with differing network types and structural arrangements, was thought to also have an impact on MD availability.

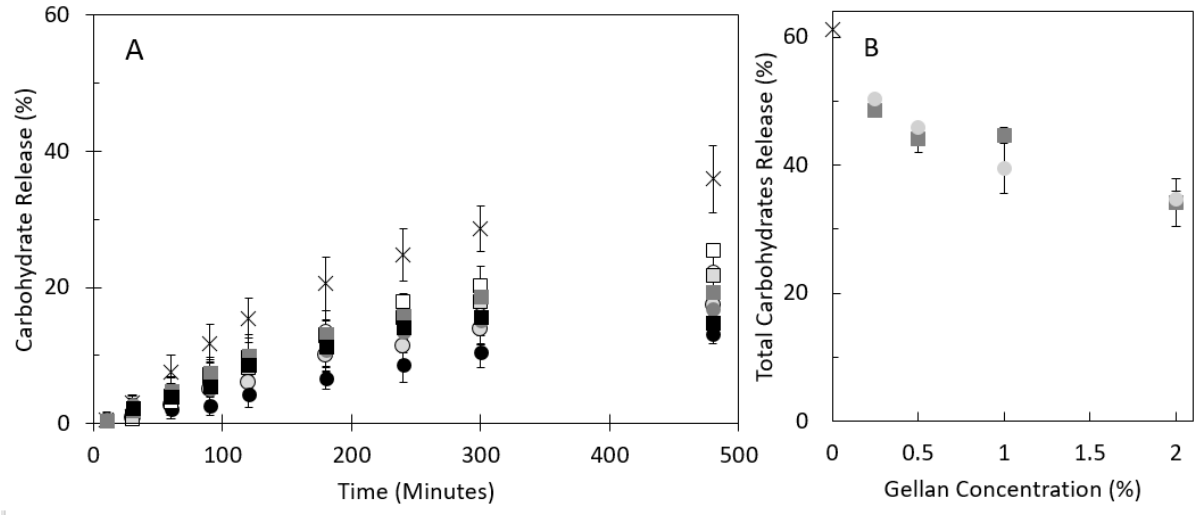

Figure 5.10. Release profiles (A) of 30% DE 2 MD without any gelling agent (X), HA gellan gum at 0.25% (○), 0.5% (●), 1% (●), and 2% (●), and with LA gellan gum at 0.25% (□), 0.5% (■), 1% (■), and 2% (■). Part B displays the total release after 48 hours for only MD (X) and each concentration of HA gellan (●) and LA gellan (■).

The structural influence of gelling agents was hypothesized to be based on the type of mixed gel network. Both HA and LA gellan gum are known to form interpenetrating polymer networks (IPNs) with MD and the structures have been described as MD aggregates within pores of the gellan network (Clark et al., 1999; Kanyuck et al., 2021a). Phase separated networks are known to form with gelatin (Kasapis et al., 1993a), agarose (Loret et al., 2005), and carrageenan (Wang and Ziegler, 2009; Gładkowska-Balewicz, 2017). Additionally, gelatin melted at the measurement temperature (37 °C). These network characteristics will be compared to explain the structural influences of the gels on release behaviour. MD with an IPN (HA and LA gellan gum) resulted in the slowest release and the lowest total release (Figure 5.11). Non-melting phase-separated gels (k-carrageenan, i-carrageenan, and agarose) resulted in greater total release than the IPNs but less than MD alone. The phase-separated melting gel (gelatin) released more than with no gelling agent.

For the IPNs, the arrangement of MD aggregates within the pores of the network reasonably could have inhibited amylase movement. Additionally, a more heterogeneous arrangement of the aggregates and inhibition of the formation of large aggregates (Clark et al., 1999; Kanyuck et al., 2021a) could have caused the lower release. Phase separated networks (all characterized as MD continuous at these concentrations) have gelling agent rich domains dispersed amongst a continuous MD phase where the gelling agents is not present (Kasapis 1993, Loret 2005). Separation into these domains means the gelling agent would have had less potential to sterically block amylase movement through the gel. Consequently, the release from phase separated gels was higher than IPNs gels (Figure 5.11). Clustering by network type confirmed structure was an important factor for comparing carbohydrate availability. In other work, hydrocolloids have been shown to

decrease the amylase digestion of retrograded starch, but differences between gelling agents has largely been nominal (no intrinsic ordering or grouping) and the association with mixed gel network type may carry over to starch applications.

Although gelatin forms a phase separated structure, the network also melted at the analysis temperature and was thought to be the cause of the difference from the other phase separated networks. This was confirmed by repeating the release measurement at 25 °C where the profile was less than MD alone and no longer significantly different from the other phase separated network (Figure 5.12). Similarity to the other phase separated networks demonstrated the importance of melting in increasing the total amount released. Melting of a gel network would suggest it was no longer able to slow amylase from entering gel, but the greater total release from gelatin could not be explained as simply.

Fractionation (self-separation) of MD within phase separated biopolymer systems have been observed for agarose (Loret et al., 2005) and gelatin (Kasapis et al., 1993d). One phase contained the larger molecular weight fraction of MD and the other phase the gelling agent mixed with a fraction of the smaller molecular weight MD chains. It was thought that phase separation may have changed the structure of helices to increase the availability of carbohydrates (Kasapis et al., 1993d). Any changes in the MD aggregation and distribution from the gelling agent could have contributed to the enzyme accessibility. DSC was used to measure the melting temperatures and enthalpy of MD to detect any changes in the aggregation behaviour with gelatin (Table 5.3) with thermograms shown in Figure 5.13. From Table 5.3 the network enthalpy of a mixed gel with gelatin was not significantly different than summation of the individual gels. Prior DSC analysis of mixed gels of gelatin

and MD was not able to achieve this resolution (Kasapis et al., 1993a). Enthalpy of MD with HA gellan was demonstrated to be not significantly different than alone (Kanyuck et al., 2021a). No change in enthalpy or melting temperature (Table 5.3) suggested any fractionation of MD did not change the helix or aggregate formation. It was possible that the smaller MW chains that separate do not participate in helix formation and thus the change was not detectable. From these results, mixed gels did not cause a measureable change in the helix formation. This suggests the greater percentage of carbohydrates released from gelatin was caused by an organisational difference. Melting of gelatin regions may have allowed the amylase increased accessibility through the MD continuous network by liquefying the gelatin phase regions. These structural differences of network type with MD were shown to be predictive of the amount of carbohydrate release.

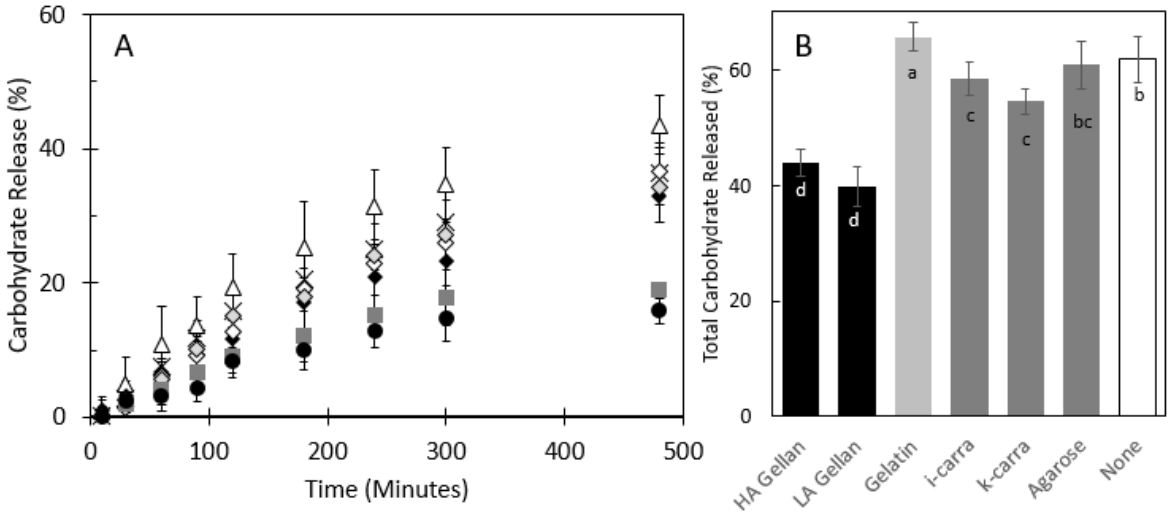

Figure 5.11. Release profiles at 37 °C from mixed gels of 30% MD comparing gelling agents forming and IPN (HA gellan (●) and LA gellan (■)) and phase separated networks (i-carrageenan (◊), k-carrageenan (♦), agarose (♦), and gelatin (△)) and no gelling agent (X). Gelatin melted at the release temperature. Total release (B) is shown for IPN (black), phase separated networks (grey), and no gelling agent (white).

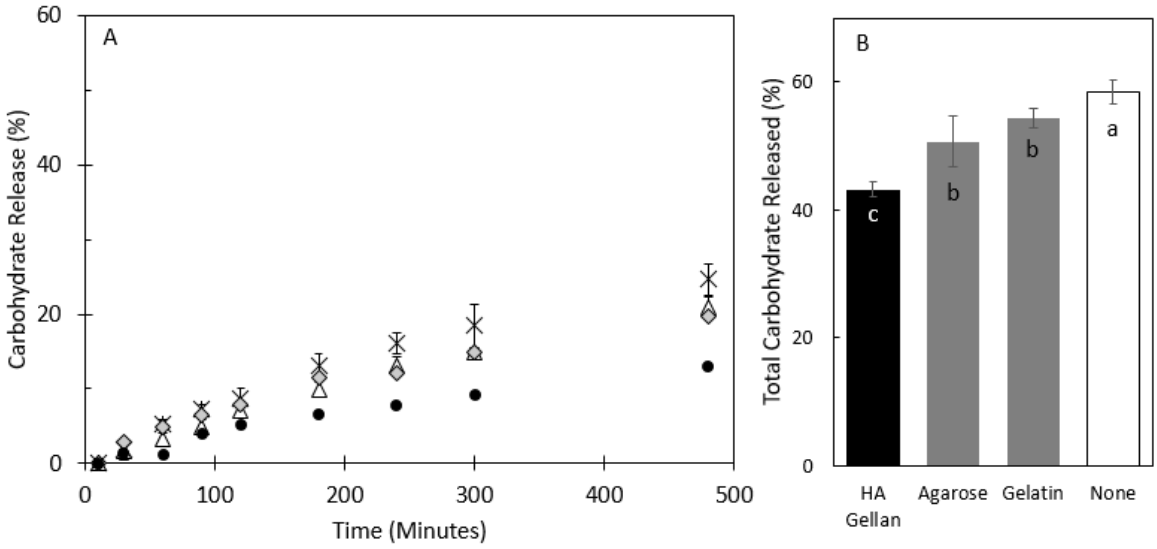

Figure 5.12**.** Maltodextrin release from gelatin (△) at non-melting conditions (25 °C) compared to no gelling agent (X), another phase separated network 1% agarose (♦), and IPN 1% HA gellan (●). Total release (B) and for IPN (black), phase separated (grey), and no gelling agent (white) where lettering indicates significantly different values.

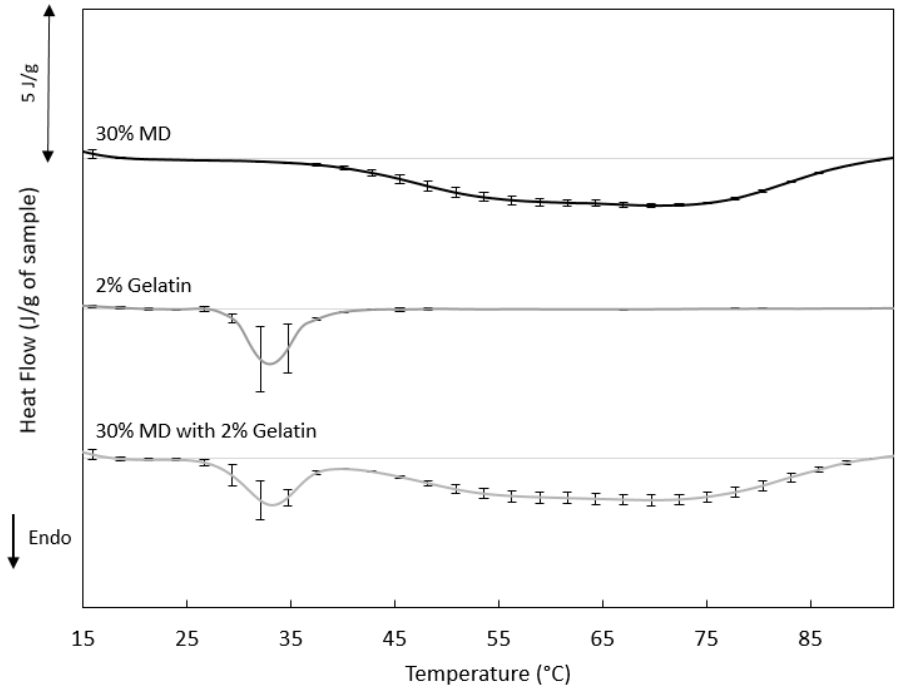

Figure 5.13. DSC heating curves for 30% MD, 2% gelatin, and 30% MD with 2% gelatin after four days of gelling at room temperature. A baseline subtractions was applied and error bars indicate the standard deviation of three unique samples. Error bars primarily represent differences in the enthalpy as there were small standard deviations (0.3°C for gelatin and 2 °C for MD) in the temperature peaks position.

Table 5.3. Peak melting temperatures and enthalpy from DSC heating thermograms for MD and gelatin independently and the mixed gel of both hydrocolloids.

		Gelatin		MD	
	Total Enthalpy	Peak (°C)	Enthalpy (J/g)	Peak (°C)	Enthalpy (J/g)
MD (30%)	3.18 ± 0.2			70 ± 2	3.18 ± 0.2
Gelatin (2%)	0.59 ± 0.2	33 ± 0.3	0.59 ± 0.2		
Summation	*3.77 ± 0.2*				
MD (30%) with gelatin (2%)	3.60 ± 0.3	33 ± 0.3		71 ± 1	

5.4. Conclusion

Carbohydrate size and a hydrocolloid's response to stimuli were shown to be important for all types of release. Gel structure, specifically the network type, was influential for the larger aggregate-forming MD but not for glucose. Glucose offered a simplified system to compare the effects of responses to stimuli (melting and swelling) of hydrocolloid gels on release. The structuring of MD introduced dependencies on amylase accessibility, self-aggregation, and the microstructure of the system. Interestingly, because MD does not undergo gelatinization, the results may provide an indication of the effects of starch retrogradation within hydrocolloid networks on the carbohydrate availability. The complex findings from this simplified two polymer system is another demonstration of the complexity of food digestion when dealing with multiple ingredients. The work presented here provides a framework for formulating and processing to achieve specific carbohydrate release profiles from gels. There was a need to better understand the swelling behaviour of HA gellan gum in comparison to other hydrocolloids, and this work was carried out in chapter 6.

Chapter 6. Swelling of high acyl gellan gum hydrogel: characterization of network strengthening and slower release

_____

Published article

Kanyuck, K. M., Mills, T. B., Norton, I. T., & Norton-Welch, A. B

Carbohydrate Polymers. 2021. (259), 117758.

Abstract

This study examined the mechanism of swelling for high acyl (HA) gellan gum and the impacts on the hydrogel mechanical properties and the release of a model active (glucose). Controlling the material properties and the release of entrapped actives during use in aqueous environments, such as the stomach or bodily fluids, are crucial in designing functional applications. Swelling of HA gellan gum was controlled by varying the osmotic environment with salts and solvents, and effects on the gel network were characterized by uniaxial compression tests, DSC, and rheology. Low ionic strength solutions caused the greatest degree of swelling (up to 400 %) and corresponded to a more brittle gel with a greater modulus and greater network enthalpy. Swelling slowed the release of glucose by decreasing the diffusion flux. The osmotic environment was found to produce different functional properties, and it is crucial to consider these changes in the design of formulations.

Author Contributions

Kelsey M. Kanyuck: Conceptualization, Methodology, Formal analysis, Investigation, Writing - original draft.

Tom B. Mills: Supervision, Writing - review & editing.

Ian T. Norton: Supervision, Funding acquisition, Writing - review & editing.

Abigail B. Norton-Welch: Supervision, Funding acquisition, Writing - review & editing

6.1. Introduction

Hydrocolloid gels are frequently used to create soft-solid structures composed predominately of water in the food, pharmaceutical, and tissue engineering industries. Gellan gum is a carbohydrate hydrocolloid that forms physical gels and is commonly used in each of these industries (Coutinho et al., 2010; Morris et al., 2012; Stevens et al., 2016; Osmałek et al., 2018; Palumbo et al., 2020). Cytocompatibility, easy processability, mucoadhesion, tuneable mechanical properties, and food-grade status offer many attractive benefits for using gellan gum (Morris et al., 2012; Stevens et al., 2016; Palumbo et al., 2020). There are two types of gellan gum available: the native or high acyl (HA) and a modified version termed low acyl (LA). The repeating unit of LA gellan gum is →3)-β-D-glucose-(1 → 4)-β-D-glucoronic acid-(1 → 4)-β-D-glucose-(1 → 4)-α-L-rhamnose-(1→ and HA gellan gum has additional substitutions of glyceryl and acetyl units on the 3-linked glucose (Figure 2.4) (Sworn, 2009; Morris et al., 2012).

Both gellan variants form gels by a coil-helix transition occurring upon cooling (after dispersing in hot water 80-90 °C) (Morris et al., 2012). The acetate group on the HA gellan polymer prevents aggregation of double helix chains and follows a fibrous gelation model through end to end associations (Morris et al., 1996; Morris et al., 2012). The removal of acyl groups from HA gellan yields a completely different gel texture in LA from modification to the helix structure and aggregation mechanism. HA gellan forms a soft and easily deformable gel, while the gel of LA gellan is firm and brittle (Morris et al., 2012). LA gellan requires monovalent cations to promote double helix formation and divalent cations to allow aggregation of helices, while the HA gellan gelation does not require salt (but it does

promote gelation) (Miyoshi and Nishinari, 1999; Mazen et al., 1999). Recent studies have demonstrated that aggregates of HA gellan, created during the drying process, contribute to the shear storage modulus (Shinsho et al., 2020). Additional reports suggested a heterogeneous gel structure with crystalline regions and amorphous regions (Yang et al., 2019) presumed to be the helices and aggregates, respectively.

The response of gellan gum gels to submersion into aqueous solutions is of interest in both the pharmaceutical and food industries for examining digestion (Lin and Metters, 2006; Norton et al., 2014a) and tissue engineering for response to body conditions (Pereira et al., 2011; De Silva et al., 2013). A common property of charged gel networks, including gellan, is the uptake of water to increase the volume and mass of the gel (defined as swelling). Theory of polymer swelling postulates three driving causes of swelling: polymer-solvent interactions, elasticity, and Donnan potential (Annaka et al., 2000; Sakai, 2020). Elastic pressure holds the gel network together while the Donnan potential and polymer-solvent interactions drive dissolution. Equation 6.1 proposes the total osmotic pressure (Π) causing swelling for a charged gel is driven by the summation of polymer-solvent mixing (Π_{mix}), chain elasticity ($\Pi_{elastic}$), and Donnan potential ions (Π_{ion}) (Annaka et al., 2000; Sakai, 2020):

$$\Pi = \Pi_{mix} + \Pi_{elastic} + \Pi_{ion} \quad \text{(Eq. 6.1)}$$

For charged hydrocolloid gels with complexed counter ions, the Donnan potential is the greatest influence. Higher concentrations of counter ions inside the gel and low concentration of ions in solutions (in the case of DI water) drives water into the gel (Annaka et al., 2000; Coutinho et al., 2010). The maximum swelling is limited by the crosslink density

(Moe et al., 1993) and the extent depended on the osmotic gradient (Annaka et al., 2000; Coutinho et al., 2010).

Large increases in the mass of HA gellan gels have been reported upon submersion in aqueous environments (Liu et al., 2013; Cassanelli et al., 2018a; Chen et al., 2020; de Souza et al., 2021). In water, a 2% HA gellan gel increased in mass by 192% (Cassanelli et al., 2018a). Swelling of freeze dried HA gellan gum gels have been measured, but it is known the freeze drying process partially destroys the gel structure (Cassanelli et al., 2018b) so a true comparison cannot be made. Increases in mass ranged from 1,150% to 32,000% for the freeze dried gel (Liu et al., 2013; Chen et al., 2020; de Souza et al., 2021). In simulated body conditions (typically high salt), both increased (De Silva et al., 2013; Osmałek et al., 2018) and decreased (Pereira et al., 2011; Osmałek et al., 2018) modulus have been observed but none of these looked at the effect of ion concentration on the swelling.

Swelling of modified LA gellan gum gels was driven by salt concentration (Annaka et al., 2000; Coutinho et al., 2010). An increased modulus was observed from submersion of LA gellan in salt solutions (Nitta et al., 2006; Tanaka and Nishinari, 2007; Hossain and Nishinari, 2009; De Silva et al., 2013; Yu et al., 2017), acidic solutions (Norton et al., 2014a), and even DI water (Nitta et al., 2006; Hossain and Nishinari, 2009). It was thought to arise from aggregation of unaggregated helices by the additional counter ions (Nitta et al., 2006; Tanaka and Nishinari, 2007; Hossain and Nishinari, 2009; De Silva et al., 2013; Yu et al., 2017). The hypothesis of ions migrating from an external solution during soaking and causing this further aggregation has been generally accepted (Morris et al., 2012). The behaviour of hardening in DI water has also been observed but cannot be explained by the

cation theory (Nitta et al., 2006; Hossain and Nishinari, 2009). Hossain and Nishinari (Hossain and Nishinari, 2009) proposed that the swelling caused “stiffening of network chains” which led to the increased modulus but no further analysis or mechanism was given. The behaviour of HA gellan may provide additional understanding because it does not aggregate through counterions, but no comparison has yet been made.

Lack of a fundamental understanding of HA gellan swelling and the interesting swelling-hardening of LA gellan necessitate further examination to understand gellan gum behaviour. No studies have comprehensively examined the origin of HA gellan swelling or the structural changes taking place during swelling. Several researches have highlighted the need to examine changes in material properties during usage in aqueous solutions (Stevens et al., 2016; Yu et al., 2017). This work will investigate the mechanism of swelling of HA gellan gum, the effects of swelling on the network structure, and the impact on release of a small molecule. This work hypothesized that HA gellan swelling is driven by an osmotic imbalance which causes a rearrangement of chains to an extended structure and is accompanied by a physical strengthening to the network. Swelling of HA gellan gum gels was controlled by altering salt concentration gradients and the resulting physical properties and network structure were examined. Additionally, the effects of solvent properties were compared to elucidate mechanisms for the physical change. Lastly, release of glucose from gellan gels under high-swelling and low-swelling environments were compared to determine the impact of swelling.

6.2. Materials and methods

6.2.1. Materials

HA (LT100) and LA (F) gellan gum were acquired from CP Kelco (Atlanta, USA). The linear polymer is comprised of a repeating sequence of a β-D-glucose, one β -D glucoronate, one β -D-glucose, and one α-L-rhamnose and the chemical structure shown in Figure 2.4 (Sworn, 2009; Morris et al., 2012). HA gellan has acetyl and glyceryl substitutions on the first glucose of the repeating unit at O(2) and O(6) respectively while the acyl groups are removed for LA gellan gum (Morris et al., 2012). The total degree of acylation for LT100 indicated a glycerate group on 90% of those units and an acetyl group on 40% of the units (Kasapis et al., 1999). The molecular weight of HA gellan gum is 1-2 x 10^6 Da and LA gellan gum is 2-3 x 10^5 Da (CP Kelco specifications; Shinsho et al., 2020). Further characterization of this polymer by FTIR and NMR has been published by de Souza et al. (2021). Cations present within the commercial gellan gums were analysed by ICP-OES (Optima 8000 by PerkinElmer, Waltham, USA). Counterions of the HA gellan powder were predominately potassium and contained 19,000 ppm K+, 3,600 ppm Na+, 2,200 ppm Ca^2+ and below LoQ of Mg^2+. Similarly, the LA gellan was also +potassium-type and contained 46,000 ppm K+, 6,300 ppm Na+, 1,400 ppm Ca^2+ and 580 ppm Mg^2+. Materials were used as described without any further purification. The DI water was prepared with a reverse osmosis milli-Q water system (Merck, Kenilworth, USA). On the logarithmic plots, DI water is considered as 0.0001 mM salt to allow it to be within the bounds of the x-axis. Solutions were prepared from salts (KCl and NaCl, $CaCl_2$) and glucose and purchased from Sigma Aldrich (St. Louis, USA).

6.2.2. Sample preparation

All gels were prepared by dispersing the hydrocolloid powder at 2% w/w in 90 °C DI water with stirring for two hours to hydrate the polymers. Salts are present in the hydrocolloid powders (see section 6.2.1) but not additional salts were added. Samples used for glucose release were prepared at 4% and mixed with an 80° C glucose solution (at 60%) prior to the cooling and setting of the gel (they were mixed as two solutions). A final concentration of 30% glucose and 2% gellan gum was achieved. Hot solutions were poured into 20mm diameter cylindrical plastic moulds and set at room temperature (20°C ± 1°C) for at least 24 hours before analysis. All samples were prepared in at least triplicate and error bars represent standard deviation.

Solvent properties were examined by submerging gels in solutions of DI water with added ethanol, glucose, or glucose with KCl. The 'solvent %' refers to the amount of ethanol or glucose added to the mixture on a total weight ratio. The samples with glucose and KCl were each formulated at a final concentration of 100 mM KCl. All solutions were prepared 24 hours before usage.

6.2.3. Swelling measurement

Swelling of gellan gum gels was measured by increases in mass after soaking in aqueous solutions. Gels were cut into ~20 mm height pieces from the cylindrical moulds (20 mm diameter) and the mass of 7.5 g ± 1 g weighed. The gel was then placed into 150 mL of solution at room temperature. Salt concentrations of the solutions ranged from 0.0001 mM to 1000 mM as indicated in each figure. After 48 hours the gel was removed using a strainer, pat dry to remove surface water, and weighed. Swelling was quantified using the ratio of

initial mass to final mass by the equation where M is the measured sample mass after swelling and M_0 is the initial mass:

$$\text{Swelling Ratio } (q) = M/M_0 \quad \text{(Eq. 6.2)}$$

This parameter was proposed by Djabourov et al. (2013) and chosen to mimic the values used during release studies. Distinction should be made from another common swelling ratio 'Q' which measures the swelling of a freeze dried gel. As it is known the process of freeze drying partially destroys the gellan network (Cassanelli et al., 2018b), these gels were not freeze dried prior to measurement. Comparison to values obtained from freeze-dried samples are not equivalent.

6.2.4. Gel compression and fracture

A compression test was used to measure the physical properties of fresh and swollen gels with a TA.XT.plus Texture Analyser (Stable Micro Systems, Godalming, UK). Analysis was completed immediately after the 48 hour period of submersion. Prior to submersion in the water, all samples had dimensions of 20 mm diameter and 20 mm height. Upon swelling, these dimensions changed. For gels that had swelled, the new radius was measured and accounted for in the calculations and the height was cut to maintain a constant 20 mm. The compression used two parallel plates with an upper plate diameter of 80 mm which was larger than the dimensions of the sample. Gels were placed on the bottom plate and the upper plate was moved downward at 2 mm/s until fracture occurred. Sample height was recorded during the experiment, and the surface area was calculated by measuring diameter of each individual sample. The Young's modulus was determined by the slope of

the initial linear relationship between stress and strain. True stress and true strain were calculated to account for the changing dimensions of the gel during compression.

6.2.5. Differential scanning calorimetry (DSC)

Changes in enthalpy and entropy of the gel from submersion in water were analysed with DSC. The instrument was a µDSC3evo by Setaram Instrumentation (Caluire, France) which feature sample cell tubes with ~0.9 mL volume made of Hastelloy and able to be tightly sealed (up to 20 bar). Samples were prepared by cutting cylindrical pieces from the gels to fill the samples cells with 750 mg ± 50 mg. Identical mass of DI water was added to the reference cell within ± 10 mg. A heating and cooling cycle began with a hold at 5 °C for 10 minutes and then increased at 1 °C/min up to 95 °C. After a 10 minute hold at 95 °C, the temperature was cooled at 1 °C/min down to 5 °C (to be referred to as the first run). This cycle was repeated again immediately after and termed the second run. Gels were prepared and analysed at least 4 separate times for each sample.

6.2.6. Rheology

Oscillatory rheology was performed with a Kinexus Rheometer (Malven Panalytical Ltd, Malvern, UK) using a 20 mm parallel plate geometry. Circular slices of a 20 mm diameter were carefully cut to a height of 1.5-2.5 mm and placed directly on the geometry. Differing height between samples was accounted for by loading to a normal force between 0.2 and 0.3 N so the gap ranged from 1.5 mm to 2.5 mm. A strain sweep was conducted from 0.01% to 100% at a frequency of 1 Hz and a temperature of 20 °C and all samples had a linear viscoelastic region (LVER) greater than 1%. Prior to conducting the temperatures sweeps the temperature was held constant for 5 minutes at 5° C to allow equilibration and following

was raised at 1 °C/min from 5 °C to 90 °C. A frequency of 1 Hz and a strain of 0.1% was used. Three replicates were analysed for each sample and error bars show the standard deviation.

6.2.7. Release

To compare release of a small molecule (glucose) from gels, a model system was used. Gels were placed into 150 mL of aqueous solution (DI water or 50 mM KCl) at 37 °C to mimic body temperature. A shaker with 200 RPM was used for mixing the bulk solution and the gels were held in place with dialysis tubing. Gels were prepared with 30% glucose and set for 24 hours prior to measurement (section 6.2.2). Before analysis, gels were cut into 1 mL pieces (1 cm height) and four were utilized in each release experiment (5 g total). The concentration of glucose in the aqueous solution was measured at each time point with a refractometer (Rudolph Research J357 automatic refractometer from Hackettstown, USA). For every sample, the release after 24 hours was 100 ± 5% of the expected glucose concentration and thus values were normalized to the maximum release to minimize the effect of sample variability.

6.3. Results and discussion

6.3.1. Swelling of gellan gum gels

Submersion of gellan gels into water caused enlargement of the network and an absorption of water resulting in a higher mass. Swelling of HA gellan and LA gellan are shown over the course of 7 days in Figure 6.1 and additional data is shown in Table 6.1. HA gellan had a much greater swelling ratio than for LA gellan and both had greater swelling in DI water than in 50mM KCl. Neither gellan appeared to reach a single equilibrium swelling value, with HA gellan continuing to increase while LA gellan began to decrease after 180 minutes (Table 6.1). For LA gellan gum, the maximum swelling ratio was reached at 180 minutes while HA gellan continued to increase logarithmically up to 14 days. In agreement with previous work, the maximum swelling of LA gellan occurred between 120 and 180 minutes (Nitta et al., 2006). An initial structural rearrangement was followed by a low degree of dissolution of polymer chains for LA gellan in DI water. The absence of HA gellan gum dissolution in DI water was interesting. These differences in apparent equilibrium likely reflect the essential participation of cations in the gelation of LA gellan but not HA gellan.

The unique ability for HA gellan to increase in size by 400%, without indication of chain dissolution, was of particular interest. A practical time point of 2 days after submersion in water was chosen for future measurements, when the change appeared to slow for HA gellan, although this does not represent a true equilibrium value. Characterization of this swelling by controlling solution properties and measuring the resulting structural and mechanical properties were the subject of this research.

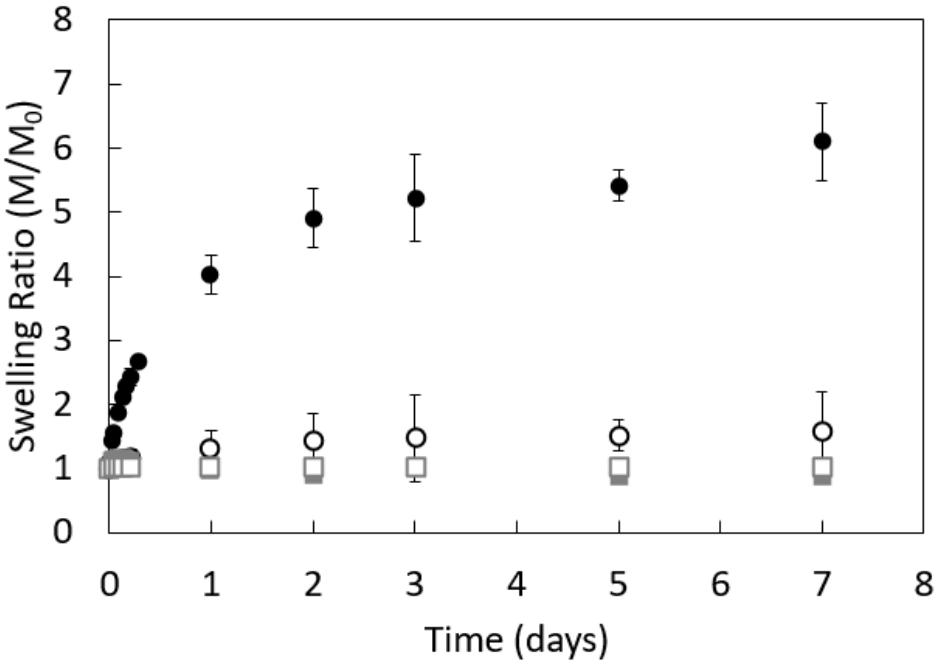

Figure 6.1. Changes in swelling ratio of 2% HA gellan (●) and LA gellan (■) during submersion in deionized water (filled symbol) and in 50 mM KCl (unfilled symbol ○ and □) for up to 7 days at room temperature.

Table 6.1. Swelling ratio of HA gellan and LA gellan gum gels after submersion in 150mL of solution the indicated solution. Averages are reported with ± the standard deviation.

	60 mins	**120 mins**	**180 mins**	**24 hours**	**2 days**	**7 days**	**14 days**
2% HA gellan gum in DI water	1.57 ± 0.06	1.87 ± 0.06	2.11 ± 0.09	4.03 ± 0.3	5.03 ± 0.4	6.10 ± 0.6	7.10 ± 0.6
2% HA gellan gum in 50mM KCl	1.09 ± 0.01	1.12 ± 0.02	1.14 ± 0.01	1.31 ± 0.02	1.42 ± 0.01	1.59 ± 0.03	1.66 ± 0.03
2% LA gellan gum in DI water	1.15 ± 0.02	1.15 ± 0.06	1.19 ± 0.02	0.99 ± 0.02	0.91 ± 0.05	0.86 ± 0.04	0.82 ± 0.03
2% LA gellan gum in 50mM KCl	1.03 ± 0.01	1.04 ± 0.004	1.05 ± 0.003	1.04 ± 0.004	1.03 ± 0.003	1.04 ± 0.01	1.04 ± 0.01

6.3.2. Ionic influence on HA gellan gum swelling

Swelling is driven by the total osmotic contribution (Π) and is a combination of polymer-solvent mixing (Π_{mix}), chain elasticity ($\Pi_{elastic}$), and the Donnan potential (Π_{ion}) for charged polymers (Eq. 6.1). Helix formation is assumed to be unchanged by the swelling and instead causes a tertiary rearrangement of the polymer. A change in the hydrodynamic volume would be reflected in Π_{mix} . The existing gel network resists swelling by $\Pi_{elastic}$ and acts to hold the gel together. Cationic polymers are well known to swell from a high Π_{ion} if the salt concentration outside the gel is lower than inside the gel (Annaka et al., 2000). The term swelling has sometimes been used to describe the change from a compact rigid polymer in a glassy state to an extended large pored rubbery network (Lin and Metters, 2006), however in this work the transition is from a soft loose network to a more rigid and extended network. Both cases involve an increased proportion of water per unit of polymer, but with differing effects on the material properties.

The following experiments will control for the Donnan contribution (Π_{ion}) to examine the effect of swelling on the HA gellan gum gel network. Effects of external ionic concentration on the swelling of a 2% HA gellan gel are shown in Figure 6.2. In DI water and low concentrations of chloride ions (0.01 mM and below), the swelling ratio of 2% HA gellan was at a maximum of 5.0 (Figure 6.2 zone 1). Sigmoidal shape of the curve was consistent with Donnan equilibrium (whereby swelling is caused from an imbalance of ions inside and outside the gel) and also supported by the similarity of the ions (Annaka et al., 2000). The end of the linear portion of the sigmoid and beginning to approach an asymptote (between 10 and 50 mM) is thought to be the equivalence point. Here the internal ionic concentration is likely equal to the outside concentration and would correspond to a Donnan effect of

near zero (Figure 6.2 zone 2). Calculating the internal gel ionic concentration from the ICP data (section 6.2.1) estimates a 15 mM cationic concentration (10 mM for K+ alone) in a 2% gel. Falling between these two concentrations (of 10 and 50mM), the measured values are consistent with an expected equivalence point (15 mM). High ionic concentrations in the external solution (above 50 mM) and the Donnan effect alone should actually promote deswelling (swelling ratio lower than 1 and a loss of water from the gel). In this region, contributions from Π_{mix} must cause a net positive swelling force. Not until 1,000 mM KCl does the swelling ratio drop below one (Figure 6.2).

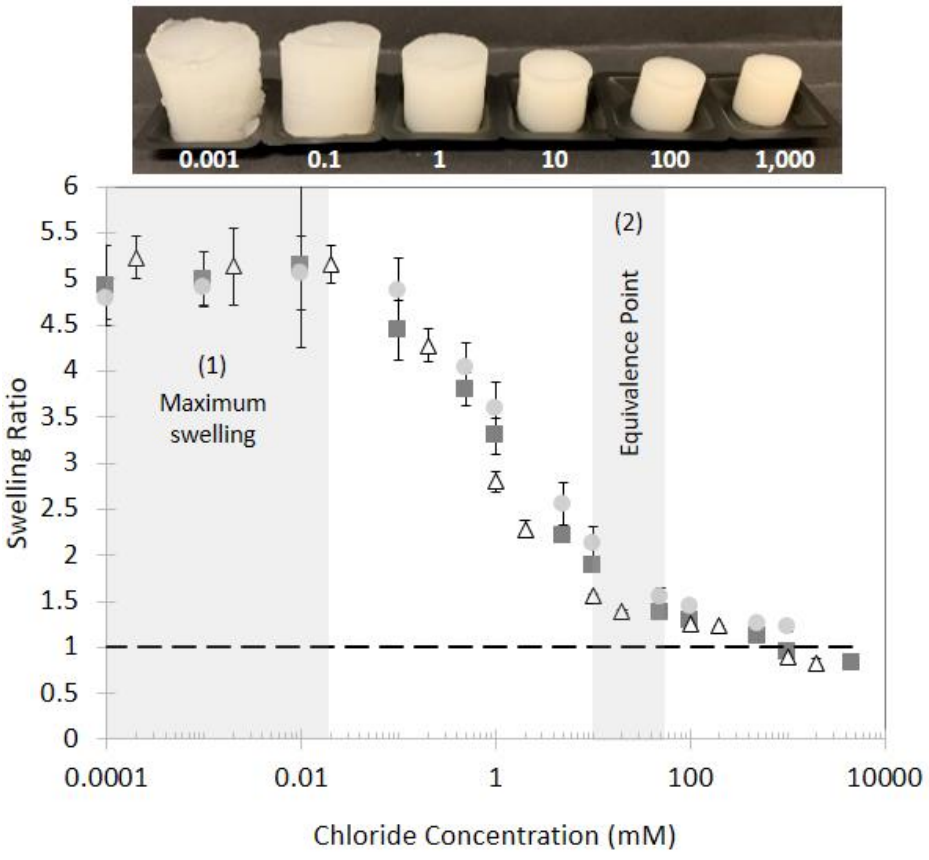

Figure 6.2. Influence of salt concentrations on swelling of 2% HA gellan gels after soaking in 150mL of the indicated solution of KCl (■), NaCl (●), and $CaCl_2$ (Δ) for 48 hours and images show the change in appearance for gellan soaked in KCl solutions. Maximum swelling occurred in zone 1 and the equivalence salt concentration was estimated between 10 and 50 mM salt in zone 2.

Contribution of the Donnan effect to the total swelling was estimated by comparing the maximum swelling ratio (5.0) to the ionic balanced swelling (1.4). A large proportion (90%) of the swelling in DI water was consistent with osmosis-driven salt imbalance. The other 10% of swelling is likely a contribution from Π_{mix} (Eq. 6.1). For LA gellan, a comparable salt dependant swelling has been previously established (Annaka et al., 2000; Nitta et al., 2006; Coutinho et al., 2010). In addition to the increase in mass of 400% from the Donnan effect, soaking gellan in water also led to a network strengthening that could not be explained by the change in concentration.

6.3.2.1. Mechanical properties

Mechanical properties of these swollen gels were compared using uniaxial compression testing to measure the Young's Modulus (Figure 6.3) and the strain to fracture (Figure 6.4). Submerging HA gellan gels in aqueous solution caused an increase in modulus (Figure 6.3) but interestingly was not directly related to the swelling (R^2 = 0.11). Whether in DI water or up to 10 mM KCl, the higher modulus was consistent (13 kPa ± 0.8 kPa) while the swelling ratio ranged from 5.0 to 1.9 (Figure 6.2). At concentrations of salt greater than 50 mM, there was an increasing modulus predicted to be caused from 'salting-out' which is common for hydrocolloids at high ionic strengths. The lowest modulus of the soaked samples occurred in the equivalence salt (zone 2) where the modulus was similar to the fresh (not soaked) gellan gel. The increase in modulus at low ionic concentrations cannot be attributed to an increase in polymer or counter ion concentration as both parameters actually decreased during the swelling. Modulus increases at high degrees of swelling has been explained by a deviation from Gaussian behaviour caused from extensive stretching of the polymer chains (Skouri et al., 1995; Djabourov et al., 2013). Additionally, it is possible new

bonds were formed during swelling which will be examined by DSC in a following section. Strain to fracture of swollen gels was well correlated (R^2 = 0.96) to the ratio of swelling (Figure 6.4). Images of the compressed and fractured gels are shown in (Figure 6.4). Water removal from gels during compression (like a sponge) was not observed from the HA gellan gels as previously reported for the LA gellan variant (Nakamura et al., 2001). The increased brittleness of gels (with a lower strain to fracture) appears to be caused by the extension of polymer chains during swelling. As swelling causes the network to expand, space between junction zones must get larger and the gel more rigid, thus forming a network less able to deform without fracture.

Previous measurement of the change in modulus of soaked HA gellan gels did not account for the salt concentration. For a 2% HA gellan gel, De Silva et al. (2013) found no change in the Young's Modulus or strain to fracture for a gel submerged in PBS for up to 14 days. Both an increase and a decrease in modulus were observed for a 0.4% HA gellan in a comparison of different bodily fluids (Osmałek et al., 2018). Applying the effect of ionic concentration from the current work, the discrepancy between these authors' work likely originates from differing ionic strengths.

Here there appears to be two factors at play in changes to the modulus with the varying ionic strengths: Donnan effect swelling and salting out of the polymer. Between 0 and 10mM the changes are driven by an ionic-imbalance salt swelling (the Donnan effect). This range is characterized by high swelling, increased modulus, and the most brittle gels. The range from 0.1 to 10mM is roughly the linear region of the sigmoidal curve where the greatest change in swelling ratio with salt was observed (largest slope). The modulus did not

vary with swelling ratio. Between 10 and 50mM was the equivalence point of ionic concentration inside and outside the gel. Swelling ratio at this point is not zero though, as swelling was still driven by the other contributions (Eq. 6.1). At the ionic equivalence point, the Young's Modulus is at a minimum. Matching the internal and external solution properties resulted in the smallest changes from the original gel. At even higher ionic concentrations (greater than 100 mM), salting-out of the polymer likely had caused the increased modulus. Molecular origins of this higher modulus at low ionic strength (<10 mM) were examined further.

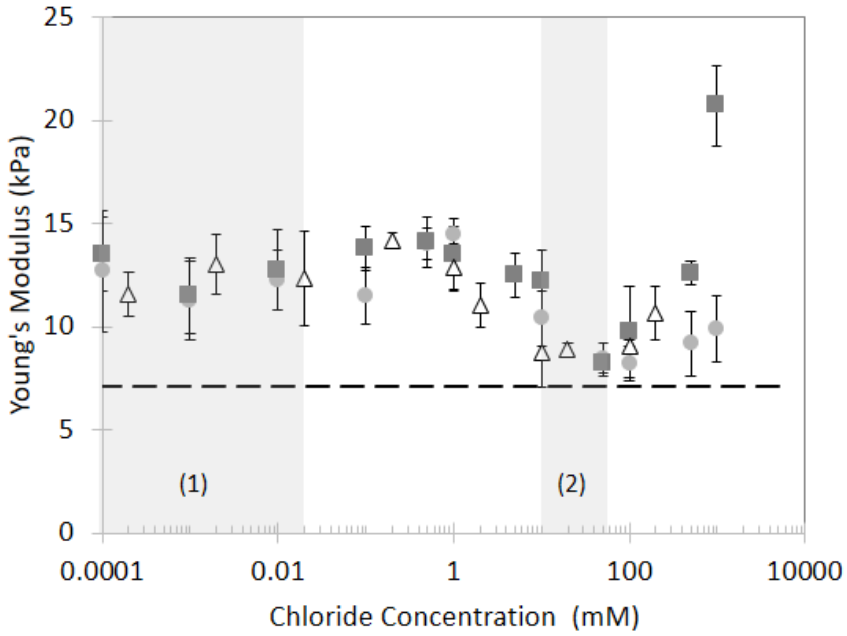

Figure 6.3. Influence of ionic effect on the Young's Modulus of 2% HA gellan gels after soaking in 150mL solutions of KCl (■), NaCl (●), and $CaCl_2$ (Δ) compared to a fresh sample (dotted line) for 48 hours. Maximum swelling occurred in zone 1 and the equivalence salt concentration was estimated between 10 and 50 mM salt in zone 2.

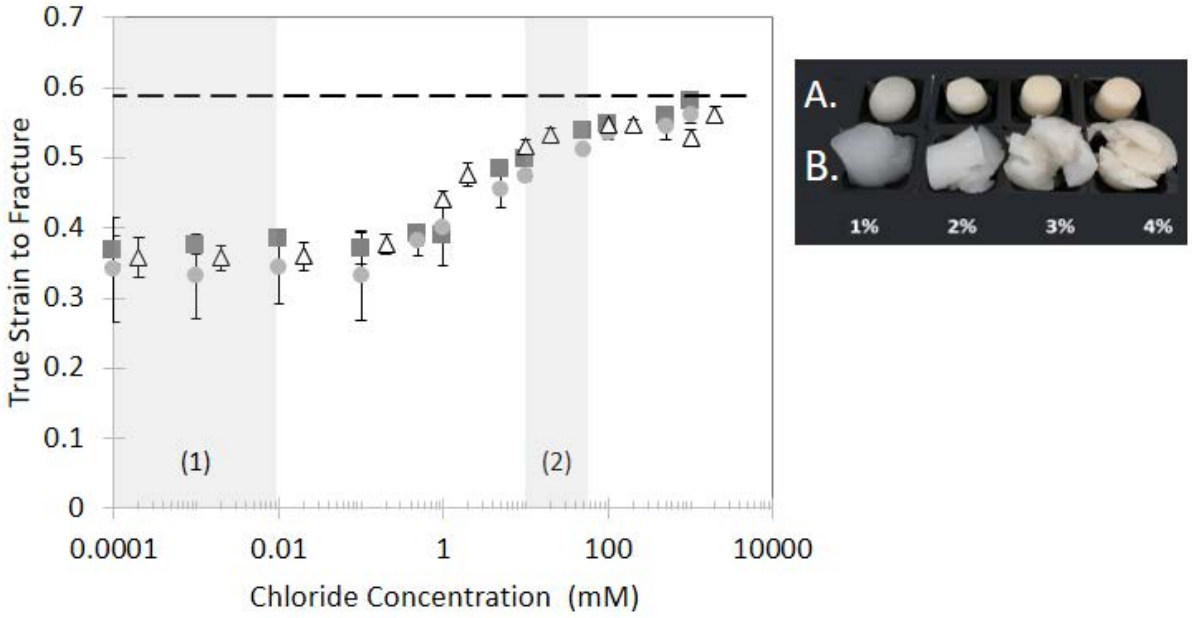

Figure 6.4. Changes in gel fracture of 2% HA gellan after soaking in 150mL of of KCl (■), NaCl (●), and $CaCl_2$ (Δ) compared to a fresh sample (dotted line). Maximum swelling occurred in zone 1 and the equivalence salt concentration was estimated between 10 and 50 mM salt in zone 2. Image shows the appearance of HA gellan gum gels at the indicated concentration (A) before treatment and (B) fractured gels after soaking in DI water.

6.3.3. Characterization of gel network changes

The increased gel strength observed upon submersion in low ionic strength solutions was hypothesized to be caused by hydrophobic-driven helix formation. A low correlation to the swelling itself (R^2 = 0.11) suggested an alternative mechanism to just "stiffening of chains" as proposed for the LA gellan (Hossain and Nishinari, 2009). The effective gellan concentration was lower and the salt concentration was lower; both of these are typically thought to drive gelation. Therefore a different mechanism must have caused the increased modulus. First, the networks of swollen and standard gels were compared with DSC and then mixed solvents were compared to understand solubility characteristics of the gels.

6.3.3.1. DSC

To examine changes in the network during swelling of gels, fresh (no soaking in water) and swollen gels were examined by DSC. Gels soaked in DI water were compared to gels soaked in 50 mM KCl to compare the maximum swelling (DI water) to the estimate of equal salt concentrations (50mM KCl). Thermograms of the heating curves are shown in Figure 6.5 and the enthalpy and transition temperatures are shown in Table 6.2. Enthalpies were normalized to the weight of the polymer to account for the differences in concentration between the swollen samples and fresh gel. An endothermic peak between 65 and 76 °C is known to be the coil-helix transition of HA gellan gum (Mazen et al., 1999; Huang et al., 2004; Murillo-Martínez and Tecante, 2014). A peak representing this helix to coil transition was observed for each of the samples with some variation in melting temperature due to the differences in salt. Ionic concentration is well known to effect the gelation temperature of HA gellan gum (Mazen et al., 1999; Huang et al., 2004; Flores-Huicochea et al., 2013). The decreased melting temperature of the sample soaked in DI water was indicative of the lower salt environment. Alternatively, soaking in 50 mM KCl resulted in a higher melting temperature (an increase of 4 °C). This concentration was an estimation of the equivalent concentration (between 10 and 50mM KCl) and in practice the selected 50mM KCl was marginally higher than the gel itself. The higher melting temperature was a reflection of this higher salt level.

Comparing enthalpies of melting for gel networks gives an indication of internal energy associated with the helix-coil transition. Differences in melting temperature were taken into consideration by calculating the entropy and Gibbs free energy (ΔG) associated with each melting event. In the soaked samples there was considerable sample to sample variability in

temperature (suggested by the large error bars). The μDSC technique utilizes only a small (~750 mg) portion of sample and this high variability would be consistent with heterogeneity within the gel. Due to the lack of helix aggregation, there is little cooperation between helices and DSC peaks are normally wide (Morris et al., 2012). Gels soaked in DI water resulted in greater enthalpy and ΔG compared to a fresh gel (enthalpy of 45 J/g compared to 27 J/g from Table 6.2 $p < 0.05$). Soaking in 50 mM KCl did not result in a significant change in the enthalpy ($p > 0.05$) but did cause an increase in ΔG compared to the fresh gel. The greater ΔG could be explained by the greater salt content (Mazen et al., 1999). Generally, salt environments can be expected to drive further helix crosslink formation (Mazen et al., 1999). The same is not expected of submersion in DI water. The process of swelling and the lower salt environment appeared to decrease the solubility of HA gellan and drive helix formation. These new bonds may have been the cause of the network strengthening (increased modulus) observed during swelling. Alternatively, extensive stretching of chains, past the point of a Gaussian assumption, has also led to a higher modulus (Skouri et al., 1995). Although the enthalpy of HA gellan (per gram) increased during swelling, the effective concentration decreased by 4-5x causing much complexity for assigning an origin of behaviour. It is likely that both factors were influential in the change of modulus.

An unusual exothermic peak (between 24 and 26 °C) was observed in the fresh sample but not present in the gel soaked in DI water. A slow-cooled (1 °C/min in the μDSC) HA gellan gel also did not exhibit this exothermic transition. A pre-melting step is common in DSC analysis and may be the reason this peak has not been previously reported. It is proposed the peak represents an ordering or semi-crystallization of the amorphous chains in aggregates.

Dissolution of HA gellan chains is not complete after 2 hours of heating and some aggregates of up to 10 chains is expected to be present in the sample (Shinsho et al., 2020). When soaking the gels in water, the aggregates must have dissolved and correspondingly the exothermic peak was not present. A much lower effective concentration and lower ionic solution are reasonable to have caused the breakup.

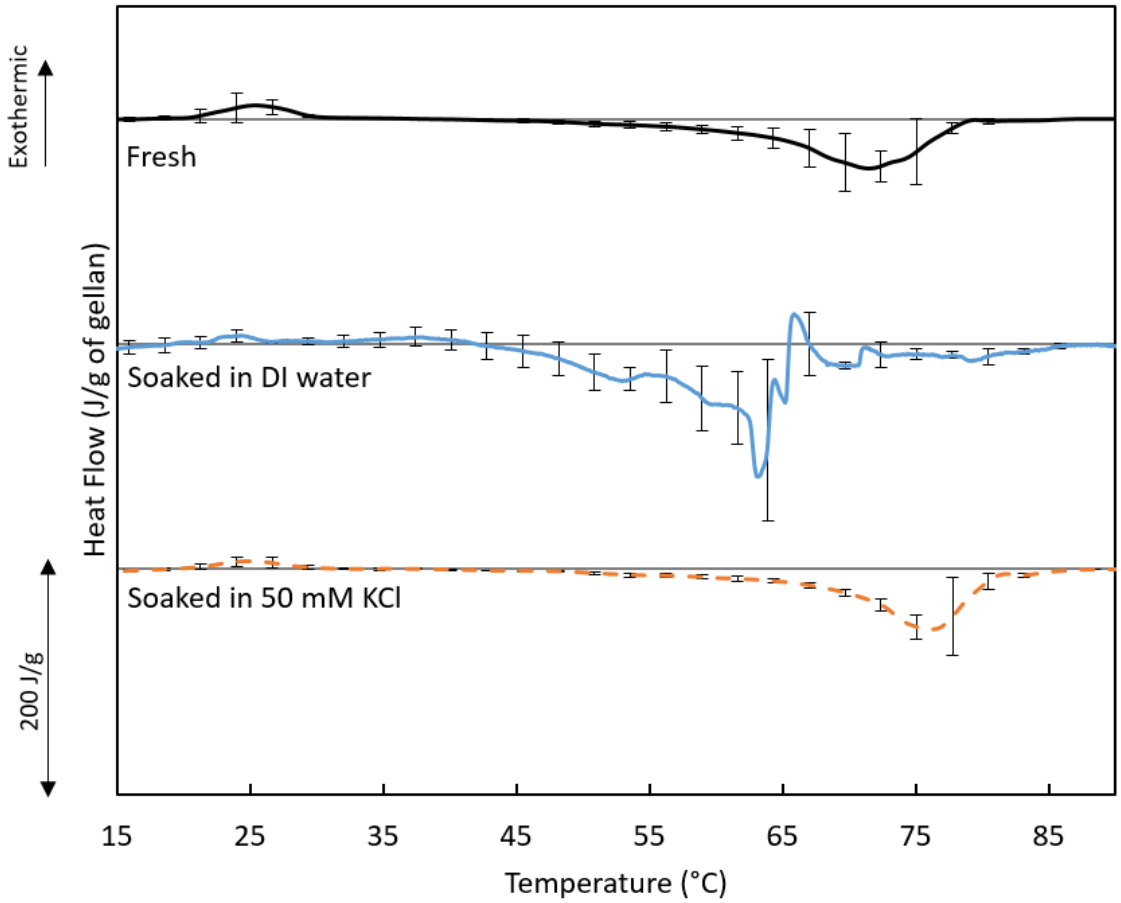

Figure 6.5. DSC heating thermograms for 2% HA gellan gum fresh (without any treatment) and after soaking in deionized (DI) water or 50 mM KCl for 48 hours. Swelling took place outside of the DSC cells and changes in HA gellan concentration were accounted by normalizing to total the polymer weight in each sample. Error bars represent the standard deviation of five replicates where the deviation was mainly from differences in temperatuare ranges for 'soaked in DI water' and differences in area between 'fresh' and 'soaked in 50mM KCl' samples.

Table 6.2. Enthalpy of melting (J/g of polymer) and peak melting temperature (°C) for 2% HA gellan gum from Figure 6.5 and calculated entropy and Gibbs free energy (ΔG). Values were normalized to the grams of gellan gum in each sample and are reported as the average with one standard deviation. Means were compared for each column and different lettering is indicative of a significant difference between sample means.

	Exothermic Peak		**Endothermic Peak**			
	Enthalpy (J/g)	**Peak Temp (°C)**	**Enthalpy (J/g)**	**Peak Temp (°C)**	**Entropy (J/g·K)**	**ΔG**
Fresh	4.2 ± 2.6 [a]	26.1 ± 1.2 [a]	27.1 ± 8.7 [a]	72.1 ± 2.2 [b]	0.079	4.1
DI water	*	*	45.4 ± 0.5 [b]	61.0 ± 4.0 [a]	0.136	5.6
50mM KCl	2.5 ± 1.7 [a]	24.4 ± 1.3 [a]	28.5 ± 6.9 [a]	75.8 ± 1.5 [c]	0.082	4.6

* Indicates peak was not significantly different than baseline

6.3.3.2. Temperature dependence of modulus

Rheological tests were used to measure the effect of temperature on the modulus to elucidate the importance of each thermal transition. During heating, the modulus gradually decreased with a steep drop approaching the melting temperatures (Figure 6.6). Melting temperature by µDSC of 72 and 61 °C for fresh gellan gum and soaked in DI water respectively were in good agreement with the rheologically determined gel melting points. Consistent with theory, the helix-coil transition temperature from DSC aligns with the sol-gel transitions temperature measured with rheology (Flores-Huicochea et al., 2013; Yang et al., 2019). Aggregate ordering at 25 °C did not result in a measureable shift during the heating ramp and suggested minimal contribution to the gel modulus (Figure 6.6).

From these experiments, it was hypothesized the further helix formation was driven by a hydrophobic effect. Orientation of the HA gellan molecule during double helix formation has

the glyceryl groups internal to the double helix (Morris et al., 1996). Hydrogen bonds are known to occur within the helix (Chandrasekaran et al., 1992) but hydrophobicity of the glyceryl groups may also contribute to the stability of the helix. Increased stability of helices of HA over LA gellan was demonstrated to be from the glyceryl groups internal to the helix (Morris et al., 1996). Hydrophobic interactions have been suggested to contribute to chain associations of HA gellan (Tako et al., 2009) but were not examined. The following section will use varying solvents to probe a hypothesized hydrophobic-driven helix-coil transition.

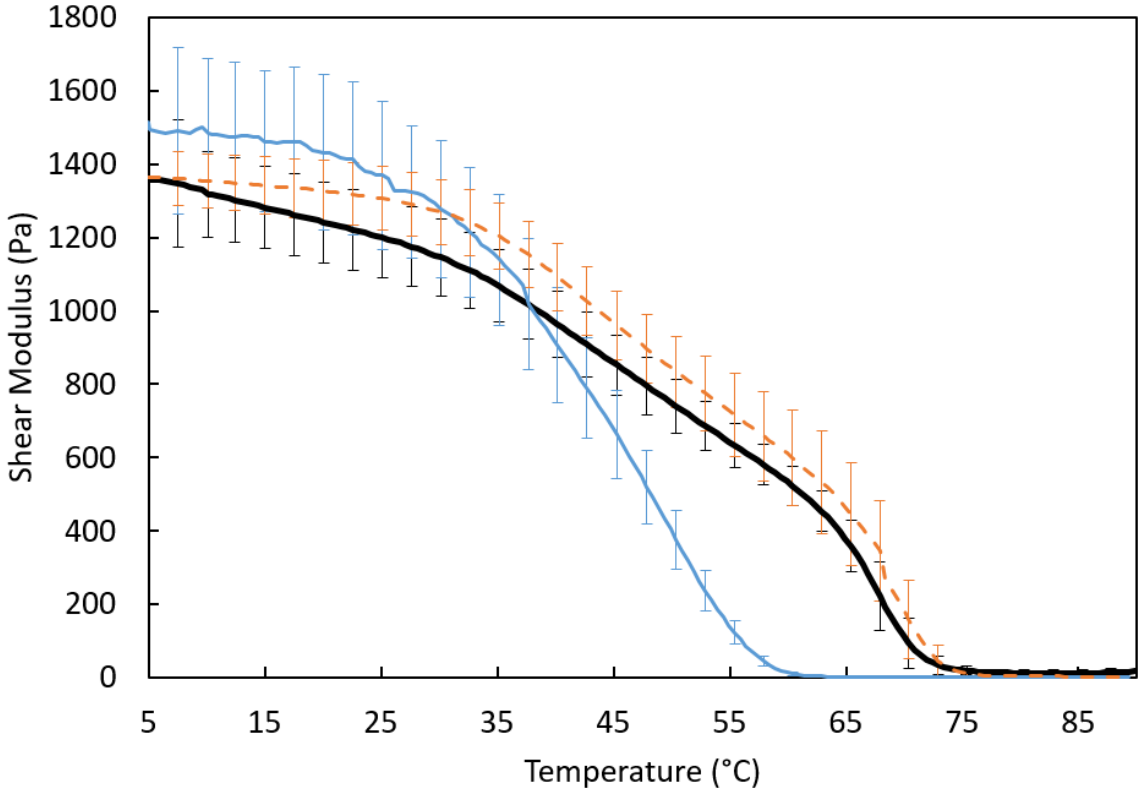

Figure 6.6. Temperature dependence of storage modulus for 2% HA gellan (black) and after soaking in deionized water (blue) and 50mM KCl (dashed orange) utilizing small deformation rheology with controlled heating.

6.3.3.3. Mixed solution swelling

Mixed solvents of water with glucose and ethanol were used to examine the solvent effects on swelling ratio, Young's Modulus, and strain to fracture (Figure 6.7). Without added salts, increasing ratios of organic solvents resulted in decreasing swelling ratios following a continuous swelling pattern (Figure 6.7A). This is explained by the lower dielectric constant of ethanol and glucose than water and shown by the high correlation (R^2 = 0.99 for ethanol and R^2 = 0.97 for glucose) between ratio of swelling and dielectric constant of the mixture (Wyman, 1931). For up to 30% of either solvent, there was little effect of the solvent concentration on the modulus, and a slight (20-30%) increase for ethanol compared to pure water. Similar to the effects of salt, the correlation between swelling ratio and modulus was low (R^2 = 0.12 for glucose and R^2 = 0.71 for ethanol) emphasizing a differing underlying mechanisms. Greater ratios of ethanol led to an increasing in modulus but a decrease for glucose. Although not shown on the graph, a 50% ethanol solution resulted in a modulus of 56,000 Pa modulus and was too large to include in Figure 6.7. Ethanol is thought to decrease swelling and increase the modulus by a de-hydration of the polymer chains (Cassanelli et al., 2018a). For pectin, the greatest gel strength (rupture force) was also at the point of greatest hydrophobic interactions at 23% ethanol (w/w) (Oakenfull and Scott, 1984). The balance between solubility and molecular interactions are likely both contributing here. At high concentrations of ethanol there was likely a dehydration-based stiffening, while at low concentrations little change was observed.

To view the effect of glucose without the swelling contribution, a 100 mM KCl concentration was kept constant while changing the ratio of glucose. The concentration of 100 mM KCl

was chosen as the control for zero swelling. As intended, the swelling ratio for the glucose mixed solvent with KCl was near to one for every concentration of glucose, although the swelling did decrease with glucose ranging from 1.3 to 0.72 (Figure 6.7A). When minimizing the swelling, glucose was shown to decrease the modulus and increase the strain to fracture. However there was high correlation between the swelling and modulus (R^2 = 0.88) suggesting swelling was still playing a role in the modulus. For both glucose and ethanol, at low ratios there was little impact of solvent changes on the modulus, but there was a decrease in swelling from the decreasing dielectric constant. Interdependencies between swelling, modulus, and solvent properties are clear from the cumulation of results. The observed swelling of HA gellan gum was consistent with both a swelling process and a de-solvation process. A reduction in salt ions in the surrounding environment appeared to cause both an influx of water by the Donnan effect and a coil-helix transitions. Further testing may allow a better understanding of the properties, but what does seem clear is an importance of both hydrophobic interactions and hydrogen bonds to the gelation of HA gellan gum.

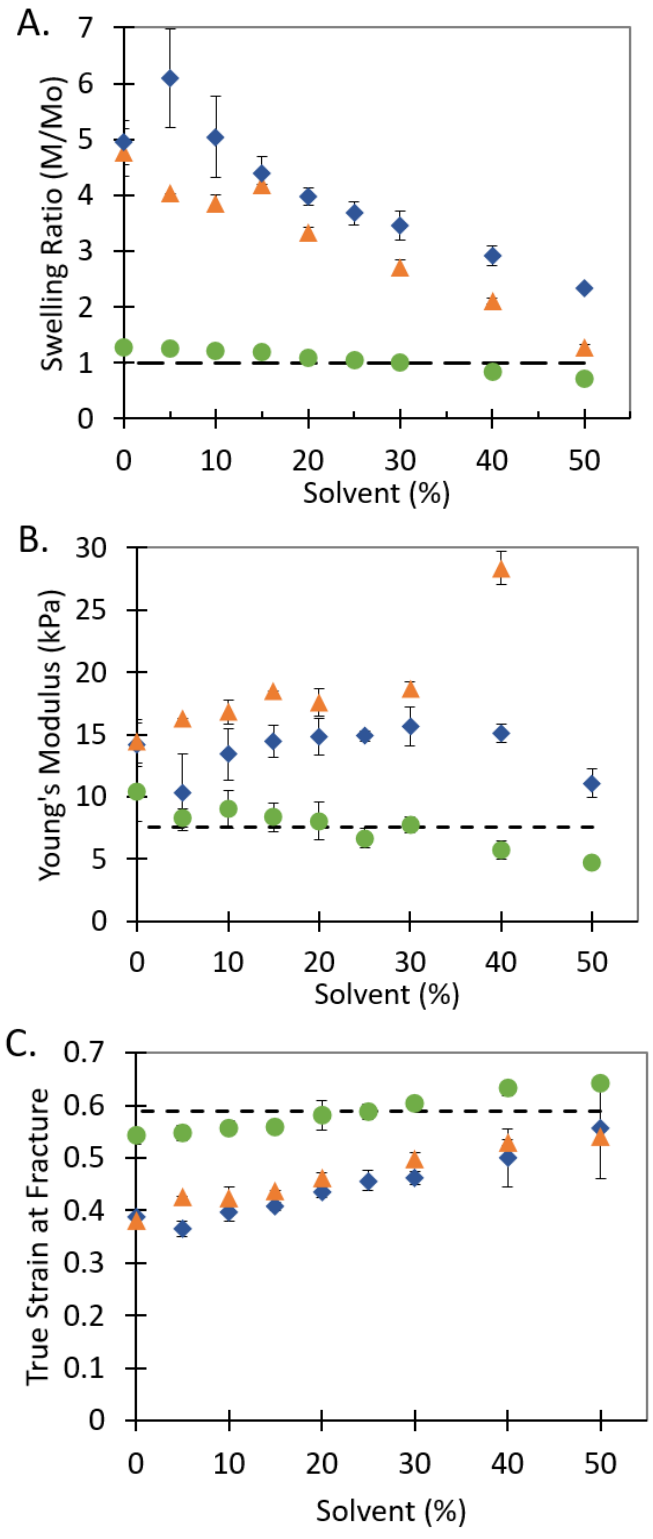

Figure 6.7. Solvent effects on swelling ratio (A), Young's Modulus (B), and strain at fracture (C) of 2% HA gellan gels after soaking in 150mL of water mixed with the indicated percentage of glucose (♦), glucose plus 100mM KCl (●), and ethanol (▲) for 48 hours and compared to a fresh gel (dotted line).

6.3.4. Importance of swelling in release

If HA gellan is submerged in water prior to use, the texture and water ratios would be vastly different during utilization as shown in section 6.3.2. Even if the gel was not modified prior to use, during digestion or tissue application the solvent properties of the environment would dictate how the gel responds. It is therefore important to measure the influence of swelling on functionality of the gel. For designing food and drug biomaterials, the effect of the characterized swelling on release of an active molecule is crucial.

A small and uncharged molecule, glucose, was chosen as the active of interest for these experiments. Release from a similar gelling agent (LA gellan) which displayed a lower ratio of swelling was included as a reference material. Comparison of swelling of the polymers was shown in Figure 6.1 and the swelling of LA gellan was small (1.1 swelling ratio at 300 minutes). Release profiles of 30% glucose from 2% HA gellan and LA gellan are shown in Figure 6.8. In DI water, release from HA gellan was considerably slower than LA gellan (at 120 minutes LA gellan was 38% greater) (Figure 6.8 filled symbols). Under these low ionic conditions, HA gellan swelled considerably during the release experiment (at 120 and 300 minutes a 1.9 and 2.4 swelling ratio respectively). It was hypothesized that swelling decreased release rates of glucose and was tested by conducting the glucose release experiment in ionic conditions that would minimize swelling. Under these ionic conditions (50 mM KCl), the difference between HA and LA gellan was only 17% at 120 minutes (Figure 6.8 empty symbols). When swelling was inhibited in HA gellan, the release was quicker and more similar to that of the control gel (LA gellan). However, there was still some swelling (1.1 at 120 minutes) which may explain the remaining difference. LA gellan also displayed a

small increase in release rate with KCl which corresponded to a decrease in swelling ratio from 1.15 to 1.04 at 120 minutes. Release from HA gellan was quicker when swelling was reduced (in 50 mM KCl) and very similar to LA gellan at comparable swelling ratios. Thus, it can be concluded that swelling of HA gellan caused the decreased release rate and the mechanism was subsequently investigated.

Pore size of a gel network allows prediction of how compounds of interest would move through the gel. Molecules considerably smaller than the pore size display little effect to the diffusion through the network, while larger molecules should become trapped in the pores and the release inhibited (Lin and Metters, 2006; Mills et al., 2011). Pore size of typical hydrogels in literature range from 100 to 5 nm (Lin and Metters, 2006). Freeze dried HA and LA gellan gum have reported average pore sizes 800-1100 μm and 400-600 μm respectively (Cassanelli et al., 2018a). Swelling polymers must have structural flexibility and low crosslink density to allow this rearrangement (Moe et al., 1993). From this understanding, the pore size of both HA and LA gellan is estimated to be much larger than glucose (~1 nm) so trapping in the network pores was unsupported. Additionally, during swelling pores would have increased in size and had the opposite of the observed effect; instead the swelling actually slowed the release. Network dimensions of these gels suggest glucose was not sterically inhibited during release, so another theory was investigated.

In large-pored gels, the effect of a gel network is principally to prevent convection-based mixing so that diffusion is the driving force through the network (Mills et al., 2011). Examining the slower release based on the principles of diffusion suggests two possible mechanisms. First, the swelling of the polymer would increase the distance a glucose

molecule must travel within the gel to reach the edge. Second, swelling (corresponding to an increase in volume and mass) would lower the effective concentration of glucose inside the gel. Both of these would have caused a lower flux and the slower measured release of glucose from the HA gellan. The decreased flux of glucose due to swelling was confirmed by the release profile quickening when swelling was inhibited. Increasing dimensions of HA gellan during swelling slowed release of the small molecule glucose.

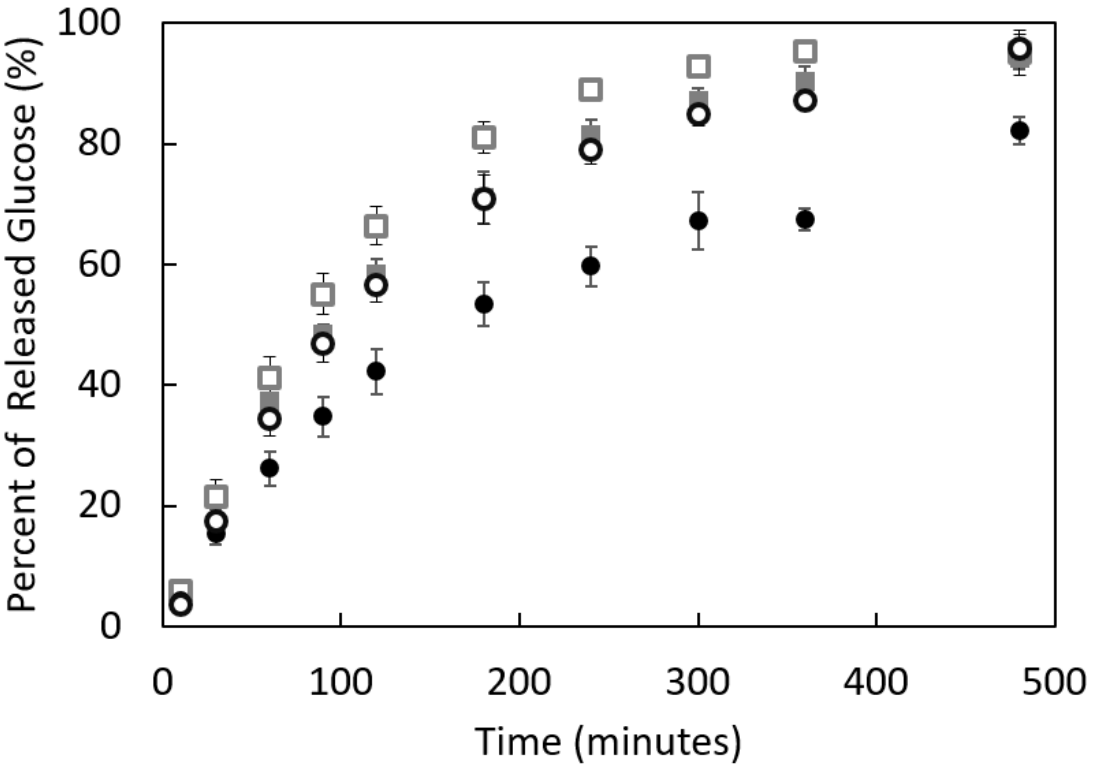

Figure 6.8. Release of glucose from gels prepared with 30% glucose and 2% HA gellan (●) and 2% LA gellan (■) into a bulk phase of deionized water (filled symbols) and 50mM KCl (unfilled symbols ○ and □ respectively).

6.4. Conclusion

In low ionic environments, HA gellan gum gels displayed high swelling and an increased modulus caused by an osmotic imbalance, which had the effect of slowing the release rate of a model molecule. Unlike typical polymers for which swelling increases release of a small molecule entrapped in the gel network, the swelling of HA gellan caused a slower release. The magnitude and rate of swelling generated this unique impact. The unusual swelling ability also provided a structural implication consistent with the previously proposed gelation mechanism of a loose and fibrous network without helix aggregation. Additionally, the swell-strengthening behaviour highlighted the contribution of hydrophobic interactions in helix formation for this hydrocolloid. This work begins to suggest that swelling of HA gellan could be harnessed to capture temperature sensitive compounds into a prefabricated gel under suitable conditions. The high degree of swelling and gel hardening, and the tunability of such with ionic environment, provide many opportunities to use HA gellan as a functional ingredient in biopolymer gels.

Chapter 7. Conclusions and Future Work

7.1. Conclusions

This thesis examined the structural-functional relationships of maltodextrin (MD) and high acyl (HA) gellan gum with respect to material properties and release of carbohydrates. The development and optimization of these gels for optimal texture and release profiles provided a solution to reducing gastrointestinal stress in athletes by creating structures that slow the release of carbohydrates. Material properties and release behaviours from gels could be selected by controlling the microstructure of the polymers.

Maltodextrin gel networks were shown to be dependent on temperature and length of gelation time. Structuring of the gels could be controlled by selection of specific concentrations and holding temperatures. From the changes in enthalpy and entropy of the gel networks, it was concluded that shifts in temperature modified which chain sizes participated in gelation. This modification to the gelation mechanism could be utilized to control helix and gel formation.

A range of textures from paste-like to firm and brittle were produced from microstructure changes by varying the gelling temperature from high (60 °C) to low (5 °C). Characterization of MD gelation alone was essential in the subsequent work to compare to the structures formed in a mixed gel. Additionally, the ability to selectively control helix formation with temperature was crucial in determining the contribution of helices to the mixed gel material properties and carbohydrate availability.

Triggered release from these characterized gels were examined in Chapter 5. The gels which were more brittle and had higher enthalpy (formed a lower temperatures) resulted in lower

available carbohydrates. Whereas glucose and maltose could freely diffuse out of a hydrocolloid gel network, MD required the use of the digestive enzyme amylase to facilitate its release it into smaller pieces.

The mixed gel of HA gellan gum and MD was characterized as an IPN. Alone, the texture of MD was not appropriate for a consumer product, and therefore it was necessary to add a secondary hydrocolloid (HA gellan gum) which was the focus of Chapter 4. From a series of experiments to characterize the network type, it was concluded that the mixed gel formed between HA gellan gum and MD best fit the IPN model through exhibiting apparent associative interactions and no indication of intermolecular binding. This network type was in agreement with the proposed type for LA gellan gum and MD (Clark et al., 1999). Self-aggregation of maltodextrin introduced difficulty to comparing this non-ideal system to theoretical representations and emphasized the importance of using multiple methods for characterization. If only one property was modelled, such as the Young's Modulus, an erroneous prediction of a phase separated network could have been made.

Mixed gels of MD with HA gellan gum were characterized and the material properties of various formulations were examined to map the range of achievable textures. Textures similar to commercial sweets were created over a range from soft and chewy to firm and brittle. Release of carbohydrates from these mixed gels was examined in Chapter 5.

Addition of a gelling hydrocolloid decreased the amount of available carbohydrate compared to that of MD alone. The type of network was shown to be important in the amount of available carbohydrates, with phase separated networks resulting in a greater availability than IPNs. From these results, it was concluded that changes in the

microstructure that effected the physical properties also modified the availability of MD for triggered-release.

Swelling of HA gellan gum gels in DI water increased the mass by 4x and slowed the release of glucose. An interesting behaviour of high swelling (400%) for HA gellan was observed during the course of the work which led to an examination of the mechanism of swelling and its effect on the release of glucose. Driving factors of swelling for HA gellan gum were consistent with other anionic hydrocolloids gels which swell due to an osmotic balance of the counter ions. From the swelling behaviour in various solutions and the increase in modulus and enthalpy, it can be concluded that hydrophobic interactions play a role in the gelation of HA gellan gum. The gelation mechanism of non-aggregated helixes forming a loose fibrous network was also consistent with high amount of swelling observed. Contrary to the swelling of most gels which quickens the release, swelling of HA gellan gum was shown to slow the release of glucose from the gel. Swelling did not significantly affect release of MD which was likely due to the different mechanism of release.

7.2. Future Work

This thesis provided a fundamental characterization of maltodextrin DE 2 gels and the effects of additional gelling agents on the material properties and release profiles. Suggested extensions from this work include both an expansion in the formulation of the gels and an increased complexity of the method used to measure release.

Formulation complexity to reflect a final food product: The work presented in this thesis only used a single carbohydrate source at a time and no additives were included in the formulation. Additional experiments should examine any interactions with flavours, colours,

preservatives, and other ingredients used in commercial food gels. To achieve an ideal sugar release profile, it is likely a mixtures of carbohydrate sources (MD with glucose or maltose) will be needed. Interactions between these two carbohydrates should be examined and the release profiles of mixtures tested. Additionally, looking at a larger carbohydrate such as starch would likely allow for a slower release of carbohydrates than MD. However, starch is also a more complex system. Further complications will certainly arise because of the gelatinization and retrogradation processes which would both be impacted by the hydrocolloid system (Zhang et al., 2018). Results from this thesis will add to the structural understanding of carbohydrates and gelling hydrocolloid systems which have been predominately focused on starches and flours.

Maltodextrin gelation: This work focused on a DE 2 potato maltodextrin as the carbohydrate of interest. Maltodextrin is commercially produced from several sources (corn, wheat, etc.) and of DE values both higher and lower. Future work should examine the application of the current findings to the wide range of maltodextrin available. It has been demonstrated that high DE value maltodextrin tend not to aggregate (DEs of 20 or greater) so there is likely an upper limit where this work is applicable. Less work has compared different sources of maltodextrin, so it is of considerable interest.

Expanded methodology to include *in vivo* or human testing: This thesis utilized a simplified model of release to focus on the structural differences between the gels. Therefore, the release method did not include break-up of the gels. Past work has demonstrated the importance of chewing, fracture, and breakup of gels on release (Morris, 1994; Khin et al., 2021). Future work should include oral processing steps (such as chewing) into experiments

to examine this effect. Additionally, using gastric and intestine fluids for *in vivo* tests and eventually human studies will be important to examine the true digestion behaviour.

Chapter 8. References

Alevisopoulos, S., Kasapis, S., & Abeysekera, R. (1996). Formation of kinetically trapped gels in the maltodextrin—gelatin system. *Carbohydrate Research,* 293(1), 79-99.

Amici, E., Clark, A. H., Normand, V., & Johnson, N. B. (2000). Interpenetrating network formation in Gellan− agarose gel composites. *Biomacromolecules,* 1(4), 721-729.

Andersson, M., Axelsson, A., & Zacchi, G. (1997). Diffusion of glucose and insulin in a swelling N-isopropylacrylamide gel. *International Journal of Pharmaceutics,* 157(2), 199-208.

Annable, P., M. G. Fitton, B. Harris, G. O. Phillips, & P. A. Williams. (1994). Phase behaviour and rheology of mixed polymer systems containing starch. *Food Hydrocolloids,* 8(3), 351-359.

Annaka, M., Ogata, Y., & Nakahira, T. (2000). Swelling behavior of covalently cross-linked gellan gels. *The Journal of Physical Chemistry B,* 104(29), 6755-6760.

Brodkorb, A., Egger, L., Alminger, M., Alvito, P., Assunção, R., Ballance, S., Bohn, T., Bourlieu-Lacanal, C., Boutrou, R., Carrière, F., Clemente, A., Corredig, M., Dupont, D., Dufour, C., Edwards, C., Golding, M., Karakaya, S., Kirkhus, B., Le Feunteun, S., Lesmes, U., Macierzanka, A., Mackie, A. R., Martins, C., Marze, S., McClements, D. J., Ménard, O., Minekus, M., Portmann, R., Santos, C. N., Souchon, I., Singh, R. P., Vegarud, G. E., Wickham, M. S. J., Weitschies, W., & Recio, I. (2019). INFOGEST static in vitro simulation of gastrointestinal food digestion. *Nature Protocols,* 14(4), 991-1014.

Brouns, F. & Kovacs, E. (1997). Functional drinks for athletes. *Trends in Food Science & Technology,* 8(12), 414-421.

Brown, C., Foster, T. J., Norton, I. T., & Underdown, J. (1995). Influence of shear on the microstructure of mixed biopolymer systems. In S. E. Harding, S. E. Hill and J. R. Mitchell (Ed.), *Biopolymer Mixtures* (65-83). Nottingham: Nottingham University Press.

Bulpin, P. V., Cutler, A. N., & Dea, I. (1984). Thermally-reversible gels from low DE maltodextrins. In G.O. Phillips, D. J. Wedlock & P. A. Williams (Ed.), *Gums and Stabilizers for the Food Industry* 2, (475-484) Pergamon Press Ltd., Oxford .

Busnel, J. P., Clegg, S. M., & Morris, E. R. (1988). Melting behaviour of gelatin gels: origin and control. In G.O. Phillips, D. J. Wedlock & P. A. Williams (Ed.), *Gums and Stabilisers for the Food Industry 4, Eds.* (105-115). Oxford: IRL.

Butler, M. F. & M. Heppenstall-Butler. (2003). Phase separation in gelatin/dextran and gelatin/maltodextrin mixtures. *Food Hydrocolloids,* 17(6), 815-830.

Butler, M., E. Heinrich, & P. Rayment. (2008). Process for production of compounds, which are starch containing particles coated, embedded or encapsulated by at least one biopolymers. 11/906,052(US 20080 107777A1).

Butterworth, P. J., Warren, F. J., & Ellis, P. R. (2011). Human α-amylase and starch digestion: An interesting marriage. *Starch-Stärke,* 63(7), 395-405.

Cain, F. W., A. H. Clark, P. J. Dunphy, M. G. Jones, I. T. Norton, & S. B. Ross-Murphy. (1990). U.S. Patent No. 4,956,193. Edible plastic dispersion.(U.S. Patent No. 4,956,193).

Cassanelli, M., Norton, I., & Mills, T. (2018a). Role of gellan gum microstructure in freeze drying and rehydration mechanisms. *Food Hydrocolloids,* 75, 51-61.

Cassanelli, M., Norton, I., & Mills, T. (2018b). Interaction of mannitol and sucrose with gellan gum in freeze-dried gel systems. *Food Biophysics,* 1-12.

Castro, N., Durrieu, V., Raynaud, C., & Rouilly, A. (2016). Influence of DE-value on the physicochemical properties of maltodextrin for melt extrusion processes. *Carbohydrate Polymers,* 144, 464-473.

Chandrasekaran, R., Radha, A., & Thailambal, V. G. (1992). Roles of potassium ions, acetyl and L-glyceryl groups in native gellan double helix: an X-ray study. *Carbohydrate Research,* 224, 1-17.

Chen, B., Y. Cai, T. Liu, L. Huang, X. Zhao, M. Zhao, X. Deng, & Q. Zhao. (2020). Formation and performance of high acyl gellan hydrogel affected by the addition of physical-chemical treated insoluble soybean fiber. *Food Hydrocolloids,* 101, 105526.

Chronakis, I. S. (1998). On the molecular characteristics, compositional properties, and structural-functional mechanisms of maltodextrins: a review. *Critical Reviews in Food Science and Nutrition,* 38(7), 599-637.

Chronakis, I. S. & S. Kasapis. (1995). Preparation and Analysis of Water Continuous Very Low Fat Spreads. *LWT - Food Science and Technology,* 28(5), 488-494.

Chronakis, I. S., Kasapis, S., & Richardson, R. K. (1996). Small deformation rheological properties of maltodextrin—milk protein systems. *Carbohydrate Polymers,* 29(2), 137-148.

Clark, A. H. (1991). Structural and Mechanical Properties of Biopolymer Gels. In E. Dickinson (Ed.), *Food Polymers, Gels, and Colloids - Proceedings of an International Symposium organized by the Food Chemistry Group of The Royal Society of Chemistry at Norwich from 28th-30th March 1990* (322-338). Elsevier.

Clark, A. H., Eyre, S., Ferdinando, D. P., & Lagarrigue, S. (1999). Interpenetrating Network Formation in Gellan− Maltodextrin Gel Composites. *Macromolecules,* 32(23), 7897-7906.

Clark, A. H. (1996). Biopolymer gels. *Current Opinion in Colloid & Interface Science,* 1(6), 712-717.

Coutinho, D. F., S. V. Sant, H. Shin, J. T. Oliveira, M. E. Gomes, N. M. Neves, A. Khademhosseini, & R. L. Reis. (2010). Modified Gellan Gum hydrogels with tunable physical and mechanical properties. *Biomaterials,* 31(29), 7494-7502.

De Silva, D. A., Poole-Warren, L. A., Martens, P. J., & in het Panhuis, M. (2013). Mechanical characteristics of swollen gellan gum hydrogels. *Journal of Applied Polymer Science,* 130(5), 3374-3383.

de Souza, F. S., de Mello Ferreira, I. L., da Silva Costa, M. A., da Costa, M. P. M., & da Silva, G. M. (2021). Effect of pH variation and crosslinker absence on the gelling mechanism of high acyl gellan: Morphological, thermal and mechanical approaches. *Carbohydrate Polymers,* 251, 117002.

Dhital, S., Gidley, M. J., & Warren, F. J. (2015). Inhibition of α-amylase activity by cellulose: Kinetic analysis and nutritional implications. *Carbohydrate Polymers,* 123, 305-312.

Dhital, S., Warren, F. J., Butterworth, P. J., Ellis, P. R., & Gidley, M. J. (2017). Mechanisms of starch digestion by α-amylase—Structural basis for kinetic properties. *Critical Reviews in Food Science and Nutrition,* 57(5), 875-892.

Djabourov, M., Nishinari, K., & Ross-Murphy, S. B. (2013). *Physical Gels from Biological and Synthetic Polymers*: Cambridge University Press.

Dokic, P., Jakovljevic, J., & Dokic-Baucal, L. (1998). Molecular characteristics of maltodextrins and rheological behaviour of diluted and concentrated solutions. *Colloids and Surfaces A: Physicochemical and Engineering Aspects,* 141(3), 435-440.

Draget, K. I. (2009). Alginates. In G. O. Phillips & P. A. Williams (Eds.), *Handbook of hydrocolloids* (807-828). Woodhead Publishing Limited.

Engmann, J., Servais, C., & Burbidge, A. S. (2005). Squeeze flow theory and applications to rheometry: A review. *Journal of non-newtonian fluid mechanics*, 132(1-3), 1-27.

Evageliou, V., R. K. Richardson, & E. R. Morris. (2000). Co-gelation of high methoxy pectin with oxidised starch or potato maltodextrin. *Carbohydrate Polymers,* 42(3), 233-243.

Fabek, H., Messerschmidt, S., Brulport, V., & Goff, H. D. (2014). The effect of *in vitro* digestive processes on the viscosity of dietary fibres and their influence on glucose diffusion. *Food Hydrocolloids,* 35, 718-726.

Flores-Huicochea, E., Rodríguez-Hernández, A. I., Espinosa-Solares, T., & Tecante, A. (2013). Sol-gel transition temperatures of high acyl gellan with monovalent and divalent cations from rheological measurements. *Food Hydrocolloids,* 31(2), 299-305.

Funami, T., Noda, S., Nakauma, M., Ishihara, S., Takahashi, R., Al-Assaf, S., Ikeda, S., Nishinari, K., & Phillips, G. O. (2008). Molecular structures of gellan gum imaged with atomic force microscopy in relation to the rheological behavior in aqueous systems in the presence or absence of various cations. *Journal of Agricultural and Food Chemistry,* 56(18), 8609-8618.

German, M. L., Blumenfeld, A. L., Yuryev, V. P., & Tolstoguzov, V. B. (1989). An NMR study of structure formation in maltodextrin systems. *Carbohydrate Polymers,* 11(2), 139-146.

German, M. L., Blumenfeld, A. L., Guenin, Y. V., Yuryev, V. P., & Tolstoguzov, V. B. (1992). Structure formation in systems containing amylose, amylopectin, and their mixtures. *Carbohydrate Polymers,* 18(1), 27-34.

Gidley, M. J. & Bulpin, P. V. (1987). Crystallisation of malto-oligosaccharides as models of the crystalline forms of starch: minimum chain-length requirement for the formation of double helices. *Carbohydrate Research,* 161(2), 291-300.

Gidley, M. J., Cooke, D., Darke, A. H., Hoffmann, R. A., Russell, A. L., & Greenwell, P. (1995). Molecular order and structure in enzyme-resistant retrograded starch. *Carbohydrate Polymers,* 28(1), 23-31.

Gidley, M. J. (2013). Hydrocolloids in the digestive tract and related health implications. *Current Opinion in Colloid & Interface Science,* 18(4), 371-378.

Gładkowska-Balewicz, I. (2017). Mixed fluid gels formation, structure and rheological properties. *Doctoral Dissertation,*.

Gong, B., Cheng, L., Gilbert, R. G., & Li, C. (2019). Distribution of short to medium amylose chains are major controllers of *in vitro* digestion of retrograded rice starch. *Food Hydrocolloids,* 96, 634-643.

Goñi, I., A. Garcia-Alonso, & F. Saura-Calixto. (1997). A starch hydrolysis procedure to estimate glycemic index. *Nutrition Research,* 17(3), 427-437.

Gunning, A. P. & V. J. Morris. (1990). Light scattering studies of tetramethyl ammonium gellan. *International Journal of Biological Macromolecules,* 12(6), 338-341.

Hofman, D. L., Van Buul, V. J., & Brouns, F. J. (2016). Nutrition, health, and regulatory aspects of digestible maltodextrins. *Critical Reviews in Food Science and Nutrition,* 56(12), 2091-2100.

Hossain, K. S. & Nishinari, K. (2009). Chain release behavior of gellan gels. In M. Tokita & K. Nishinari (Eds.), *Gels: Structures, properties, and functions* (177-186). Springer.

Huang, Y., Singh, P. P., Tang, J., & Swanson, B. G. (2004). Gelling temperatures of high acyl gellan as affected by monovalent and divalent cations with dynamic rheological analysis. *Carbohydrate Polymers,* 56(1), 27-33.

Janssen, A. M., Van de Pijpekamp, Anne M, & Labiausse, D. (2009). Differential saliva-induced breakdown of starch filled protein gels in relation to sensory perception. *Food Hydrocolloids,* 23(3), 795-805.

Jenkins, D. J., Leeds, A. R., Gassull, M. A., Cochet, B., & Alberti, K. G. M. (1977). Decrease in postprandial insulin and glucose concentrations by guar and pectin. *Annals of Internal Medicine,* 86(1), 20-23.

Jeukendrup, A. E. & Jentjens, R. (2000). Oxidation of carbohydrate feedings during prolonged exercise. *Sports Medicine,* 29(6), 407-424.

Jönsson, B., Wennerström, H., Nilsson, P. G., & Linse, P. (1986). Self-diffusion of small molecules in colloidal systems. *Colloid and Polymer Science,* 264(1), 77-88.

Kang, D., Z. Cai, Y. Wei, & H. Zhang. (2017). Structure and chain conformation characteristics of high acyl gellan gum polysaccharide in DMSO with sodium nitrate. *Polymer,* 128, 147-158.

Kanyuck, K. M., Mills, T. B., Norton, I. T., & Norton-Welch, A. B. (2019). Temperature influences on network formation of low DE maltodextrin gels. *Carbohydrate Polymers,*(218C), 170-178.

Kanyuck, K. M., Norton-Welch, A. B., Mills, T. B., & Norton, I. T. (2021a). Structural characterization of interpenetrating network formation of high acyl gellan and maltodextrin gels. *Food Hydrocolloids,* 112, 106295.

Kanyuck, K. M., Mills, T. B., Norton, I. T., & Norton-Welch, A. B. (2021b). Swelling of high acyl gellan gum hydrogel: Characterization of network strengthening and slower release. *Carbohydrate Polymers,* 259, 117758.

Kasapis, S., Morris, E. R., Norton, I. T., & Brown, C. R. T. (1993a). Phase equilibria and gelation in gelatin/maltodextrin systems - Part III: Phase separation in mixed gels. *Carbohydrate Polymers,* 21(4), 261-268.

Kasapis, S., Morris, E. R., Norton, I. T., & Clark A. H. (1993b). Phase equilibria and gelation in gelatin/maltodextrin systems — Part I: gelation of individual components. *Carbohydrate Polymers,* 21(4), 243-248.

Kasapis, S., Morris, E. R., Norton, I. T.,, & Clark A. H. (1993c). Phase equilibria and gelation in gelatin/maltodextrin systems — Part IV: composition-dependence of mixed-gel moduli. *Carbohydrate Polymers,* 21(4), 269-276.

Kasapis, S., Morris, E. R., Norton, I. T., & Gidley, M. J. (1993d). Phase equilibria and gelation in gelatin/maltodextrin systems - Part II: Polymer incompatibility in solution. *Carbohydrate Polymers,* 21(4), 249-259.

Kasapis, S. (1995). Review: phase separated, glassy and rubbery states of gellan gum in mixtures with food biopolymers and co-solutes. *International Journal of Food Science & Technology,* 30(6), 693-710.

Kasapis, S., Giannouli, P., Hember, M. W., Evageliou, V., Poulard, C., Tort-Bourgeois, B., & Sworn, G. (1999). Structural aspects and phase behaviour in deacylated and high acyl gellan systems. *Carbohydrate Polymers,* 38(2), 145-154.

Kasapis, S. (2008). Phase separation in biopolymer gels: a low-to high-solid exploration of structural morphology and functionality. *Critical Reviews in Food Science and Nutrition,* 48(4), 341-359.

Khang, G., Lee, S. K., Kim, H. N., Silva-Correia, J., Gomes, M. E., Viegas, C., Dias, I. R., Oliveira, J. M., & Reis, R. L. (2015). Biological evaluation of intervertebral disc cells in different formulations of gellan gum-based hydrogels. *Journal of Tissue Engineering and Regenerative Medicine,* 9(3), 265-275.

Khin, M. N., Goff, H. D., Nsor-Atindana, J., Ahammed, S., Liu, F., & Zhong, F. (2021). Effect of texture and structure of polysaccharide hydrogels containing maltose on release and hydrolysis of maltose during digestion: In vitro study. *Food Hydrocolloids,* 106326.

Koh, L. W., Kasapis, S., Lim, K. M., & Foo, C. W. (2009). Structural enhancement leading to retardation of *in vitro* digestion of rice dough in the presence of alginate. *Food Hydrocolloids,* 23(6), 1458-1464.

Lau, M. H., Tang, J., & Paulson, A. T. (2000). Texture profile and turbidity of gellan/gelatin mixed gels. *Food Research International,* 33(8), 665-671.

Lillford, P. J. (1988). The polymer/water relationship--its importance for food structure. In JMV Blanshard & JR Mitchell (Eds.), *Food structure: its creation and evaluation* (75-92). : London: Butterworths, 1988.

Lillford, P. J., Clark, A. H., & Jones, D. V. (1980). Distribution of water in heterogeneous food and model systems. In Rowland, S. P. (Ed) *Water in polymers* (Vol. 127) (177-195). ACS Symposium Series.

Lin, C. & Metters, A. T. (2006). Hydrogels in controlled release formulations: network design and mathematical modeling. *Advanced Drug Delivery Reviews,* 58(12-13), 1379-1408.

Liu, L., Wang, B., Gao, Y., & Bai, T. (2013). Chitosan fibers enhanced gellan gum hydrogels with superior mechanical properties and water-holding capacity. *Carbohydrate Polymers,* 97(1), 152-158.

Lorén, N., Langton, M., & Hermansson, A. (1999). Confocal laser scanning microscopy and image analysis of kinetically trapped phase-separated gelatin/maltodextrin gels. *Food Hydrocolloids,* 13(2), 185-198.

Lorén, N. & Hermansson, A. (2000). Phase separation and gel formation in kinetically trapped gelatin/maltodextrin gels. *International Journal of Biological Macromolecules,* 27(4), 249-262.

Lorén, N., Nydén, M., & Hermansson, A. (2009a). Determination of local diffusion properties in heterogeneous biomaterials. *Advances in Colloid and Interface Science,* 150(1), 5-15.

Lorén, N., Shtykova, L., Kidman, S., Jarvoll, P., Nydén, M., & Hermansson, A. (2009b). Dendrimer diffusion in κ-carrageenan gel structures. *Biomacromolecules,* 10(2), 275-284.

Loret, C., Frith, W. J., & Fryer, P. J. (2004a). Mechanical properties of maltodextrin gels: Small and large deformation. In G. O. Phillips & P. A. Williams (Eds.), *Gums and Stabilisers for the Food Industry 12* (116-123). : The Royal Society of Chemistry.

Loret, C., V. Meunier, W. J. Frith, & P. J. Fryer. (2004b). Rheological characterisation of the gelation behaviour of maltodextrin aqueous solutions. *Carbohydrate Polymers,* 57(2), 153-163.

Loret, C., Schumm, S., Pudney, P. D., Frith, W. J., & Fryer, P. J. (2005). Phase separation and molecular weight fractionation behaviour of maltodextrin/agarose mixtures. *Food Hydrocolloids,* 19(3), 557-565.

Loret, C., Frith, W. J., & Fryer, P. J. (2006a). Microstructures Designed to Control the Mechanical Properties of Mixed Biopolymer Gels. In G. O. Phillips & P. A. Williams (Eds.), *Gums and Stabilisers for the Food Industry 13* (185-192). : Royal Society of Chemistry.

Loret, C., Frith, W. J., & Fryer, P. J. (2006b). Mechanical and structural properties of maltodextrin/agarose gel composites. *Applied Rheology,* 16(5), 248.

Lundin, L., Norton, I. T., Foster, T. J., Williams, M., Hermansson, A. M., & Bergstrom, E. (2000). Phase Separation in Mixed Biopolymer Systems. In P A. Williams, G O Phillips (Ed.), *Food Colloids, Biopolymers and Materials 10* (1). Royal Society of Chemistry.

Mandel, A. L., Des Gachons, C. P., Plank, K. L., Alarcon, S., & Breslin, P. A. (2010). Individual differences in AMY1 gene copy number, salivary α-amylase levels, and the perception of oral starch. *PloS One,* 5(10).

Manoj, P., Kasapis, S., & Chronakis, I. S. (1996). Gelation and phase separation in maltodextrin-caseinate systems. *Food Hydrocolloids,* 10(4), 407-420.

Maughan, R. J. (1991). Fluid and electrolyte loss and replacement in exercise. *Journal of Sports Sciences,* 9(S1), 117-142.

Mazen, F., Milas, M., & Rinaudo, M. (1999). Conformational transition of native and modified gellan. *International Journal of Biological Macromolecules,* 26(2-3), 109-118.

McClements, D. J. & Xiao, H. (2014). Excipient foods: designing food matrices that improve the oral bioavailability of pharmaceuticals and nutraceuticals. *Food & Function,* 5(7), 1320-1333.

McClements, D. J. (2017). Designing biopolymer microgels to encapsulate, protect and deliver bioactive components: Physicochemical aspects. *Advances in Colloid and Interface Science,* 240, 31-59.

McClements, D. J. (2021). Food hydrocolloids: Application as functional ingredients to control lipid digestion and bioavailability. *Food Hydrocolloids,* 106404.

McRorie Jr, J. W. & McKeown, N. M. (2017). Understanding the physics of functional fibers in the gastrointestinal tract: an evidence-based approach to resolving enduring misconceptions about insoluble and soluble fiber. *Journal of the Academy of Nutrition and Dietetics,* 117(2), 251-264.

Mills, T., Spyropoulos, F., Norton, I. T., & Bakalis, S. (2011). Development of an *in-vitro* mouth model to quantify salt release from gels. *Food Hydrocolloids,* 25(1), 107-113.

Minekus, M., Alminger, M., Alvito, P., Ballance, S., Bohn, T. , Bourlieu C, Carrière F, Boutrou R, Corredig M, Dupont D, Dufour C, Egger L, Golding M, Karakaya S, Kirkhus B, Le Feunteun S, Lesmes U, Macierzanka A, Mackie A, Marze S, McClements DJ, Ménard O, Recio I, Santos CN, Singh RP, Vegarud GE, Wickham MS, Weitschies W, Brodkorb A. (2014). A standardised static *in vitro* digestion method suitable for food–an international consensus. *Food & function*, 5(6), 1113-1124.

Miyoshi, E., Takaya, T., & Nishinari, K. (1998). Effects of glucose, mannose and konjac glucomannan on the gel–sol transition in gellan gum aqueous solutions by rheology and DSC. *Polymer Gels and Networks,* 6(3-4), 273-290.

Miyoshi, E. & Nishinari, K. (1999). Rheological and thermal properties near the sol-gel transition of gellan gum aqueous solutions. In Anonymous *Physical Chemistry and Industrial Application of Gellan Gum* (68-82). Springer.

Moates, G. K., Noel, T. R., Parker, R., & Ring, S. G. (1997). The effect of chain length and solvent interactions on the dissolution of the B-type crystalline polymorph of amylose in water. *Carbohydrate Research,* 298(4), 327-333.

Moe, S. T., Elgsaeter, A., Skjåk-Bræk, G., & Smidsrød, O. (1993). A new approach for estimating the crosslink density of covalently crosslinked ionic polysaccharide gels. *Carbohydrate Polymers,* 20(4), 263-268.

Morris, E. R., Rees, D. A., & Robinson, G. (1980). Cation-specific aggregation of carrageenan helices: domain model of polymer gel structure. *Journal of Molecular Biology,* 138(2), 349-362.

Morris, E. R. (1992). The effect of solvent partition on the mechanical properties of biphasic biopolymer gels: an approximate theoretical treatment. *Carbohydrate Polymers,* 17(1), 65-70.

Morris, E. R. (1994). Rheological and organoleptic properties of food hydrocolloids.In K. Nishinari & E. Doi (Eds.), *Food hydrocolloids* (201-210). : Springer.

Morris, E. R. (1995). Polysaccharide synergism—more questions than answers.In S. E. Harding, S. E. Hill and J. R. Mitchell (Ed.), *Biopolymer Mixtures* (247-288). Nottingham, UK: Nottingham University Press.

Morris, E. R., Gothard, M., Hember, M., Manning, C. E., & Robinson, G. (1996). Conformational and rheological transitions of welan, rhamsan and acylated gellan. *Carbohydrate Polymers,* 30(2-3), 165-175.

Morris, E. R. (2009). Functional interactions in gelling biopolymer mixtures.In Stefan Kasapis, Ian T. Norton and Johan B. Ubbink (Ed.), *Modern biopolymer science* (167-198). : Elsevier.

Morris, E. R., Nishinari, K., & Rinaudo, M. (2012). Gelation of gellan–a review. *Food Hydrocolloids,* 28(2), 373-411.

Morris, V. J. (1986). Multicomponent gels. In G. O. Phillips, D. J. Wedlock and P. A. Williams (Eds.) *Gums and Stabilisers for the Food Industry* 3, 87-99. Elsevier Applied Science Publishers.

Morris, V. J., Kirby, A. R., & Gunning, A. P. (1999). A fibrous model for gellan gels from atomic force microscopy studies. In K. Nishinari (Ed.), *Physical Chemistry and Industrial Application of Gellan Gum* (102-108). Springer.

Murillo-Martínez, M.,M. & Tecante, A. (2014). Preparation of the sodium salt of high acyl gellan and characterization of its structure, thermal and rheological behaviors. *Carbohydrate Polymers,* 108(1), 313-320.

Nakamura, K., Shinoda, E., & Tokita, M. (2001). The influence of compression velocity on strength and structure for gellan gels. *Food Hydrocolloids,* 15(3), 247-252.

Nickerson, M. T., Farnworth, R., Wagar, E., Hodge, S. M., Rousseau, D., & Paulson, A. T. (2006). Some physical and microstructural properties of genipin-crosslinked gelatin–maltodextrin hydrogels. *International Journal of Biological Macromolecules,* 38(1), 40-44.

Nishinari, K., Watase, M., Rinaudo, M., & Milas, M. (1996a). Characterization and properties of gellan-κ-carrageenan mixed gels. *Food Hydrocolloids,* 10(3), 277-283.

Nishinari, K., Miyoshi, E., Takaya, T., & Williams, P. A. (1996b). Rheological and DSC studies on the interaction between gellan gum and konjac glucomannan. *Carbohydrate Polymers,* 30(2-3), 193-207.

Nishinari, K., H. Zhang, & S. Ikeda. (2000). Hydrocolloid gels of polysaccharides and proteins. *Current Opinion in Colloid & Interface Science,* 5(3), 195-201.

Nishinari, K. & Fang, Y. (2016). Sucrose release from polysaccharide gels. *Food & Function,* 7(5), 2130-2146.

Nishinari, K. & Fang, Y. (2021). Molar mass effect in food and health. *Food Hydrocolloids,*(106110).

Nitta, Y., Ikeda, S., & Nishinari, K. (2006). The reinfocement of gellan gel network by the immersion into salt solution. *International Journal of Biological Macromolecules,* 38(2), 145-147.

Noda, S., Funami, T., Nakauma, M., Asai, I., Takahashi, R., Al-Assaf, S., Ikeda, S., Nishinari, K., & Phillips, G. O. (2008). Molecular structures of gellan gum imaged with atomic force microscopy in relation to the rheological behavior in aqueous systems. 1. Gellan gum with various acyl contents in the presence and absence of potassium. *Food Hydrocolloids,* 22(6), 1148-1159.

Normand, V., Plucknett, K. P., Pomfret, S. J., Ferdinando, D., & Norton, I. T. (2001). Large deformation mechanical behavior of gelatin–maltodextrin composite gels. *Journal of Applied Polymer Science,* 82(1), 124-135.

Norton, A. B., Hancocks, R. D., & Grover, L. M. (2014a). Poly (vinyl alcohol) modification of low acyl gellan hydrogels for applications in tissue regeneration. *Food Hydrocolloids,* 42, 373-377.

Norton, I. T. & Frith, W. J. (2001). Microstructure design in mixed biopolymer composites. *Food Hydrocolloids,* 15(4), 543-553.

Norton, J. E., Wallis, G. A., Spyropoulos, F., Lillford, P. J., & Norton, I. T. (2014b). Designing food structures for nutrition and health benefits. *Annual Review of Food Science and Technology,* 5, 177-195.

Oakenfull, D. & Scott, A. (1984). Hydrophobic Interaction in the Gelation of High Methoxyl Pectins. *Journal of Food Science,* 49(4), 1093-1098.

Osmałek, T. Z., Froelich, A., Jadach, B., & Krakowski, M. (2018). Rheological investigation of high-acyl gellan gum hydrogel and its mixtures with simulated body fluids. *Journal of Biomaterials Applications,* 32(10), 1435-1449.

Palumbo, F. S., Federico, S., Pitarresi, G., Fiorica, C., & Giammona, G. (2020). Gellan gum-based delivery systems of therapeutic agents and cells. *Carbohydrate Polymers,* 229, 115430.

Peppas, N. A. & Sahlin, J. J. (1989). A simple equation for the description of solute release. III. Coupling of diffusion and relaxation. *International Journal of Pharmaceutics,* 57(2), 169-172.

Pereira, D. R., Silva-Correia, J., Caridade, S. G., Oliveira, J. T., Sousa, R. A., Salgado, A. J., Oliveira, J. M., Mano, J. F., Sousa, N., & Reis, R. L. (2011). Development of gellan gum-based microparticles/hydrogel matrices for application in the intervertebral disc regeneration. *Tissue Engineering Part C: Methods,* 17(10), 961-972.

Picone, C. S. F. & Cunha, R. L. (2011). Influence of pH on formation and properties of gellan gels. *Carbohydrate Polymers,* 84(1), 662-668.

Picout, D. R., Richardson, R. K., & Morris, E. R. (2000a). Ca 2+ -induced gelation of low-methoxy pectin in the presence of oxidised starch. Part 2. Quantitative analysis of moduli. *Carbohydrate Polymers,* 43(2), 123-131.

Picout, D. R., Richardson, R. K., & Morris, E. R. (2000b). Co-gelation of calcium pectinate with potato maltodextrin. Part 1. Network formation on cooling. *Carbohydrate Polymers,* 43(2), 133-141.

Piculell, L., Bergfeldt, K., & Nilsson, S. (1995). Factors determining phase behaviour of multi component polymer systems. *Biopolymer Mixtures,* 13-35.

Radosta, S. & Schierbaum, F. (1990). Polymer-Water Interaction of Maltodextrins. Part III: Non-freezable Water in Maltodextrin Solutions and Gels. *Starch-Stärke,* 42(4), 142-147.

Ramírez, C., Millon, C., Nunez, H., Pinto, M., Valencia, P., Acevedo, C., & Simpson, R. (2015). Study of effect of sodium alginate on potato starch digestibility during *in vitro* digestion. *Food Hydrocolloids,* 44, 328-332.

Ranawana, V., Clegg, M. E., Shafat, A., & Henry, C. J. (2011). Postmastication digestion factors influence glycemic variability in humans. *Nutrition Research,* 31(6), 452-459.

Reuther, F., Damaschun, G., Gernat, C., Schierbaum, F., Kettlitz, B., Radosta, S., & Nothnagel, A. (1984). Molecular gelation mechanism of maltodextrins investigated by wide-angle X-ray scattering. *Colloid & Polymer Science,* 262(8), 643-647.

Reuther, F., Plietz, P., Damaschun, G., Pürschel, H., Kröber, R., & Schierbaum, F. (1983). Structure of maltodextrin gels—a small angle X-ray scattering study. *Colloid and Polymer Science,* 261(3), 271-276.

Ross-Murphy, S. B. (1995). Small deformation rheological behaviour of biopolymer mixtures. In S. E. Harding, S. E. Hill and J. R. Mitchell (Ed.), *Biopolymer Mixtures* (85-98). Nottingham: Nottingham University Press.

Sakai, T. (2020). *Physics of Polymer Gels*: John Wiley & Sons.

Sala, G., Stieger, M., & van de Velde, F. (2010). Serum release boosts sweetness intensity in gels. *Food Hydrocolloids,* 24(5), 494-501.

Sanderson, G. R., Bell, V. L., Clark, R. C., & Ortega, D. (1988). The Texture of Gellan Gum Gels. In D. J. Wedlock & P. A. Williams (Ed.), *Gums and Stabilisers for the Food Industry 4* (219-229). Oxford: IRL.

Santoro, M. M. & Bolen, D. W. (1992). A test of the linear extrapolation of unfolding free energy changes over an extended denaturant concentration range. *Biochemistry,* 31(20), 4901-4907.

Sasaki, T. & Kohyama, K. (2011). Effect of non-starch polysaccharides on the in vitro digestibility and rheological properties of rice starch gel. *Food Chemistry,* 127(2), 541-546.

Schierbaum, F., Kettlitz, B., Radosta, S., Reuther, F., Richter, M., & Vorwerg, W. (1984). Zum stand der kenntnisse uber struktureigenschafts- beziehungen von maltodextrin. *Acta-Alimentaria-Polonica,* 10(69).

Schierbaum, F., Radosta, S., Vorwerg, W., Yuriev, V. P., Braudo, E. E., & German, M. L. (1992). Formation of thermally reversible maltodextrin gels as revealed by low resolution H-NMR. *Carbohydrate Polymers,* 18(3), 155-163.

Schierbaum, F., Reuther, F., Braudo, E. E., Plashchina, I. G., & Tolstoguzov, V. B. (1990). Thermodynamic parameters of the junction zones in thermoreversible maltodextrin gels. *Carbohydrate Polymers,* 12(3), 245-253.

Schierbaum, F., Vorwerg, W., Kettlitz, B., & Reuther, F. (1986). Interaction of linear and branched polysaccharides in starch gelling. *Molecular Nutrition & Food Research,* 30(10), 1047-1049.

Shi, X. & Passe, D. H. (2010). Water and solute absorption from carbohydrate-electrolyte solutions in the human proximal small intestine: a review and statistical analysis. *International Journal of Sport Nutrition and Exercise Metabolism,* 20(5), 427-442.

Shinsho, A., Brenner, T., Descallar, F. B., Tashiro, Y., Ando, N., Zhou, Y., Ogawa, H., & Matsukawa, S. (2020). The thickening properties of native gellan gum are due to freeze drying–induced aggregation. *Food Hydrocolloids,* 105997.

Siepmann, J. & N. A. Peppas. (2011). Higuchi equation: Derivation, applications, use and misuse. *International Journal of Pharmaceutics,* 418(1), 6-12.

Skouri, R., Schosseler, F., Munch, J. P., & Candau, S. J. (1995). Swelling and elastic properties of polyelectrolyte gels. *Macromolecules,* 28(1), 197-210.

Srikaeo, K. & Paphonyanyong, W. (2020). Texture, microstructure and *in-vitro* starch digestibility of waxy rice cooked with hydrocolloids. *Food Research,* 4(4), 1089-1097.

Stein, W. D. & Litman, T. (2014). *Channels, carriers, and pumps: an introduction to membrane transport*: Elsevier.

Stevens, L. R., Gilmore, K. J., & Wallace, G. G. (2016). Tissue engineering with gellan gum. *Biomaterials Science,* 4(9), 1276-1290.

Sworn, G. (2009). Gellan gum. In G. O. Phillips & P. A. Williams (Eds.), *Handbook of Hydrocolloids* (204-227). Woodhead Publishing Limited.

Tako, M., Teruya, T., Tamaki, Y., & Konishi, T. (2009). Molecular origin for rheological characteristics of native gellan gum. *Colloid and Polymer Science,* 287(12), 1445.

Tanaka, F. (2003). Thermoreversible gelation driven by coil-to-helix transition of polymers. *Macromolecules,* 36(14), 5392-5405.

Tanaka, S. & Nishinari, K. (2007). Unassociated molecular chains in physically crosslinked gellan gels. *Polymer Journal,* 39(4), 397-403.

Tharakan, A., Norton, I. T., Fryer, P. J., & Bakalis, S. (2010). Mass transfer and nutrient absorption in a simulated model of small intestine. *Journal of Food Science,* 75(6), E339-E346.

van den Berg, L., van Vliet, T., van der Linden, E., van Boekel, M., & van de Velde, F. (2007). Breakdown properties and sensory perception of whey proteins/polysaccharide mixed gels as a function of microstructure. *Food Hydrocolloids,* 21(5-6), 961-976.

van der Sman, R. (2015). Biopolymer gel swelling analysed with scaling laws and Flory–Rehner theory. *Food Hydrocolloids,* 48, 94-101.

van Vliet, T. & Walstra, P. (1995). Large deformation and fracture behaviour of gels. *Faraday Discussions,* 101, 359-370.

Vilela, J. A. P. & Cunha, R. L. D. (2016). High acyl gellan as an emulsion stabilizer. *Carbohydrate Polymers,* 139, 115-124.

Vorwerg, W., Schierbaum, F. R., Reuther, F., & Kettlitz, B. (1988). Formation of thermally reversible networks from starch polysaccharides. In Kramer, O. (Ed.) *Biological and synthetic polymer networks* (127-139). Springer.

Wang, X. & Ziegler, G. R. (2009). Phase Behavior of the ι-Carrageenan/Maltodextrin/Water System at Different Potassium Chloride Concentrations and Temperatures. *Food Biophysics,* 4(2), 119-125.

Wang, Y. & Wang, L. (2000). Structures and properties of commercial maltodextrins from corn, potato, and rice starches. *Starch-Stärke,* 52(8-9), 296-304.

Wang, Z., Yang, K., Brenner, T., Kikuzaki, H., & Nishinari, K. (2014). The influence of agar gel texture on sucrose release. *Food Hydrocolloids,* 36, 196-203.

Wee, M. S. & Henry, C. J. (2020). Reducing the glycemic impact of carbohydrates on foods and meals: Strategies for the food industry and consumers with special focus on Asia. *Comprehensive Reviews in Food Science and Food Safety,* 19(2), 670-702.

Wesdorp, L. H., Madsen, R. A., Norton, I. T., & Brown, C. R. T. (1995). U.S. Patent No. 5,464,645. Process of making a water continuous dispersion with more than 50% dispersed phase and products thereof. (U.S. Patent No. 5,464,645).

Williams, P. A. & Phillips, G. O. (2009). Introduction to food hydrocolloids. In G. O. Phillips & P. A. Williams (Eds.), *Handbook of hydrocolloids* (1-22). Elsevier.

Woolnough, J. W., Monro, J. A., Brennan, C. S., & Bird, A. R. (2008). Simulating human carbohydrate digestion *in vitro*: a review of methods and the need for standardisation. *International Journal of Food Science & Technology,* 43(12), 2245-2256.

Wyman, J. (1931). The dielectric constant of mixtures of ethyl alcohol and water from-5 to 40. *Journal of the American Chemical Society,* 53(9), 3292-3301.

Yang, K., Wang, Z., Brenner, T., Kikuzaki, H., Fang, Y., & Nishinari, K. (2015). Sucrose release from agar gels: Correlation with sucrose content and rheology. *Food Hydrocolloids,* 43 (Supplement C), 132-136.

Yang, X., Hou, Y., Gong, T., Sun, L., Xue, J., & Guo, Y. (2019). Concentration-dependent rheological behavior and gelation mechanism of high acyl gellan aqueous solutions. *International Journal of Biological Macromolecules,* 131, 959-970.

Yu, I., Kaonis, S., & Chen, R. (2017). A study on degradation behavior of 3D printed gellan gum scaffolds. *Procedia CIRP,* 65, 78-83.

Zhang, B., Bai, B., Pan, Y., Li, X., Cheng, J., & Chen, H. (2018). Effects of pectin with different molecular weight on gelatinization behavior, textural properties, retrogradation and *in vitro* digestibility of corn starch. *Food Chemistry,* 264, 58-63.

Zhang, G. & Zhou, D. (2016). Crystalline and Amorphous Solids. In Qiu, Y., Chen, Y., Geoff, G.Z. Yu, L., & Mantri, R.V. (Ed.), *Developing Solid Oral Dosage Forms: Pharmaceutical Theory and Practice*: Academic Press.

Zhang, J., Daubert, C. R., & Foegeding, E. A. (2005). Characterization of polyacrylamide gels as an elastic model for food gels. *Rheologica Acta,* 44(6), 622-630.

Appendix

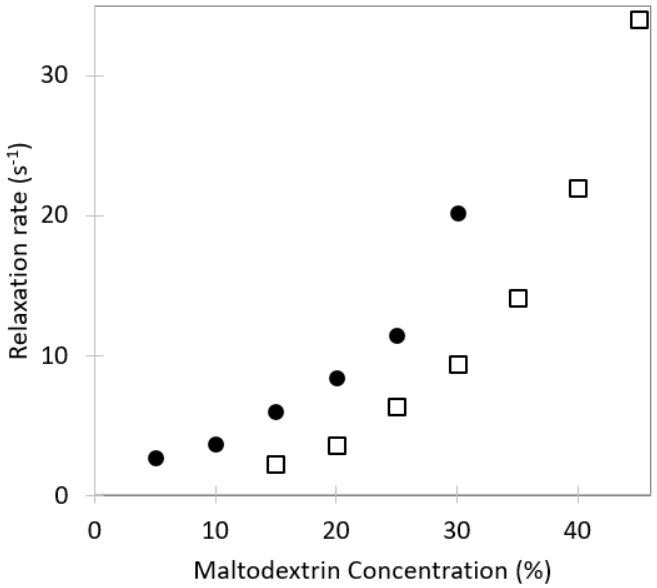

Appendix A. NMR relaxation rates ($1/T_2$) used to estimate phase separation volumes for MD (□), MD with 1% HA gellan (●). A Bruker mq20 minispec benchtop NMR was used for the measurement with a CPMG pulse sequence and tau of 0.25 ms.